

ETD Archive

2011

Glia Specific Innate Responses and Their Influence on Murine Coronavirus Inducedencephalomyelitis

Parul Kapil
Cleveland State University

Follow this and additional works at: <https://engagedscholarship.csuohio.edu/etdarchive>

 Part of the [Biology Commons](#)

[How does access to this work benefit you? Let us know!](#)

Recommended Citation

Kapil, Parul, "Glia Specific Innate Responses and Their Influence on Murine Coronavirus Inducedencephalomyelitis" (2011). *ETD Archive*. 153.
<https://engagedscholarship.csuohio.edu/etdarchive/153>

This Dissertation is brought to you for free and open access by EngagedScholarship@CSU. It has been accepted for inclusion in ETD Archive by an authorized administrator of EngagedScholarship@CSU. For more information, please contact library.es@csuohio.edu.

**GLIA SPECIFIC INNATE RESPONSES AND THEIR INFLUENCE ON MURINE
CORONAVIRUS INDUCED ENCEPHALOMYELITIS**

PARUL KAPIL

Bachelor of Science

Ch Charan Singh University, Haridwar, India

July 1999

Master in Microbiology

Gurukul Kangri Vishwavidalya

July 2001

Submitted in partial fulfillment of requirements for the degree

DOCTOR OF PHILOSOPHY IN REGULATORY BIOLOGY

at the

CLEVELAND STATE UNIVERSITY

December, 2011

© Copyright by Parul Kapil 2011

This thesis/dissertation has been approved for
the Department of Biological, Geological,
and Environmental Sciences and for the
College of Graduate Studies of
Cleveland State University

By

Dr. Cornelia Bergmann, Chairperson Date

Cleveland Clinic

Dr. Robert Silverman Date

Cleveland Clinic

Dr. Crystal Weyman Date

Biological, Geological, and Environmental Sciences

Dr. Vincent Tuohy Date

Cleveland Clinic

Dr. William Baldwin Date

Cleveland Clinic

Dr. Bruce Lamb Date

Cleveland Clinic

DEDICATIONS

This thesis is dedicated to my parents, Rameshwar and Rekha Sharma, for their endless love support and encouragement.

ACKNOWLEDGMENT

Writing this section is a bittersweet experience as one side it marks as an end of an era of my life as a graduate student while other side it indicates beginning of a new future. In my journey of past 5 years I have gained several experiences and I am indebted to the many people.

First I would like to thank Department of Biology, Geology and Environmental Sciences, CSU, Cleveland, OH for providing me opportunity to pursue my lifetime carrier goal in research. I would also like to acknowledge my gratitude towards my mentor Dr. Cornelia Bergmann. Dr. Bergmann not only provided opportunity to work in her lab and helped me in my research, manuscript and thesis writing, but she also guided me to become an independent thinker.

I am immensely thankful to my advisory committee members, Dr. Crystal Weyman, Dr. Robert Silverman, and Dr. Vincent Tuohy. Each committee member was always very helpful and always had time for my questions and their intriguing questioning always encouraged me to move forward. Dr. Weyman always inspired me by her enthusiasm towards research and always helped me not only in academically but also in my in my administrative needs. Dr. Silverman provided very insightful advice in my project and also shared some valuable mice strains with us that lead to some new discoveries and important part of my thesis. Dr. Tuohy always challenged me to do better and supported me to achieve the goal. He would always ensure before my committee meeting that I am not too nervous.

I would like to thank to members of my thesis examination committee, Dr. William Baldwin and Dr. Bruce Lamb for their willingness to take time out of their busy schedule to supervise in my dissertation exam. I would also like to thank Dr. Jeffrey Dean, Chair of the BGES and Dr. Anton Komar, assistant chair of BGES and graduate program director and advising for their help and support.

I consider it an honor to work with our collaborator Dr. Stephen Stohlman, and would like to thank him for all the mice injection and for teaching me lot of laboratory techniques. Perhaps it is right to say that a supportive working atmosphere increase the productivity and I would like to share my achievements with my colleagues in the lab. I was blessed to be working with such a nice bunch of people. They were not only supportive but always stimulated me intellectually. I am indebted to old and new members of the lab not only for their input on my projects but also helped me plenty of times in my personal endowers too. I would like to thank Dr. Derek Ireland, Dr. Crisitina Marques, Dr. Carine Savarin, Dr. Shweta Puntambekar, Dr. Teresa Aquino, Dr. Gabriel Parra, Dr. Timothy Phares, Dr. Niranjan Butchi and S Dr. habbir Hussain for their support and help. I would also like to thank Mrs. Mi Widness, Ms. Kate Stenson, Ms. Megan Mconnell, and Mr. Jeoffery Tarcy for the technical support. I would especially like to thank Mrs. Jennifer Powers for her help in cell sorting.

I owe my deepest gratitude to my parents, Mr. Rameshwar Dayal Sharma and Mrs. Rekha Sharma. They always have been pillar of strength for me and always supported and inspired me in every situation. My quest to the knowledge started from the very nice saying my dad use to tell me "Knowledge is the best

addiction". Thank you Mummy-papa! My younger brother and also my best friend, Ashu deserves a major share in my success too who always believed in me and help me believing in myself too. He always stood behind me and cheered up for me. He would sit down in my time of despair and listen me complaining for hours and then hug me and say it will be all right. Thanks Bhai! I would also like to thank my father-in-law Mr. Ishwar Chand Sharma for his support and wishes.

One good friend is worth of thousand relatives; I would like to thanks my friends Mr. Neeraj Joshi and Mrs. Anupurna Kaul for their constant support and love.

Finally I would like to thank love of my life my loving and caring husband, Dr. Nikunj Sharma. This thesis would have been a dream without his unending support and inspiration. He always stood by me. He always encouraged me through every experimental failure and celebrated each of my achievements. He always dealt with my mood swings in the process with a smile and always tried to provide best of conditions. Love you sweetheart!

**GLIA SPECIFIC INNATE RESPONSES AND THEIR INFLUENCE ON MURINE
CORONAVIRUS INDUCED ENCEPHALOMYELITIS**

PARUL KAPIL

ABSTRACT

Control of viral infections of the central nervous system (CNS) is challenging, as the host has to balance anti-viral activity and immune mediated damage to non- renewable cells. The present study focuses on the role of glia and macrophages in regulating initial viral control and subsequent T cell activity in a murine model of neurotropic coronavirus induced encephalomyelitis. As induction of IFN α/β , pro- and anti-inflammatory factors depend on activation of pattern recognition receptors (PRR), macrophages, microglia and oligodendroglia were isolated from the CNS of infected mice to characterize their gene expression patterns. Oligodendroglia did not induce *Ifn α/β* expression following intracranial inoculation of both virus or the PRR agonist poly I:C, consistent with limited expression of PRRs and factors critical in the IFN α/β pathway. By contrast, induction of *Ifn α/β* by infected microglia and macrophages coincided with a broad and high basal expression pattern of IFN α/β signaling components and a protective antiviral state. Furthermore, an anti-inflammatory property of IFN α/β was suggested by abrogation of early *Il1ra* expression in both microglia and macrophage in the absence of IFN α/β signaling. Microglia and macrophages also induced a mixture of pro-inflammatory (*Il12*) and anti-inflammatory (*Il1ra*, *Ym1/2*) genes, which shape the adaptive immune response. IL12 and Ym1/2 stimulate T cells towards IFN γ and IL13 producing cells, respectively. The absence of IL12

decreased IFN γ and increased IL10 production, resulting in amelioration in clinical disease without altering virus control. Under the influence of distinct T cell mediated stimuli both microglia and macrophage retained a mixed pro- and anti-inflammatory phenotype defined by increased expression of *iNos* and *Arg1*, respectively. Sustained expression of *Arg1* and increased phagocytic activity indicated an overall bias towards an anti-inflammatory phenotype with time. Finally, analysis of the role of PKR, an IFN α/β induced anti-viral gene, demonstrated only a modest direct anti-viral role. Surprisingly however, PKR deficiency reduced production of the anti-inflammatory cytokine IL10 by CD4 T cells, coincident with increased diffuse demyelination. These results demonstrate how a tightly linked network between innate and adaptive responses regulates viral control as well as tissue damage and disease in a viral encephalomyelitis model.

TABLE OF CONTENTS

LIST OF FIGURES	xv
LIST OF TABLES	xxvii
CHAPTERS	
I. INTRODUCTION	1
1.1 Host Barriers and Innate Immune Responses Associated With CNS Infection	2
1.2 Activation of CNS Resident Cells Following Viral Infection.....	4
1.3 Experimental Models to Study Immune Responses in CNS.....	5
1.4 Coronavirus (JHMV) Mouse Model to Study Encephalitis and Demyelination in CNS	6
1.5 Role of Immune Response Following JHMV: Virus Clearance versus Pathogenesis	9
1.5.1 Innate immune response following JHMV and their interaction with adaptive immune response.....	9
1.5.2 Adaptive immune response	11
1.5.3 Anti-inflammatory response	12
II. OLIGODENDROGLIA ARE LIMITED IN TYPE I INTERFERON INDUCTION AND RESPONSIVENESS <i>IN VIVO</i>	14
2.1 Abstract	14
2.2 Introduction.....	15

2.3	Results	19
2.3.1	Limited expression of PRR and signal transduction molecules in oligodendroglia.....	19
2.3.2	IFN α/β is not induced in oligodendroglia.....	23
2.3.3	Oligodendroglia induce ISG delayed relative to microglia.....	26
2.3.4	Inability of oligodendroglia to induce <i>Ifnα/β</i> genes is virus independent.....	29
2.4	Discussion	32
III.	PKR: UNCONVENTIONAL ROLE OF AN ANTI-VIRAL FACTOR FOLLOWING CNS INFECTION	38
3.1	Abstract	38
3.2	Introduction.....	40
3.3	Results	44
3.3.1	PKR deficiency does not alter IFN α/β induction, reduces NF κ B mediated gene expression and only affects virus replication modestly in the CNS following JHMV infection.....	44
3.3.2	Increased CNS T cell infiltration, but accumulation of CD4 T cells in the perivascular space in the absence of PKR	48
3.3.3	Absence of PKR influences CD4 T cell function	51
3.3.4	PKR deficiency results in more diffuse demyelination, but does not contribute to clinical disease or survival.....	53

3.3.5	Dual deficient mice in PKR and RNaseL depicts overall similar phenotype as RNaseL ^{-/-} mice	55
IV.	IL12, BUT NOT IL23, DEFICIENCY AMELIORATES VIRAL ENCEPHALITIS WITHOUT AFFECTING VIRAL CONTROL.....	62
4.1	Abstract	62
4.2	Introduction.....	63
4.3	Results	67
4.3.1	IL12 enhances JHMV induced encephalitis	67
4.3.2	IL12 does not alter CNS inflammation	71
4.3.3	IFN γ is compromised in the absence of IL12	72
4.3.4	Viral induced demyelination is IL12 and IL23 independent.....	75
4.3.5	IL12 regulation of innate cytokine, chemokine and anti-inflammatory cytokines	77
4.4	Discussion	79
V.	KINETIC ANALYSIS OF PRO VERSUS ANTI-INFLAMMATORY GENES EXPRESSED BY MICROGLIA/MACROPHAGES DURING CORONAVIRUS MEDIATED CNS INFECTION.....	86
5.1	Abstract	86
5.2	Introduction.....	87
5.3	Results	92

5.3.1	The innate phase of JHMV infection is associated with abundant monocyte recruitment	92
5.3.2	JHMV replicates in microglia and infiltrating macrophages early during the infection.....	93
5.3.3	Activation of microglia/macrophage following JHMV infection	95
5.3.4	Expression of cytokines polarizing pro- and anti-inflammatory macrophages in the CNS following JHMV infection	97
5.3.5	T cell mediated influence on M1/M2 profiles of microglia and macrophages following JHMV infection	99
5.3.6	Increasing phagocytic activity of microglia and macrophage following infection	101
5.3.7	IFN α/β signaling plays an important role in induction of anti-inflammatory cytokine IL1Ra.....	103
5.4	Discussion	105
VI.	DISCUSSION	109
VII.	MATERIALS AND METHODS.....	114
7.1	Mice.....	114
7.2	Virus Infection and Clinical Disease	115
7.3	Intracranial Inoculation of Poly (I:C).....	115

7.4	Isolation of the Mononuclear Cells and Determination of the Virus	
	Tite	115
7.5	Flow Cytometry	116
7.6	Purification of Cells by Flow Activated Cell Sorting (FACS)	117
7.7	Correlation between Cell Number and Ct Value	119
7.8	<i>Ex Vivo</i> Stimulation Of Splenocytes	119
7.9	Intracellular Detection of Cytokines	120
7.10	Phagocytic Assay For Macrophage And Microglia	120
7.11	ELISA	121
7.12	Histology and Fluorescent Staining	122
7.13	Real Time PCR	123
	REFERENCES	130
	APPENDICES	166
A.	LIST OF ABBREVIATIONS	167

LIST OF FIGURES

1. Role of TLR Signaling in Glial Cells Following CNS Infection (adapted from Carpentier et al., 2008). (A) Virus recognition, (B) Glial Cell Activation, (C) Recruitment and Activation of Peripheral Cells. 5
2. Mouse Hepatitis Virus (MHV) Replication (Bergmann et al.,2006). 8
3. Oligodendroglia are limited in basal and inducible expression of viral RNA sensing PRRs. Microglia and oligodendroglia purified from spinal cords of naïve (A) or JHMV infected (B) PLP-GFP mice were assayed for *Mda5*, *Rig-I*, *Tlr3*, and *Tlr7* transcripts at the indicated times p.i. Data represent the average of 3 separate experiments \pm standard error of the mean (SEM). * denotes $p \leq 0.05$ comparing microglia to oligodendroglia at each timepoint; # indicates $p \leq 0.05$ compared to basal levels for each cell population. 21
4. MDA5 and RIG-I upregulation is IFN α/β dependent. Wt and IFNAR $^{-/-}$ mice infected with JHMV were used to compare induction of Mda5 and Rig-I mRNA in oligodendroglia and microglia purified from spinal cords. Data are average of 3 individual experiments \pm SEM as described in Fig. 3. * denotes $p \leq 0.05$ comparing wt to IFNAR $^{-/-}$ populations at each timepoint. 22
5. Oligodendroglia do not induce IFN α/β transcripts during JHMV infection. Microglia and oligodendroglia purified from spinal cords of naïve or JHMV infected PLP-GFP mice were assessed for (A) JHMV-N transcripts or (B) *Ifn β* and *Ifn α 4* transcripts. Data are average values \pm

- SEM of 3 independent experiments. BD indicates below detection. * denotes $p \leq 0.05$ comparing microglia to oligodendroglia. 24
6. Oligodendroglia are limited in basal and inducible expression of PRR associated signaling factors during JHMV infection. Microglia and oligodendroglia from naïve or JHMV infected mice were assayed for *Ikk ϵ* , *Irf3* and *Irf7* transcripts as indicated in Fig. 3. Data represent the average of 3 separate experiments \pm SEM. * denotes $p \leq 0.05$ comparing microglia to oligodendroglia at each timepoint; # indicates $p \leq 0.05$ compared to basal levels for each cell population..... 25
7. Oligodendroglia have limited IFN α/β receptor signaling capacity. Microglia and oligodendroglia from naïve or JHMV infected mice were assayed for transcripts encoding the IFNAR1, soluble IFNAR2 (IFNAR2^s) and IFNAR2 transmembrane (IFNAR2TM) chains (A) or *Stat1* and *Irf9* transcripts (B). Data in (A) represent the average of 2 experiments; data in (B) represent the average of 3 independent experiments \pm SEM as indicated in Fig. 3. * denotes $p \leq 0.05$ comparing microglia to oligodendroglia at each timepoint; # indicates $p \leq 0.05$ compared to basal levels for each cell population. 27
8. Delayed induction of anti-viral ISG in oligodendroglia. Microglia and oligodendroglia from naïve or JHMV infected mice were assayed for *Pkr*, *Oas2*, *Adar1*, and *Ifit2* transcripts as indicated in Fig. 3. Data represent the average of 3 separate experiments \pm SEM. * denotes

$p \leq 0.05$ comparing microglia to oligodendroglia at each timepoint; # indicates $p \leq 0.05$ compared to basal levels for each cell population. 29

9. Kinetics of CNS IFN α/β responses to Poly (I:C). Wt mice were injected intracranially with 200ug poly (I:C) to assess kinetics of Ifn β , Ifn $\alpha 4$, Ifit1, and Ifit2 mRNA induction in spinal cords. Data represent the mean \pm SEM for 3 mice per group; # indicates $p \leq 0.05$ compared to basal levels 30

10. Distinct in vivo responses of oligodendroglia and microglia to poly (I:C). Microglia and oligodendroglia purified from spinal cords at 4 or 12 hours post poly (I:C) injection were analyzed for expression of Ifn $\alpha 4$, Ifn β , Mda5, Rig-I, *Ikk ϵ* , *Irf7*, *Ifit1*, and *Ifit2* transcripts. Data are representative of two independent experiments each with 10 pooled mice per experiment. 32

11. Model for differential innate glia responses to JHMV infection..... 37

12. PKR deficiency resulted in reduced expression of NFkB induced pro-inflammatory genes, but does not alter IFN α/β dependent antiviral genes. Expression of NFkB and IFN α/β induced genes were determined using Real time PCR analysis. (A) Expression of *Ifn α/β* and dependent genes *Ifit1* and *Ifit2* from spinal cord of PKR $^{-/-}$ mice and wt mice. (B). Expression of selected NFkB dependent genes, *Il1 β* , *Il6*, *Tnfa*, *Ccl2*, *Ccl5*, and *Cxcl10* relative to *Gapdh* in spinal cords of PKR $^{-/-}$ and wt mice. Data is represented as average of n = 3 mice/ group/ time-point \pm standard error mean (SEM).* $p \geq .05$ 46

13. Virus replication in PKR^{-/-} mice is enhanced during early phase of infection but clear with similar kinetics as wt mice. Virus replication in brain was determined by plaque assay on brain supernatants at indicated time-points post infection. Data is re represented as average of n = 3 mice/ group/ time-point ± standard error mean (SEM). (n = 9 mice/group/time-point).Viral RNA was determined in spinal cords relative to *Gapdh*. * p ≥ .05. 47
14. Increased number of infiltrating T cells to the CNS in PKR^{-/-} mice. Number of infiltrating, Total lymphocytes (CD45hi), macrophages (CD45hi F4/80+), CD8 T and CD4 T cells derived from the brain of infected wt and PKR^{-/-} mice was determined using flow cytometric analysis. Data is average of three separate experiments ± standard error mean (SEM). (n = 9 mice/group/time-point). * p ≥ .05. 48
15. Trafficking of lymphocytes from perivascular space to CNS parenchyma is influenced in PKR^{-/-} mice compared to wt mice. (A) Cross-sections of spinal cords at day 10 p.i. were stained for Hematoxylin and Eosin (H & E). Enhanced perivascular inflammation is consistent with increased T cell accumulation by flow cytometric analysis. Data is representative of three separate experiments. (B) Accumulation of CD4 T cells in the perivascular space was determined using staining spinal cord sections with CD4 and laminin in PKR^{-/-} mice relative to wt mice. Staining of CD and laminin indicates the perivascular accumulation of CD4 T cells. Data is representative of n =

3 mice/ group at day 10 p.i. Quantification of frequency perivascular CD 4 T cells within total infiltrating Cd \$ T cells is presented as graph form. Data is average of total 15 sections between n = 3mice/group/time-point \pm SEM. (C) Expression of activated PKR in infiltrating CD4 T cells to the CNS was determined by double staining spinal cord sections for PKR-p and CD4 in wt mice. Data is representative of n = 3mice/group at day 7 p.i. * p \geq .05..... 50

16. CD4 T cell function is specifically affected in PKR-/- mice relative to wt mice. (A) Effector function of CD4 T cells was assessed by measuring mRNA expression of cytokines mainly produced by CD4 T cells following JHMV infection (high IFN γ , high IL10 and IL21). Data is represented as average of n = 3 mice/group/time-point \pm SEM. (B) Ability of CD8 and CD4 T cells to produce IFN γ and IL10 was determined using intracellular cytokine assay in splenocytes after stimulation with CD * and CD4 specific peptides, S510 and M133, respectively. Frequency of IL10 producing CD4 T cells is presented as representative flow graph and data is also quantified as average of n = 3/group \pm SEM. Reduced effector functions associated primarily with CD4 T cells suggests reduced IL10 may contribute to enhanced pathology. * p \geq .05..... 52

17. Demyelination but not axonal damage increased in PKR-/- mice. The extent of demyelination was determined by staining cross sections of

- spinal cord with Luxol fast Blue (LFB) from wt and PKR^{-/-} mice at day 10 p.i. Data is representative of three separate. 54
18. Clinical disease and mortality is not altered in absence of PKR. (Clinical disease and survival rate between wt and PKR^{-/-} mice was determined following intracranial JHMV infection. Data is representative of three separate (n ≥ 15 mice/group/time- point ± SEM)+ 54
19. Dually deficient mice in PKR and RNaseL (DRP^{-/-}) demonstrated high virus titers but overall similar phenotype as RNaseL^{-/-} mice. (A) Following intracranial JHMV infection, clinical scores and survival rate were determined between wt and DRP^{-/-} mice. Data is representative of three separate (n ≥ 15 mice/group/time-point ± SEM. (B) Virus replication in the CNS of wt and DRP^{-/-} mice following JHMV infection. Data are mean of n = 9 mice/group/time-point from three independent experiments ± SEM. And (C) Flow cytometric analysis of bone marrow derived CD45^{hi} infiltrating lymphocytes within the CNS following JHMV infection. Total number of CD8 and CD4 T cells isolated from the brains of infected mice. Data represents mean from three independent experiments ± SEM. * p ≥ .05. 56
20. Dual deficiency of PKR and RNaseL reverses PKR mediated reduction in expression of NFκB induced pro-inflammatory genes. Expression of NFκB induced genes Il6, Tnfα, Ccl5, and Cxcl10 were determined relative to *Gapdh* in spinal cords of DRP^{-/-} mice relative to wt mice,

using real time PCR analysis. Data is represented as average of n = 3 mice/group/time-point \pm SEM..... 57

21. JHMV infection induces Il12p40 expression within the CNS.
 Expression of Il12p40, Il12p35, and Il23p19 mRNA in the CNSs of JHMV infected mice at various time p.i. The data reflect induction relative to Gapdh, using the following formula: $(2^{[CT \{GAPDH\} - CT \{Target\}]}) \times 100$, where C_T is the threshold cycle. The data are the means of three mice per time point \pm the standard error mean (SEM). (Kapil et al., 2009)..... 68

22. IL12 deficiency decreases the symptoms of virus-induced encephalitis. JHMV infected p40^{-/-}, p35^{-/-}, and p19^{-/-} mice were examined for disease severity at various times p.i. The data are representative of two separate experiments for each strain with n>20 per experiment \pm SEM. * p \leq 0.05 (compared to wt). (Kapil et al., 2009)..... 69

23. IL12 does not influence control of infectious virus. Virus replication in the CNS of p35^{-/-} and wt mice following JHMV infection. The data are representative of two independent experiments and show the mean of four individual mice per time point \pm SEM. (Kapil et al., 2009)..... 70

24. Decreased CD4 T cell recruitment into the CNS of p35^{-/-} mice. (A) Flow Cytometric analysis of bone marrow derived CD45hi infiltrating cells within the CNS following JHMV infection. Total numbers of CD8 T cells (B) and CD4 T cells (C) isolated from the brains of infected mice.

- The Data represent the mean of three independent experiments \pm SEM. (Kapil et al., 2009)..... 72
25. IL12 enhances IFN γ production and Class II expression. Frequencies of CNS derived IFN γ secreting T cells at day 7 p.i. (A) CD8 T cells following stimulation with S510 peptide and (B) CD4 T cells with M133 peptide. Data are representative of two separate experiments analyzing cells combined from n = 4-6 individuals (C) Number of CNS derived CD4 T cells producing IFN γ after ex vivo peptide stimulation in infected wt and p35 $^{-/-}$ mice at days 7 and 10 p.i. Data represent the mean of two independent experiments \pm SEM. (D) Frequencies of CLN derived IFN γ secreting CD4 T cells at day 7 p.i. following stimulation in presence or absence of M133 peptide. Data are representative of two separate experiments analyzing cells combined from n = 4-6 individuals (E) IFN γ dependent MHC class II expression on CD45 lo microglia (boxed cells) at days 7 and 10 p.i. (F) Cell free homogenates of the infected CNS were examined for IFN γ by ELISA. Data show the mean of n= 4 per time point \pm SEM and are representative of two separate experiments. Asterisks indicate statistical significance $p \leq 0.05$, compared to wt. (Kapil et al., 2009) 74
26. IL12 and IL23 do not influence viral pathogenesis. Longitudinal sections of spinal cords from JHMV infected wt, p35 $^{-/-}$ and p19 $^{-/-}$ at day 10 p.i. The extent of demyelination as shown by luxol fast blue (LFB). Viral antigen (arrows) detected by immunohistochemical

analysis for viral nucleocapsid using mAb J.3.3. Bar = 200 microns.

(Kapil et al., 2009)..... 76

27. IL12 alters the expression of pro-inflammatory and anti-inflammatory cytokines. Brains from infected wt and p35^{-/-} mice were compared for mRNA expression of pro-inflammatory cytokines (A) *Il1 β* , *Il6* and *Tnf α* ; chemokines (B) *Cxcl10*, *Cxcl9* and *Ccl5* and the anti-inflammatory cytokines (C) *Tgf β 1* and *Tgf β 3* by real time PCR. Expression levels were normalized to *Gapdh* using the following formula: $(2^{[CT\{GAPDH\} - CT\{Target\}]}) \times 1000$, where Ct is the threshold cycle. Data represent the mean of three mice per time point \pm SEM. (D) IL10 levels in brains of infected wt and p35^{-/-} mice determined by the ELISA. Data are representative of two experiments (n = 4 per time point) \pm SEM. BD = below detection. Asterisks indicate statistical significance $p \leq 0.05$, compared to wt. (Kapil et al., 2009) 79
28. Kinetics of CD45^{hi} F4/80⁺ macrophage, and CD45^{lo} F4/80⁺ microglia in the CNS following JHMV infection. Representative density plots of CNS derived cells stained with CD45 and F4/80 at day 3, 5, 7, and 10 p.i. CNS-infiltrating cells contain a prominent population of CD45^{hi} F4/80⁺ macrophages early during the infection, while microglia are represented as CD45^{lo} F4/80⁺ cells. The data represents three separate experiments at each time point, combining cells from 3-4 mice/time point/experiment. 93

29. Kinetics of viral RNA in macrophage and microglia. Viral mRNA comprising N-protein encoding sequences was measured in microglia and macrophage populations isolated from brains of JHMV infected C57/Bl6 mice using real time PCR. Numbers depict mRNA levels relative to the house keeping gene GAPDH using the following formula $(2^{[C_T - C_T\{target\}]}) \times 1000$, where C_T is the threshold cycle. The data represent the average values of pooled cells from 5-6 mice of three individual experiments \pm SEM..... 94
30. Activation of microglia/macrophages early during JHMV infection. Comparison of transcript levels for the pro-inflammatory cytokine *Il12p40* and anti-inflammatory factors *Il1Ra* and *Ym1/2* in microglia and macrophages isolated from brains of C57BL/6 mice following JHMV infection. Data are all relative to *Gapdh* as described in Fig. 29. Data for *Il12p40* and *Il1Ra* is average of two separate experiments \pm SEM. The data for *Ym1/2* is derived from a single experiment. Data is from pooled cells from 5-6 mice per time-point. 96
31. Kinetics of cytokine expression known to polarize distinct microglia/monocyte activation states. Protein levels of the pro-inflammatory cytokine IFN- γ was measured using ELISA and are represented as ng/brain (n=9 mice/time-point). Anti-inflammatory cytokines IL-13 and IL-10 were measured at the transcriptional level using real time PCR (n=6 mice/time-point). Data are represented as

- relative to GAPDH as depicted in Fig. 29. Values represent the average of three separate experiments \pm SEM..... 99
32. Upregulation of mRNA characteristic of M1/M2. Microglia and macrophages were isolated from infected mice by FACS and RNA analyzed for IFN γ mediated upregulation of iNos as a representative M1 specific factors and *Arg1* as a typical M2 specific factor. Expression relative to *Gapdh* was determined by real time PCR. The data represent the average values of pooled cells from 5-6 mice of three individual experiments \pm SEM..... 101
33. Phagocytic activity of macrophages and microglia is increased as virus is controlled. Phagocytic ability of microglia and macrophages was determined by incubating percol gradient purified brain cells with fluorescein (494/518) labeled E coli particles (E2861) at 5 MOI (5 particles per one cell) at day 7 and day 10 p.i. The data is representative of two separate experiments. Cells were pooled together from 2-3 mice/time-point/experiment. 102
34. Upregulation of IL1R antagonist mRNA in microglia and macrophage is IFN $\alpha\beta$ dependent. (A) *Ifn α* and *Ifn β* transcripts in FACS purified microglia and macrophages were determined using real time PCR. Data represent the average of three separate experiments \pm SEM. (B). *Il1ra* transcript levels were determined in both microglia and macrophage isolated by FACS from IFNAR $^{-/-}$ and wt mice following JHMV infection. The data is from a single experiment. All data is

presented as relative to *Gapdh*. Cells were pooled together from 5-6
mice/time-point/experiment..... 104

LIST OF TABLES

5.1.	Functional Heterogeneity of Macrophages	89
7.1.	Antibodies Utilized in Flow Cytometry.....	118
7.2	Classification of Cell Types for Identification by Flow	119
7.3	List of Primer Sequences/Catalog Number for Genes Utilized in the Study.....	126

CHAPTER I

INTRODUCTION

Various RNA and DNA viruses can infect the Central nervous system (CNS) and pose a serious threat as they can induce many different pathological outcomes such as encephalitis, meningitis, and demyelination. Viruses can affect CNS homeostasis in two ways; 1. They can directly infect and destroy CNS resident cells leading to neuronal damage, 2. The immune response to the virus can mediate damage to the CNS (Griffin, 2003). Neurotropic viruses generally invade the host through peripheral routes, but can enter the (Lipton et al., 2007) CNS by axonal spread or through the hematogenous route either as free virus or by transport in infected cells. Once viruses enter in the CNS, infected cells can mount a local innate immune response, which recruits peripheral immune responses to control the virus. However, due to the unique physiological and immune features of the CNS discussed below, viruses often evade the immune system and establish persistent or latent infection. Persistent infection in the CNS can be kept under control by the immune system in the absence of overt clinical symptoms. However, immune suppression or dysregulation may lead to loss of viral control resulting in fatal damage to the CNS. Viruses that can

infect the human nervous system include Herpes Simplex Virus-1 (HSV-1), Human Cytomegalovirus (HCMV), West Nile Virus (WNV), Poliovirus, Measles virus, Rabies virus, Human Immunodeficiency virus (HIV) etc (McGavern and Kang, 2011).

1.1 Host Barriers and Innate Immune Responses Associated With CNS Infection

Controlling virus infections in the CNS is a complicated task for the host because of the potentially damaging consequences of immune responses. Damage to non-renewable cells of the CNS is associated with increased permeability of vascular endothelium and influx of inflammatory cells releasing proteolytic enzymes and pro-inflammatory molecules, which can mediate cytotoxicity. Not surprisingly, therefore, the CNS is structurally protected by meningeal coverings and the blood brain barrier to minimize invasion of micro-organism as well as peripheral leukocytes. Furthermore, limited expression of major histocompatibility (MHC) molecules on CNS resident cells and absence of dedicated lymphatic drainage system (Galea et al., 2007) make it difficult to initiate adaptive immune responses. Overall, these features protect non-renewable CNS resident cells from infection as well as an overly active immune system. Furthermore, local production of the anti-inflammatory cytokine TGF β and neurotrophins, as well as interactions between microglia and neurons through maintain an anti-inflammatory environment in the CNS (Hoek et al., 2000, Johnson et al., 1992, Neumann et al., 1998).

Nevertheless, following infection CNS resident cells quickly initiate expression of innate immune molecules. Glial cells can recognize an array of molecular patterns associated with micro-organisms (PAMPs) and endogenous danger signals (DAMPs) through receptors collectively known as Pathogen Recognition Receptors (PRRs) (Piccinini and Midwood, 2010, Hanke and Kielian, 2011). Signaling via PRRs leads to induction of a variety of innate inflammatory cytokines, type-1 Interferons ($IFN\alpha/\beta$), chemokines. Rapid production of $IFN\alpha/\beta$ slows virus replication and constrains dissemination prior to emergence of virus specific adaptive immune responses. Furthermore, PRRs such as Toll like receptors-3 (TLR3) and $IFN\alpha/\beta$ induced protein kinase RNA dependent (PKR), can induce NF κ B pathway, resulting in expression of a variety of pro-inflammatory genes (Alexopoulou et al., 2001). Although the pattern and magnitude varies with specific virus infection and the cell type infected, the most commonly induced factors are IL1, IL6, IL12, TNF α , CCL2, CCL5 and CXCL10 (Griffin, 2003). Furthermore, up-regulation of pro-inflammatory genes triggers the recruitment of leukocytes to the CNS (Engelhardt and Ransohoff, 2005, Griffin, 2003). Lymphocytes are activated in the periphery and restimulated by CNS resident cells presenting viral antigen. However, the pattern of pro-inflammatory molecules within the CNS can influence the pattern and magnitude of T cell cytokine expression. Anti-inflammatory molecules, such as IL10, TGF β further limit the noxious effect of CNS inflammation to prevent tissue damage. IL10 primarily acts to suppress macrophages and DC function by inhibiting expression of MHC class II and co-stimulatory molecules such as CD80/CD86 and

production of proinflammatory cytokines and chemokines, including IL12 (Mosser and Zhang, 2008). The successful outcome of an infection thus relies on fine-tuning between pro- versus anti-inflammatory responses to control the infection while minimizing tissue damage.

1.2 Activation of CNS Resident Cells Following Viral Infection

Two types of PRR that recognize RNA viruses include endosomal receptors, Toll Like receptors (TLRs) and cytoplasmic receptors, Retinoic acid inducible gene-I (RIG-I) like receptors (RLRs, MDA5 and RIG-I). Microglia and astrocytes are the most prominent cell types in CNS in producing a large array of cytokines and chemokines. Microglia are the CNS resident macrophages and act as immune sentinels in the CNS. Murine microglia expresses all TLRs (TLR 1-9) at basal levels (Bsibsi et al., 2002, Olson and Miller, 2004). Activation of microglia by various exogenous and endogenous TLR ligands contributes to their either neuroprotective or neurotoxic phenotype. Primary murine astrocytes also express a wide variety of TLRs at basal levels, however at lower amounts than microglia. Specifically, robust expression of TLR3 in astrocytes under physiological conditions indicates their responsiveness against viral infections. (Bsibsi et al., 2006, Carpentier et al., 2005, Suh et al., 2009). Neurons and oligodendroglia can also express/induce a more limited array of TLRs; however, their role in induction of innate immune response following CNS infection is not well defined (Bsibsi et al., 2002, Suh et al., 2009). These studies indicate that activation of innate immune responses in the CNS is not homogeneous but rather tailored according to cell type and environmental cues (figure 1).

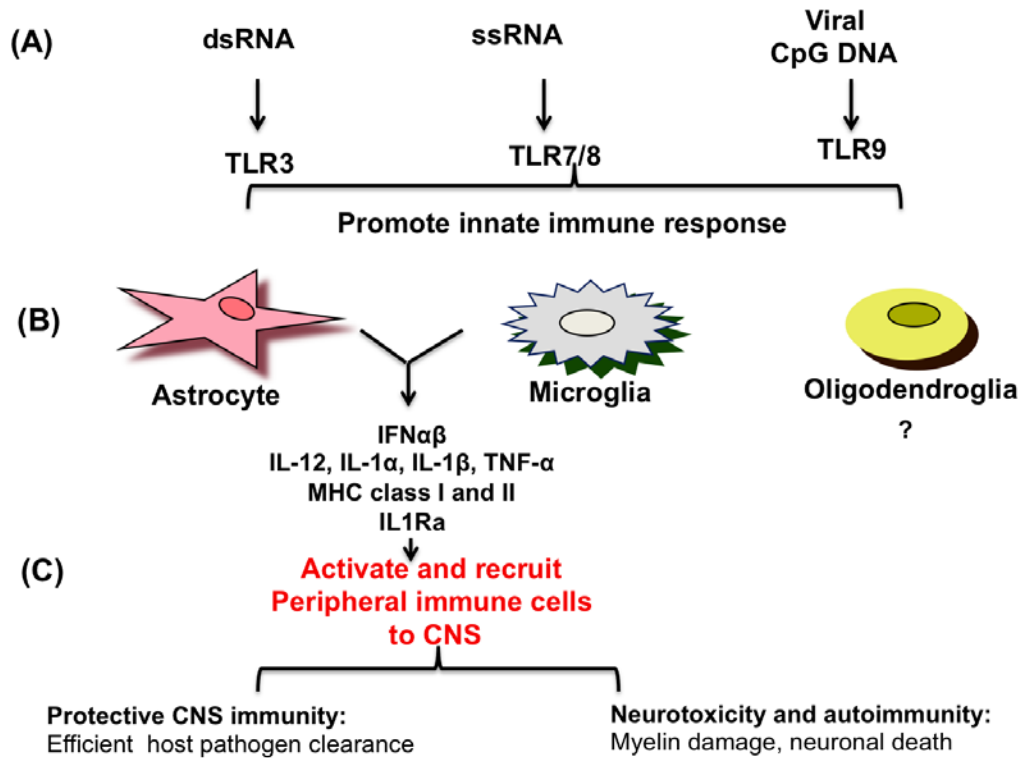


Figure 1. Role of TLR Signaling in Glial Cells Following CNS Infection (adapted from Carpentier et al., 2008). (A) Virus recognition, (B) Glial Cell Activation, (C) Recruitment and Activation of Peripheral Cells.

Error! No text of specified style in document.

1.3 Experimental Models to Study Immune Responses in CNS

Due to limitations in obtaining CNS samples to study human viral CNS infection, several experimental viral models have been developed to understand mechanism regulating immune responses in the CNS. Among infections associated with demyelination are Theiler's murine encephalomyelitis virus (TMEV) infection and neurotropic coronavirus infection. TMEV causes persistent infection in microglia and macrophage; infected microglia induce production of various innate and co-stimulatory molecules and were able to efficiently process and present virus and myelin epitopes to infiltrating CD4 T cells (Olson et al.,

2001). Furthermore, administration of IFN β resulted in reduced infiltration of myelin specific CD4 T cells and reduced demyelination, which was associated with increased expression of the anti-inflammatory cytokine IL10 in the CNS (Olson and Miller, 2009). Similarly, Stimulation of TLRs on glial cells by Herpes Simplex Virus-1 (HSV-1), induces IFN α/β , IL15, TNF α and CCL2 expression (Conrady et al., 2010). IFN α/β mediates anti-viral effects by inducing proteins such as RNaseL and Protein Kinase R (PKR) (Samuel, 2001). In addition, the absence of IL10 prevents the severity of inflammatory responses caused by HSV-1 (Dakhama et al., 2009). Furthermore, treatment with both IFN β and IL10 in mice infected with HSV-1 resulted in suppression in virus spread and prevented corneal inflammation (Minagawa et al., 1997).

These models indicate that the pattern of innate immune responses induced by various viruses is critical in dictating the outcome of an infection. To better understand the role of individual resident glia cells in mounting innate immune response and shaping the adaptive immune response in the CNS, we utilized murine gliatropic coronavirus CNS infection as a model of virus-induced encephalomyelitis.

1.4 Coronavirus (JHMV) Mouse Model to Study Encephalitis and Demyelination in CNS

Coronaviruses (CoV) are the largest positive sense single stranded RNA viruses (27-32kb genome). These belong to the group Nidovirales (nedo means nested in latin) which are characterized by their production of a nested set of mRNA with common 3' end to express various viral gene products (Figure 2

MHV replication cycle). Virions are composed of four structural proteins namely spike protein (S), enveloped protein (E), membrane protein (M) and nucleocapsid protein (N) coated genome (Figure 2). The virus assembles in the Golgi Body and accumulates in cytoplasmic membrane-bound vesicles which subsequently fuse with the plasma membrane resulting in virus exocytosis (Masters, 2006).

Coronaviruses are the cause of 1/3 of common colds. While primarily infecting the respiratory tract, coronaviruses have also been reported to cause CNS infection (Bonavia et al., 1997, Yeh et al., 2004, Xu et al., 2005). The biggest outbreak of coronavirus (Severe Acute Respiratory Syndrome-coronavirus (SARS-CoV)) infection was reported in 2002-2003 near Hongkong, which soon spread to 23 countries claiming 916 lives (WHO, retrieved 2008- 10- 13). With the exception of SARS CoV, human coronavirus infections have not received much attention due to their benign disease course. However, murine coronavirus infections of their natural rodent hosts are excellent models to study acute hepatitis, respiratory disease and encephalomyelitis associated with persistence. Specifically a virus variant of the neurotropic John Howard Muller strain of coronavirus (JHMV) has prominently been used to study control of virus replication in the CNS and immune mediated demyelination. The monoclonal antibody (mAb) selected variant of JHMV designated V2.2-v1 (characterized by point mutation and deletion in spike protein), used throughout in this study is gliatropic virus. Following intracranial inoculation virus initially replicates in ependymal cells and spreads to microglia, astrocytes, and oligodendroglia. Neurons are rarely infected. Infectious virus in the CNS peaks at day 5 post-

infection (p.i.), but is generally controlled by day 21 p.i. in a T cell dependent manner (Bergmann et al., 2006).

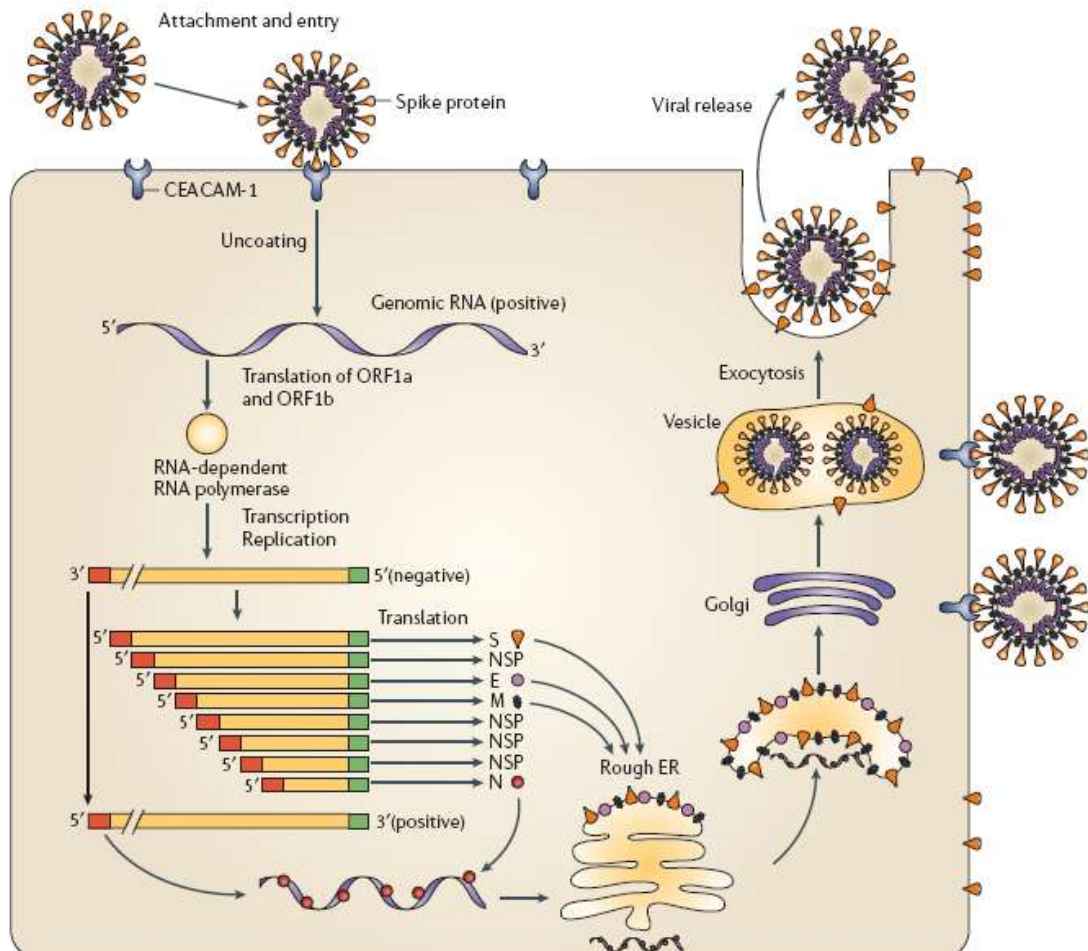


Figure 2. Mouse Hepatitis Virus (MHV) Replication (Bergmann et al.,2006).

Virus replication leads to activation of glial cells and expression of cytokines/chemokines that contribute to disruption of the blood brain barrier (BBB) integrity. The influx of T cells is associated with signs of encephalitis that can be observed ~7 days post infection (p.i.) (Fleming et al., 1986). Infiltrating T

cells control infectious virus, although viral antigen and RNA can be detected for the life of the rodent (Bergmann et al., 2006).

1.5 Role of Immune Response Following JHMV: Virus Clearance versus Pathogenesis

1.5.1 Innate immune response following JHMV and their interaction with adaptive immune response

Innate immune response in the CNS: JHMV infection initiates rapid induction of pro-inflammatory chemokines and cytokines. Early expression of CXCL1 and CCL2 is linked to CNS infiltration of neutrophils and macrophages, respectively. Macrophages constitute the major part of total early infiltrates at day 3, 5, and 7 p.i. Furthermore, abrogation of chemokines, CXCL1, CCL2, CCL5 and CXCL10 has been reported to prevent infiltration of T cells to the CNS (Liu et al., 2001, Glass et al., 2004, Hosking et al., 2009, Savarin et al., 2010). Similarly, JHMV infection induces pro-inflammatory cytokines such as IL1 β , IL6, IL12, TNF α , iNOS (inducible form of nitric oxide synthase) (Parra et al., 1997, Rempel et al., 2005). Upregulation of these pro-inflammatory cytokines even in absence of cellular infiltrates indicates a direct response of CNS resident cells to JHMV. All these cytokines are involved in enhancing leukocyte infiltration to the CNS, but can also induce apoptosis. IL12 drives the differentiation of naïve CD4 T cells towards IFN γ producing Th1 cells. Treatment with recombinant IL12 has been shown to protect from lethal hepatotropic mouse hepatitis virus (MHV) in C57Bl/6 mice, but not in IFN γ R $^{-/-}$ mice indicating IFN γ dependent protective role of IL12 during hepatitis (Schijns et al., 1996). *To evaluate the specific role of IL12*

following JHMV infection in CNS, we utilized mice deficient in IL12 only (p35^{-/-} mice), mice deficient in IL23 only (p19^{-/-} mice), and mice deficient in both IL12 and IL23 (p40^{-/-} mice) as described in chapter 4.

Interferons (IFNs): Initially coronavirus were thought to not to induce IFN α/β production. However, the importance of IFN α/β signaling in controlling viral dissemination became apparent *in vivo* following peripheral as well as CNS infection of mice deficient in type-1 IFN receptor (IFNAR^{-/-}) (Ireland et al., 2008, Cervantes-Barragan et al., 2007). The absence of classical IFN α/β producing “plasmacytoid dendritic cells (pDCs)” in the CNS emphasize the importance of the ability of CNS resident cells to produce IFN α/β (Serafini et al., 2000). Very recently, *in vitro* and *ex vivo* studies indicate that microglia/macrophage, dendritic cells, and oligodendroglia (N20.1 cell line) can produce IFN α/β following CNS as well as peripheral MHV (coronavirus) infection (Rose and Weiss, 2009, Roth-Cross et al., 2008, Li et al., 2010). However the response of fully differentiated oligodendroglia compared to microglia *in vivo* following virus infection has not been studied. *Thus, chapter 2 focuses on induction of IFN α/β and its response in microglia versus oligodendroglia in CNS following viral infection.*

IFNs play a very important role following infection, not only by inducing antiviral genes (RNaseL, Protein Kinase RNA dependent (PKR)), but also by regulating immune response via the induction of antigen presentation molecules (MHC class I and classII), pro-inflammatory genes (IL12p70, IL6, iNOS) as well as anti-inflammatory genes (IL1 receptor antagonist, IL10). We previously reported a noncanonical role of the antiviral gene RNaseL following JHMV

infection. This study indicated that while RNaseL does not contribute to overall virus replication but rather affects virus control in macrophages and microglia following CNS infection. Furthermore, RNaseL^{-/-} mice exhibited accelerated and severe demyelination and axonal damage compared to wt mice (Ireland et al., 2009). To further understand the downstream mechanism of IFN α/β mediated anti-viral response, we evaluated the role of another well-studied anti-viral gene; PKR in JHMV mediated CNS infection. *Chapter 3 focuses to understand the role PKR in virus replication as well as in modulating pro- and anti-inflammatory cytokines.*

1.5.2 Adaptive immune response

Both T cell mediated as well as humoral immune responses are pertinent to the control of JHMV infection at multiple levels.

Virus Control: The inability of irradiated mice to clear virus following JHMV infection emphasizes the importance of both T as well as B cells. Antigen specific CD8 T cells contribute a major part in controlling infectious virus from the CNS (Bergmann et al., 1999, Bergmann et al., 1993, Castro and Perlman, 1996, Stohlman et al., 1995). CD8 T cells control virus replication in different cell types using different effector mediators; virus is controlled in astrocytes and microglia by perforin dependent cytotoxicity, while IFN γ secretion is important in controlling virus replication in oligodendroglia (Bergmann et al., 2003, Bergmann et al., 2004, Gonzalez et al., 2006, Parra et al., 1999). CD4 T cells also contribute to virus control by supporting CD8 T cell function and directly affecting virus replication (Savarin et al., 2008, Stohlman et al., 2008). While T cells are indispensable in

controlling virus replication, however, virus specific antibodies provide protection from recurrence of infectious virus during persistence (Lin et al., 1999).

Pathology: One of the hallmarks of JHMV infection is demyelination. Demyelination was originally thought to be due to cytolytic infection of oligodendroglia. However, the absence or sparse demyelination in SCID or irradiated mice despite high oligodendroglia infection suggests a contribution of adaptive immunity (Wang et al., 1990, Houtman and Fleming, 1996). Restoration of demyelination after transfer of spleen as well as purified T cells supports a role of T cells in destruction of myelin (Houtman and Fleming, 1996, Fleming et al., 1993).

1.5.3 Anti-inflammatory response

Suppression of infectious virus progresses to persistent infection accompanied by chronic ongoing demyelination following JHMV infection (Weiner, 1973). The inability to completely eliminate viral antigen and RNA suggests an important role of anti-inflammatory responses designed to preserve CNS function at the expense of virus persistence. During acute JHMV encephalomyelitis anti-inflammatory cytokines IL10 and IL4 are upregulated with the same kinetics as pro-inflammatory cytokine IFN γ and TNF α (Parra et al., 1997). Lack of IL10, but not IL4 resulted in increased morbidity/mortality without altering virus clearance (Lin et al., 1998). Furthermore, a reengineered JHMV strain to produce IL10 confirmed a protective role of IL10. Increased IL10 production resulted in reduced microglial activation, expression of pro-

inflammatory cytokines and chemokines, infiltration of lymphocytes to the brain, and demyelination (Trandem et al., 2011).

The balance between pro- versus anti-inflammatory responses is critical to achieve effective viral control, but minimal tissue damage. Activation of microglia and macrophages play an important role following JHMV mediated CNS infections based on their role as primary innate responders. The plasticity of activated pro-inflammatory versus immunomodulatory microglia/macrophage thus raises an interest in their respective roles in downregulating the immune response as virus is controlled in the CNS. *In chapter 5 we explored the existence of pro as well as anti-inflammatory phenotypes across CNS resident microglia and infiltrating macrophages following JHMV infection.*

CHAPTER II

**OLIGODENDROGLIA ARE LIMITED IN TYPE I INTERFERON INDUCTION
AND RESPONSIVENESS *IN VIVO***

2.1 Abstract

Type I interferons (IFN α/β) provide a primary defense against infection. Nevertheless, the dynamics of IFN α/β induction and responsiveness by central nervous system (CNS) resident cells *in vivo* in response to viral infections are poorly understood. Mice were infected with a neurotropic coronavirus (CoV) with tropism for oligodendroglia and microglia to probe innate Antiviral Researchponses during acute encephalomyelitis. Expression of genes associated with the IFN α/β pathways were monitored in microglia and oligodendroglia purified from naïve and infected mice by fluorescent activated cell sorting. Compared to microglia, oligodendroglia were characterized by low basal expression of mRNA encoding viral RNA sensing pattern recognition receptors (PRRs), IFN α/β receptor chains, interferon sensitive genes (ISG), as well as kinases and transcription factors critical in IFN α/β signaling. Although PRRs, including CoV RNA sensing *Mda5*, and ISGs were upregulated by

infection in both cell types, the repertoire and absolute mRNA levels were more limited in oligodendroglia. Furthermore, although oligodendroglia harbored higher levels of viral RNA compared to microglia, *Ifn α / β* was only induced in microglia. Stimulation with the dsRNA analogue poly (I:C) also failed to induce *Ifn α / β* in oligodendroglia, and resulted in reduced and delayed induction of ISGs compared to microglia. The limited Antiviral Response by oligodendroglia was associated with a high threshold for upregulation of *Ikk ϵ* and *Irf7 transcripts*, both central to amplifying IFN α / β responses. Overall, these data reveal that oligodendroglia from the adult CNS are poor sensors of viral infection and suggest they require exogenous IFN α / β to establish an antiviral state.

2.2 Introduction

Type I interferons (IFN α / β) are critical innate cytokines that limit viral replication and dissemination prior to the emergence of adaptive immune responses. In addition to inducing an antiviral state, IFN α / β exert numerous other functions including induction of apoptosis, mobilizing innate cells, and regulating adaptive immune responses (Barton, 2008, Borden et al., 2007, Stetson and Medzhitov, 2006, Vilcek, 2006). As these pleiotropic effects can be detrimental if left unregulated, the innate Antiviral Response has to be controlled to minimize cell injury and maintain cellular homeostatic functions. Although an early IFN α / β response contributes to viral control and disease outcome, its precise regulation is especially critical in the central nervous system (CNS), where the health of non renewable neurons as well as resident glia is vital for the maintenance of host physiological function. IFN α / β production and signaling is

thus tightly regulated by both the basal and inducible expression of numerous factors involved in the IFN α / β pathway.

During viral infections the ability to induce IFN α / β is determined by activation of pattern recognition receptors (PRR) following interaction with pathogen associated molecular patterns, which typically constitute viral RNA or DNA structures. PRRs comprise members of the Toll-like receptor (TLR) family and the cytosolic helicase sensors, retinoic acid-inducible gene 1 (RIG-I) and melanoma differentiation-associated antigen 5 (MDA5) (Kawai and Akira, 2009, Mogensen, 2009) . PRR recognition of viral RNA triggers the activation and nuclear localization of interferon regulatory factors (IRF) IRF3 and IRF7 leading to IFN α / β induction. By binding to the IFN α / β receptor secreted IFN α / β initiates a signaling cascade leading to transcription of a variety of interferon sensitive genes (ISG). ISG encode both direct antiviral factors as well as PRR and signal transduction components, such as IRF7 and STAT1 (Borden et al., 2007). This amplification loop thus elevates the ability of cells to induce and respond to IFN α / β . In general IRF7 is considered the master switch in IFN α / β induction following various viral infections due to its role in amplifying IFN α / β production (Honda and Taniguchi, 2006). Since the pattern as well as levels of PRR, IRF and IFN α / β receptor expression and activation varies with each cell type, initial IFN α / β induction and amplification can be very distinct depending on the cell types infected (Colonna, 2007, Stewart et al., 2005). Furthermore, due to the potency of IFN α / β in inhibiting viral replication, many viruses have evolved mechanisms to antagonize the IFN α / β pathway, either at the induction or

signaling level (Levy and Garcia-Sastre, 2001, Sen, 2001). Microglia and astrocytes are primary sentinels within the CNS parenchyma responding to stimuli triggered by either microbial infection or degenerative events (Dong and Benveniste, 2001, Hanisch, 2002, Paul et al., 2007). This function is partially attributed to basal expression of a vast array of PRRs (Bsibsi et al., 2002, Carty and Bowie, 2011, Hanke and Kielian, 2011, Okun et al., 2009, van Noort and Bsibsi, 2009). *Irf3* mRNA and to a lesser extent *Irf7* mRNA, are constitutively expressed in the CNS. While *Irf7* expression is highly inducible, *Irf3* transcripts remain constant following infection (Ousman et al., 2005). However, their relative expression in different cell types has not been extensively explored. Consistent with PRR activation, microglia, astrocytes and neurons all induce IFN α/β (Paul et al., 2007). However, the vast majority of information on innate responses is derived from primary glia and neuronal cultures established from neonates and may not reflect responsiveness of fully differentiated cells. Distinct from *in vitro* studies, IFN α/β production *in vivo* is highly restricted as indicated by the small proportion (less than 5%) of infected neurons with detectable IFN α/β expression in mice infected with lymphocytic choriomeningitis virus (Delhaye et al., 2006). Furthermore, IFN α/β inducible *Irf7* transcripts mapped closely to sites of viral RNA (Ousman et al., 2005), supporting highly focal IFN α/β responses. Overall however, little is known about responsiveness of distinct CNS cell types to viral infections *in vivo*. Specifically oligodendroglia appears to express a limited TLR repertoire at basal levels compared to microglia (Hanke and Kielian, 2011,

Okun et al., 2009, Paul et al., 2007). They also do not appear to contribute to active proinflammatory cytokine secretion (Cannella and Raine, 2004).

Infection with the neurotropic mouse hepatitis virus (MHV) strain JHM (JHMOV), belonging to the positive strand RNA coronavirus (CoV) family, was used to better characterize the ability of oligodendroglia to mount innate antiviral immune responses *in vivo* based on its prominent infection and persistence in oligodendroglia (Bergmann et al., 2006). In adult mice JHMOV infection causes an acute encephalomyelitis, which resolves into a persistent infection of the spinal cord associated with demyelination. In addition to oligodendroglia, this virus also infects microglia and infiltrating macrophages during acute infection; however, neuronal and astrocyte infection is sparse (Ireland et al., 2008). CoV members are poor inducers of IFN α/β in numerous cell types due to their 5'RNA structures mimicking self RNA (Daffis et al., 2010, Zust et al., 2011). However, IFN α/β is induced in microglia, macrophages, and plasmacytoid dendritic cells (pDC) (Cervantes-Barragan et al., 2007, Roth-Cross et al., 2008). Importantly, a protective effect of IFN α/β *in vivo* was highlighted by uncontrolled MHV replication in mice deficient in IFN α/β signaling (Cervantes-Barragan et al., 2007, Ireland et al., 2008). Furthermore, protection following peripheral MHV infection is associated with TLR7 dependent IFN α/β production by pDC (Cervantes-Barragan et al., 2007). The naïve CNS is devoid of pDC (Serafini et al., 2000), implicating infected glia as primary candidates contributing to protective IFN α/β production following CNS infection. This is supported by MDA5 mediated IFN α/β production in infected microglia (Roth-Cross et al., 2008).

In the present study we compared the relative IFN α/β responsiveness of oligodendroglia and microglia following infection with JHMV or intracerebral inoculation of the double stranded (ds)RNA mimic poly (I:C). Both glia populations were isolated directly from the CNS to monitor changes in mRNA expression. The results are the first to imply an inherent block in IFN α/β transcription by oligodendroglia, coincided with limited expression of PRR and signaling molecules downstream of PRR activation. The dependence of oligodendroglia on IFN α/β from other cellular sources to induce an antiviral state *in vivo* highlight the potent monitoring functions of microglia and suggest a mechanism to preserve oligodendroglial homeostatic functions.

2.3 Results

2.3.1 Limited expression of PRR and signal transduction molecules in oligodendroglia

Induction of IFN α/β by murine CoV is mediated via TLR7 in pDC and via MDA5 in microglia/monocytes (Cervantes-Barragan et al., 2007, Roth-Cross et al., 2008). Furthermore, both MDA5 and RIG-1 act as PRR in an oligodendroglia cell line (Li et al., 2010). However, the expression of these viral sensors in oligodendroglia in the adult CNS is unknown. To analyze their capacity to initiate innate responses, oligodendroglia and microglia were isolated from spinal cords of uninfected PLP-GFP mice by FACS based on their respective CD45⁻ GFP⁺ and CD45^{lo/int} F4/80⁺ phenotypes (Malone et al., 2008). Spinal cords were used as donor tissue based on higher oligodendroglia yields compared to brains. The potential of mature oligodendroglia to recognize viral RNA in comparison to

microglia was assessed by comparing basal transcript levels of genes encoding the viral RNA sensors MDA5, RIG-I, TLR3, and TLR7 (Kawai and Akira, 2007). Whereas transcription of all four PRR was readily detected in microglia, *Mda5*, *Rig-I* and *Tlr3* transcripts were significantly reduced and *Tlr7* was below detection in oligodendroglia (Figure 3A). Basal levels of PRR mRNAs are low in the resting CNS relative to lymphoid tissue, with the exception of *Tlr3* (McKimmie et al., 2005). Nevertheless, PRR are rapidly upregulated during viral encephalitis initiated by Semliki Forest virus, Rabies virus, and Venezuelan Equine Encephalitis virus (McKimmie et al., 2005, Sharma and Maheshwari, 2009). However, the relative contribution of infiltrating leukocytes versus resident CNS cells was not directly assessed. Microglia and oligodendroglia were therefore isolated from JHMV infected mice to evaluate upregulation of PRRs during the course of infection. Microglia upregulated *Mda5*, *Rig-I*, *Tlr3* and *Tlr7* transcripts 2-5 fold over basal levels, with peak expression at days 3-5 post infection (p.i.) (Figure 3B). Relative to the modest fold increase in microglia, *Mda5* and *Rig-I* transcripts were vastly increased in oligodendroglia. *Rig-I* expression reached levels similar to microglia by day 3 p.i. mounting to an ~70 fold increase over naïve levels (Figure 3). Nevertheless, *Mda5* mRNA levels in oligodendroglia remained overall lower compared to microglia. Similarly, mRNAs encoding the endosomal PRR TLR3 and TLR7 were also induced in oligodendroglia; however, absolute levels remained low and the peak of expression was delayed relative to microglia. *Mda5* and *Rig-I* induction in oligodendroglia, as well as all RNA sensing PRR in microglia, correlated with induction of *Ifn α* and *Ifn β* mRNA

throughout days 3-5 p.i. in total CNS RNA following JHMV infection (Ireland et al., 2008, Malone et al., 2008).

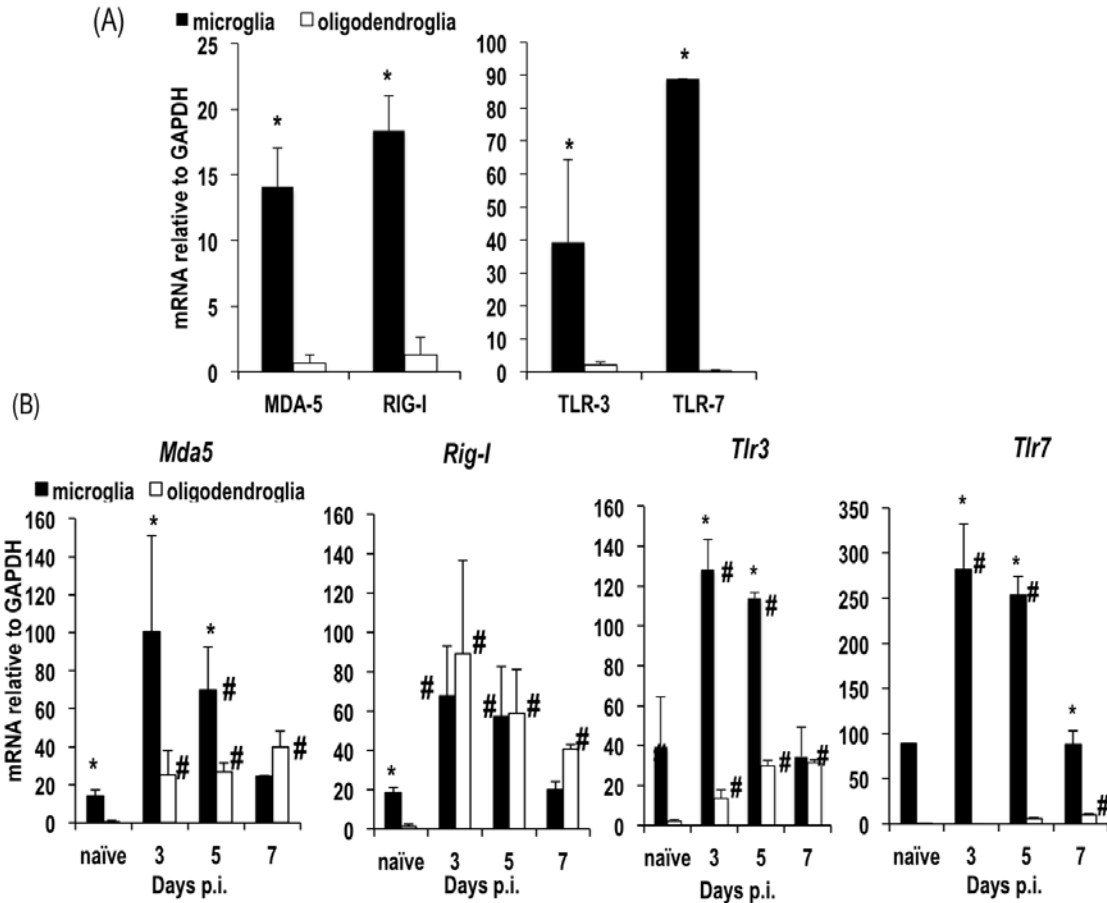


Figure 3. Oligodendroglia are limited in basal and inducible expression of viral RNA sensing PRRs. Microglia and oligodendroglia purified from spinal cords of naïve (A) or JHMV infected (B) PLP-GFP mice were assayed for *Mda5*, *Rig-I*, *Tlr3*, and *Tlr7* transcripts at the indicated times p.i. Data represent the average of 3 separate experiments \pm standard error of the mean (SEM). * denotes $p \leq 0.05$ comparing microglia to oligodendroglia at each timepoint; # indicates $p \leq 0.05$ compared to basal levels for each cell population.

To verify that the increase in PRR transcripts is directly attributed to IFN α/β signaling, mRNA expression was assessed in microglia and oligodendroglia from naïve and JHMV infected wt and IFNAR^{-/-} mice. Although *Mda5* and *Rig-I* mRNA levels were diminished by 8-9 fold in microglia from naïve

IFNAR^{-/-} relative to wt mice, they were only slightly reduced in oligodendroglia (Figure 4). These results are reminiscent of previous observations that PRR expression in neurons is controlled by basal IFN α/β signaling (Shrestha et al., 2003). Importantly, the absence of IFN α/β signaling abrogated upregulation of *Mda5* and *Rig-I* transcripts in both microglia and oligodendroglia following JHMV infection (Figure 4). Early induction of *Mda5* and *Rig-I*, both classified as ISG, thus demonstrated that oligodendroglia respond to exogenous IFN α/β *in vivo*, similar to microglia. IFN α/β thus enhances the potential to recognize invading RNA viruses, thereby facilitating early innate responses.

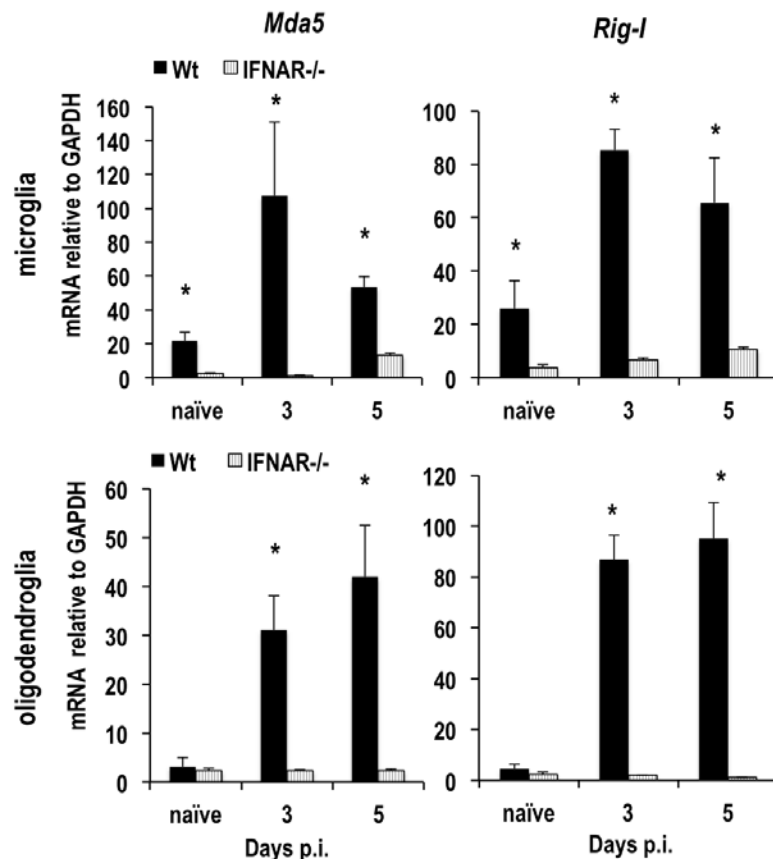


Figure 4. MDA5 and RIG-I upregulation is IFN α/β dependent. Wt and IFNAR^{-/-} mice infected with JHMV were used to compare induction of *Mda5* and *Rig-I* mRNA in oligodendroglia and microglia purified from spinal cords. Data are average of 3 individual experiments \pm SEM as described in Fig. 3. * denotes $p < 0.05$ comparing wt to IFNAR^{-/-} populations at each timepoint.

2.3.2 IFN α/β is not induced in oligodendroglia

IFN α/β signaling is crucial to prevent dissemination of gliotropic CoV within the CNS parenchyma (Ireland et al., 2008). Furthermore, IFN α/β induction in response to CoV infection has been demonstrated in microglia *in vitro* and *in vivo* (Roth-Cross et al., 2008) as well as in an oligodendroglial cell line (Li et al., 2010). Given the distinct basal and inducible levels of *Mda5* transcripts in mature CNS derived glial populations, the contribution of infected oligodendroglia and microglia to IFN α/β induction was assessed *in vivo* by comparing *Ifn β* and *Ifn α 4* mRNA relative to viral replication in each population. Viral loads were monitored by measuring viral mRNA encoding the N protein, the most abundant viral gene in infected cells (Skinner and Siddell, 1983). *JHMV-N* transcripts prevailed in microglia at day 3 p.i., but decreased by days 5 and 7 p.i. (Figure 5A). By contrast, although viral mRNA was near detection levels at day 3 p.i. in oligodendroglia, the levels increased ~20 fold relative to microglia by day 5 p.i. Despite subsiding by day 7 p.i., viral mRNA levels remained significantly elevated relative to microglia. These results not only assured that infected cells were recovered by the isolation procedure, but clearly indicated that virus predominated in microglia early, but subsequently prevailed in oligodendroglia. Concomitant with infection, sparse but detectable basal levels of *Ifn β* and *Ifn α 4* transcripts increased in microglia (Figure 5 B). *Ifn β* levels were sustained through day 5 p.i., while *Ifn α 4* levels were only transiently upregulated. The contribution of infiltrating infected monocyte derived macrophages (Ireland et al., 2009) to *Ifn α/β* induction was also assessed. Viral RNA loads in macrophages

were less than 50% of those in microglia and declined with similar kinetics; *Ifn α / β* transcripts reflected the magnitude of viral RNA transcripts similar to microglia (data not shown). By contrast, neither *Ifn α 4* nor *Ifn β* mRNA were detected in oligodendroglia from naïve or infected mice (Figure 5B), despite higher viral RNA loads as well as elevated *Mda5* and *Rig-1* mRNA expression at day 5 p.i. (Figure 4).

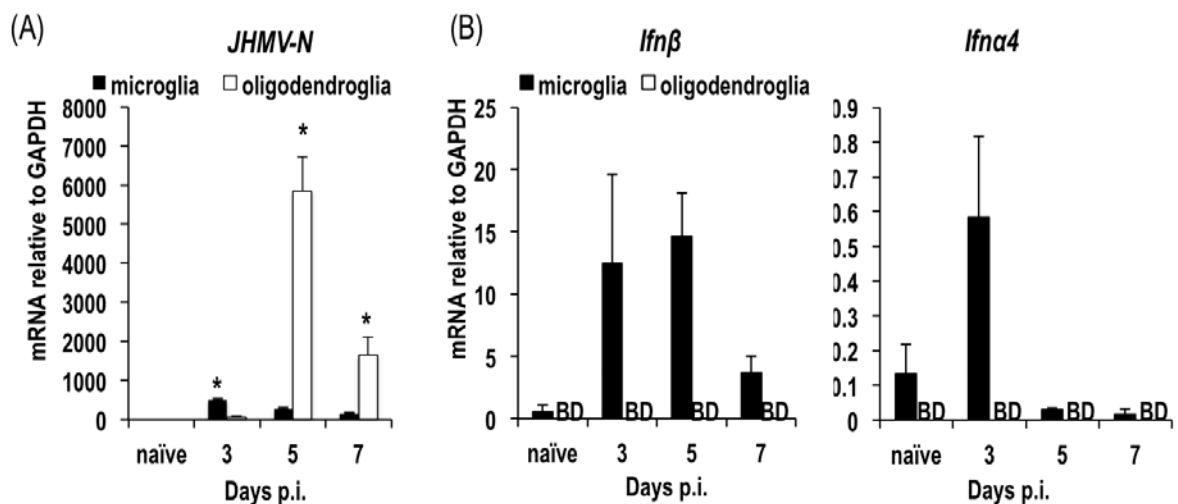


Figure 5. Oligodendroglia do not induce IFN α / β transcripts during JHMV infection. Microglia and oligodendroglia purified from spinal cords of naïve or JHMV infected PLP-GFP mice were assessed for (A) JHMV-N transcripts or (B) *Ifn β* and *Ifn α 4* transcripts. Data are average values \pm SEM of 3 independent experiments. BD indicates below detection. * denotes $p \leq 0.05$ comparing microglia to oligodendroglia.

The failure of oligodendroglia to induce *Ifn α / β* following infection suggested that MDA5 and RIG-I are not activated, and/or that downstream signaling factors are limiting. PRR signaling requires several mediators including the inducible kinase IKK ϵ (also known as Ikbke or Ikki) and the transcription factors IRF3 and IRF7. While IRF3 is constitutively expressed IRF7 is induced by IFN α / β and amplifies IFN α / β production (Honda and Taniguchi, 2006, Honda et al., 2005). Therefore to investigate the potential for PRR signaling,

oligodendroglia were examined for expression of mRNAs encoding IKK ϵ , IRF3 and IRF7. All three mRNAs were regulated in a cell type specific manner (Figure 6). Microglia from naïve mice expressed higher basal *Ikk ϵ* transcripts, which were modestly, but progressively upregulated throughout day 7 p.i. (Figure 6). By contrast *Ikk ϵ* induction was not detected in oligodendroglia until day 7 p.i., at which time levels reached those in microglia. *Irf3* mRNA was readily detected at basal levels in both microglia and oligodendroglia from naïve mice, but remained constant or even declined following infection (Figure 6). Lastly, *Irf7* transcripts were sparse in both microglia and oligodendroglia derived from naïve mice (Figure 6), consistent with lower basal CNS expression relative to *Irf3* (Ousman et al., 2005). However, in contrast to the induction of *Irf7* mRNA in microglia by day 3 p.i., induction was only modest and significantly delayed in oligodendroglia following infection (Figure 6). As the *Irf7* gene is an ISG, its upregulation in microglia was consistent with IFN α/β upregulation. By contrast, the delayed response in oligodendroglia implied more selective ISG induction and/or distinct IFN α/β receptor signaling thresholds.

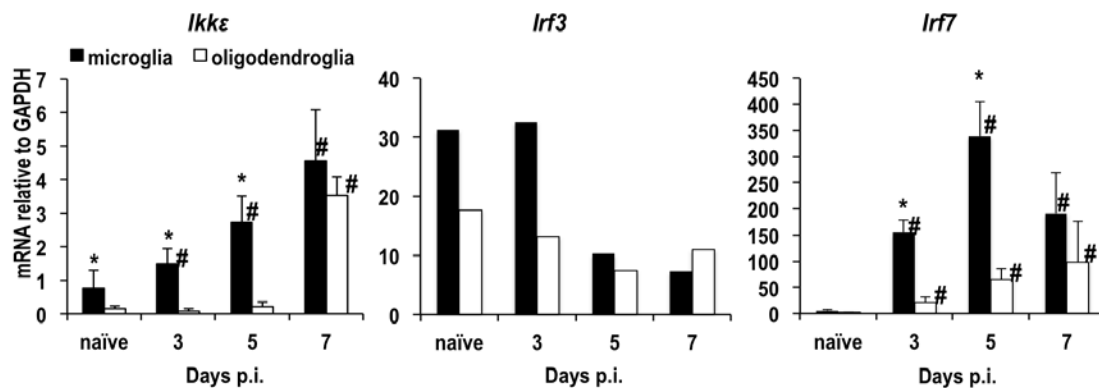


Figure 6. Oligodendroglia are limited in basal and inducible expression of PRR associated signaling factors during JHMV infection. Microglia and oligodendroglia from naïve or JHMV infected mice were assayed for *Ikk ϵ* , *Irf3* and *Irf7* transcripts as indicated in Fig. 3. Data represent the average of 3 separate experiments \pm SEM. * denotes $p \leq 0.05$ comparing microglia to oligodendroglia at each timepoint; # indicates $p \leq 0.05$ compared to basal levels for each cell population.

2.3.3 Oligodendroglia induce ISG delayed relative to microglia

Upregulation of the ISGs *Rig-I*, *Mda5*, *Tlr3* and *Irf7* support the notion that oligodendroglia respond to IFN α/β following infection. However, optimal induction was delayed and absolute levels were not as robust as in microglia. These results suggested that oligodendroglia are exposed to limiting amounts of IFN α/β in the microenvironment, or that they are intrinsically more limited than microglia in IFN α/β responsiveness. While the first possibility is difficult to address *in vivo*, the second may reflect reduced expression of the IFN α/β receptor (IFNAR) or downstream signaling components. We therefore assessed regulation of transcripts encoding the IFNAR, as well as STAT1 and IRF9, which act downstream of IFN α/β signaling. IFN α/β binds a common receptor complex consisting of two transmembrane proteins, IFNAR1 and IFNAR2. As IFNAR2 exists as a transmembrane and soluble isoform generated by alternative splicing (Domanski et al., 1995), we then examined basal expression patterns of IFNAR1, and both IFNAR2 isoforms in microglia and oligodendroglia. Basal mRNA levels of the *Ifnar1* chain were ~2fold higher in microglia compared to oligodendroglia. However, transcripts encoding both the soluble as well as the transmembrane form of *Ifnar2* were more than 5 fold higher in microglia compared to oligodendroglia (Figure 7A), suggesting more limited responsiveness of oligodendroglia to IFN α/β . *Stat1* and *Irf9* transcript levels were also elevated in microglia compared to oligodendroglia derived from naïve mice (Figure 7B). STAT1 is inducible by both IFN α/β and IFN γ , while IRF9 is constitutively

expressed in most non CNS cell types (Borden et al., 2007). Consistent with a response to IFN α/β *Stat1* mRNA indeed increased ~10-fold by day 3 p.i. and remained elevated until day 7 p.i. in microglia (Figure 7B). By contrast, a reduced capacity of oligodendroglia to respond to IFN α/β was supported by the modest upregulation of *Stat1* transcripts at days 3 and 5 p.i. The prominent increase of *Stat1* transcripts prominently at day 7 p.i. suggested IFN γ mediated upregulation. *Irf9* transcripts were only upregulated 2-fold in microglia by 3 p.i. and subsequently declined to or below basal levels (Figure 7B). Nevertheless, despite lower basal levels and apparent constitutive expression, *Irf9* transcripts in oligodendroglia rapidly increased by ~15-fold at day 3 p.i., but did not increase further at day 7 p.i. Although activation and nuclear localization of STAT1 and IRF9 remains to be evaluated, the overall limited basal levels of *Irfar1* and *Irfar2*, as well as basal and inducible levels of *Stat1* and *Irf9* transcripts in oligodendroglia during JHMV infection, support an overall paucity in ISG transcriptional activation.

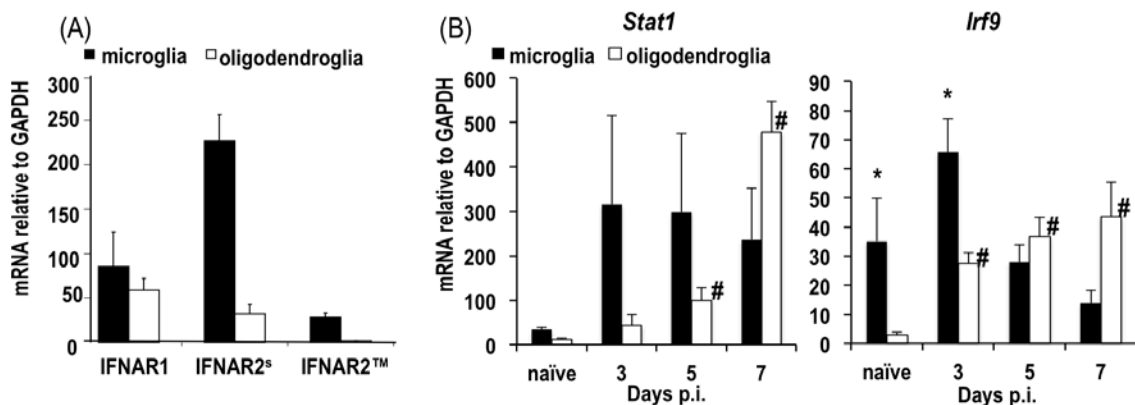


Figure 7. Oligodendroglia have limited IFN α/β receptor signaling capacity. Microglia and oligodendroglia from naïve or JHMV infected mice were assayed for transcripts encoding the IFNAR1, soluble IFNAR2 (IFNAR2^s) and IFNAR2 transmembrane (IFNAR2TM) chains (A) or *Stat1* and *Irf9* transcripts (B). Data in (A) represent the average of 2 experiments; data in (B) represent the average of 3 independent experiments \pm SEM as indicated in Fig. 3. * denotes $p \leq 0.05$ comparing microglia to oligodendroglia at each timepoint; # indicates $p \leq 0.05$ compared to basal levels for each cell population.

The notion of limited ISG transcriptional activation in oligodendroglia was further supported by analysis of a subset of ISG encoding factors with anti-viral activity. Basal levels of transcripts encoding protein kinase R (*Pkr*), and the OAS/RNaseL pathway (*Oas2*), known to modulate translational activity, were all elevated in microglia derived from naïve mice relative to oligodendroglia (Figure 8). Transcripts encoding adenosine deaminase specific for RNA (*Adar1*), which limits viral replication via introduction of RNA mutations (Bass, 1997), were also more abundant in microglia (Figure 8). By contrast, *Ifit2* RNA was expressed at similar levels in both cell types derived from naïve mice. Importantly, in microglia all transcripts, particularly *Oas2* and *Ifit2* RNA, were rapidly increased to peak levels by day 3 p.i. and declined thereafter. With the exception of *Oas2*, induction was also evident at day 3 p.i. in oligodendroglia; however, increases were most prominent by day 7 p.i., yet never reached the peak absolute values observed in microglia (Figure 8). These data demonstrate that oligodendroglia not only express lower steady state levels of ISGs, but also upregulate transcription with delayed kinetics relative to microglia in response to CoV infection. Furthermore, delayed ISG expression in oligodendroglia supported a more prominent responsiveness to IFN γ than IFN α/β . Overall the data clearly suggest that oligodendroglia require paracrine IFN α/β signals to induce ISG during gliatropic CoV infection.

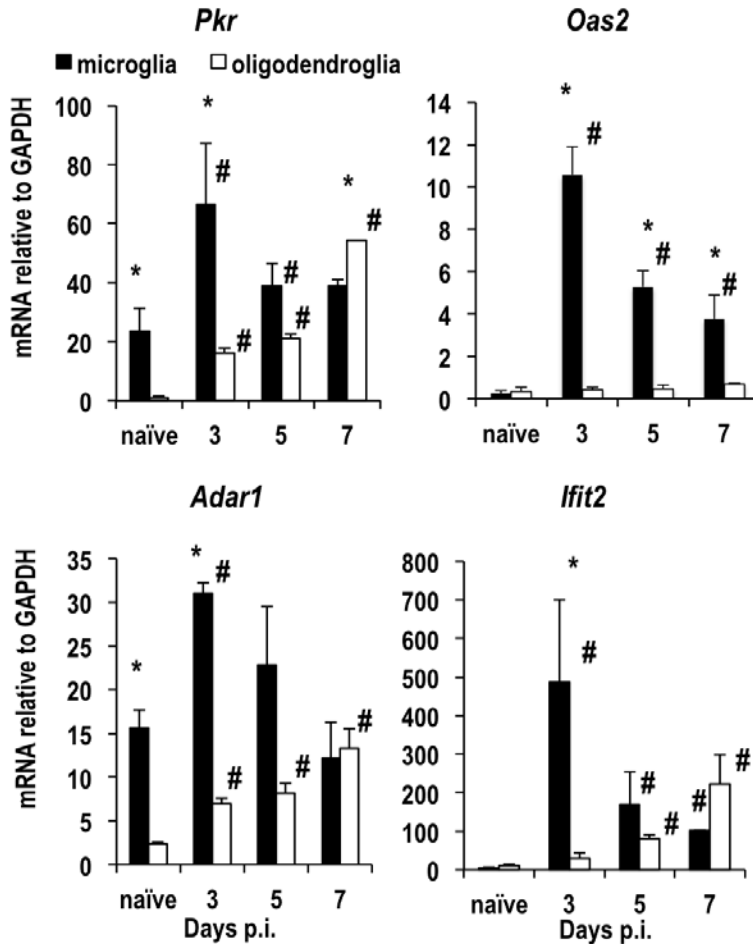


Figure 8. Delayed induction of anti-viral ISG in oligodendroglia. Microglia and oligodendroglia from naïve or JHMV infected mice were assayed for Pkr, Oas2, Adar1, and Ifit2 transcripts as indicated in Fig. 3. Data represent the average of 3 separate experiments \pm SEM. * denotes $p \leq 0.05$ comparing microglia to oligodendroglia at each timepoint; # indicates $p \leq 0.05$ compared to basal levels for each cell population.

2.3.4 Inability of oligodendroglia to induce *Ifna*/ β genes is virus independent

To test whether oligodendroglia are intrinsically limited in IFN α / β production, or if limited IFN α / β production is specific to JHMV infection, we assessed IFN α / β and ISG induction following intracranial injection of the synthetic PRR ligand Poly (I:C). Poly (I:C) is a strong agonist of both TLR3 and the RIG-like receptors RIG-I/MDA5 (Alexopoulou et al., 2001, Kato et al., 2006). IFN α / β upregulation was initially tested in total tissue to characterize the time

course of Poly (I:C) induced IFN α/β responses in the CNS. *Ifn β* expression was maximal at 2 hours and *Ifn $\alpha 4$* mRNA was elevated between 2 and 12 hours post poly (I:C) inoculation (Figure 9). By contrast, peak induction of the ISGs *Ifit1* and *Ifit2* was delayed until 12 hours (Figure 9). Cell type specific gene analysis of IFN α/β and ISG after intracranial poly (I:C) injection was thus performed in purified microglia and oligodendroglia at 4 hours as an intermediate timepoint for optimal *Ifn α/β* expression and at 12 hours.

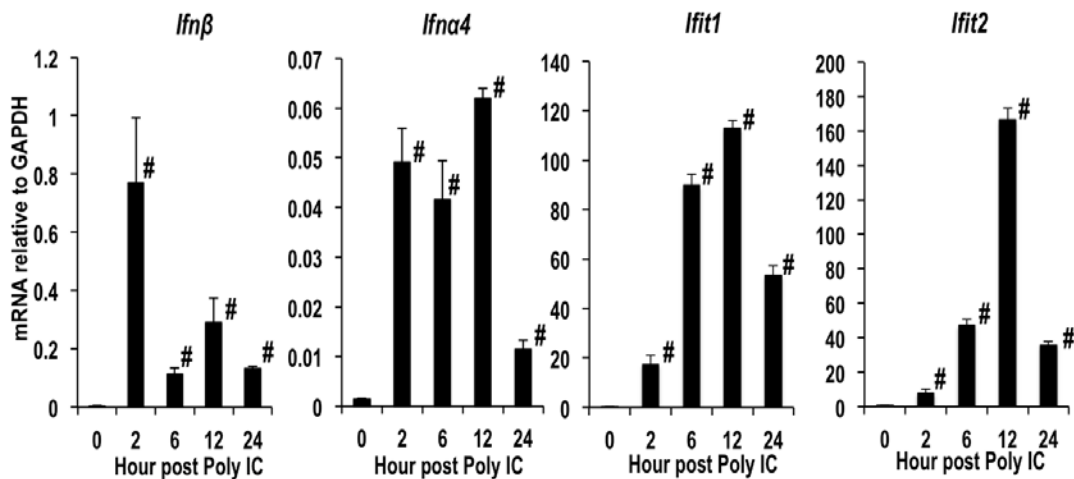


Figure 9. Kinetics of CNS IFN α/β responses to Poly (I:C). Wt mice were injected intracranially with 200 μ g poly (I:C) to assess kinetics of *Ifn β* , *Ifn $\alpha 4$* , *Ifit1*, and *Ifit2* mRNA induction in spinal cords. Data represent the mean \pm SEM for 3 mice per group; # indicates $p \leq 0.05$ compared to basal levels.

In microglia *Ifn $\alpha 4$* and *Ifn β* transcripts were clearly induced by 4 hours and expression of *Ifn β* was sustained until 12 hours (Figure 10). Importantly, the levels were 30-40 fold higher than those induced by viral infection (see Figure 5), confirming the significantly increased magnitude of the response. Nevertheless, *Ifn α/β* mRNA remained near detection thresholds in oligodendroglia (Figure 10). However, *Mda5* and *Rig-I* levels were increased in both cell populations after poly (I:C) injection relative to the modest 4-5 fold increases induced by virus

infection (Figure 10). Furthermore, similar to the trend observed during infection, *Rig-I* transcripts were significantly increased over *Mda5* transcripts in oligodendroglia. Nevertheless, *Ikk ϵ* and *Irf7* transcripts were elevated in both microglia and oligodendroglia at 4 and 12 hours after poly (I:C) (Figure 10) relative to viral injection (Figure 6). While limiting IFN α/β levels thus clearly contributed to suboptimal ISG induction in both glial populations following infection, the mechanism(s) underlying the paucity of IFN α/β induction in oligodendroglia remains elusive. Representative of antiviral ISG expression, *Ifit1* and *Ifit2* mRNA were also significantly increased in microglia at 4 hours, but subsided by 12 hours post poly (I:C) administration. By contrast, in oligodendroglia *Ifit1* and *Ifit2* levels induced at 4 hours were maintained at similar (*Ifit1*) or even increased levels (*Ifit2*) at 12 hours (Figure 10). Even under these conditions of optimal *in vivo* stimulation, oligodendroglia exhibited tentative and delayed ISG induction. These results support the notion that *in vivo* oligodendroglia are intrinsically impaired in inducing IFN α/β in response to dsRNA stimuli but also in responsiveness to IFN α/β suggesting an overall dampened capacity for innate responses.

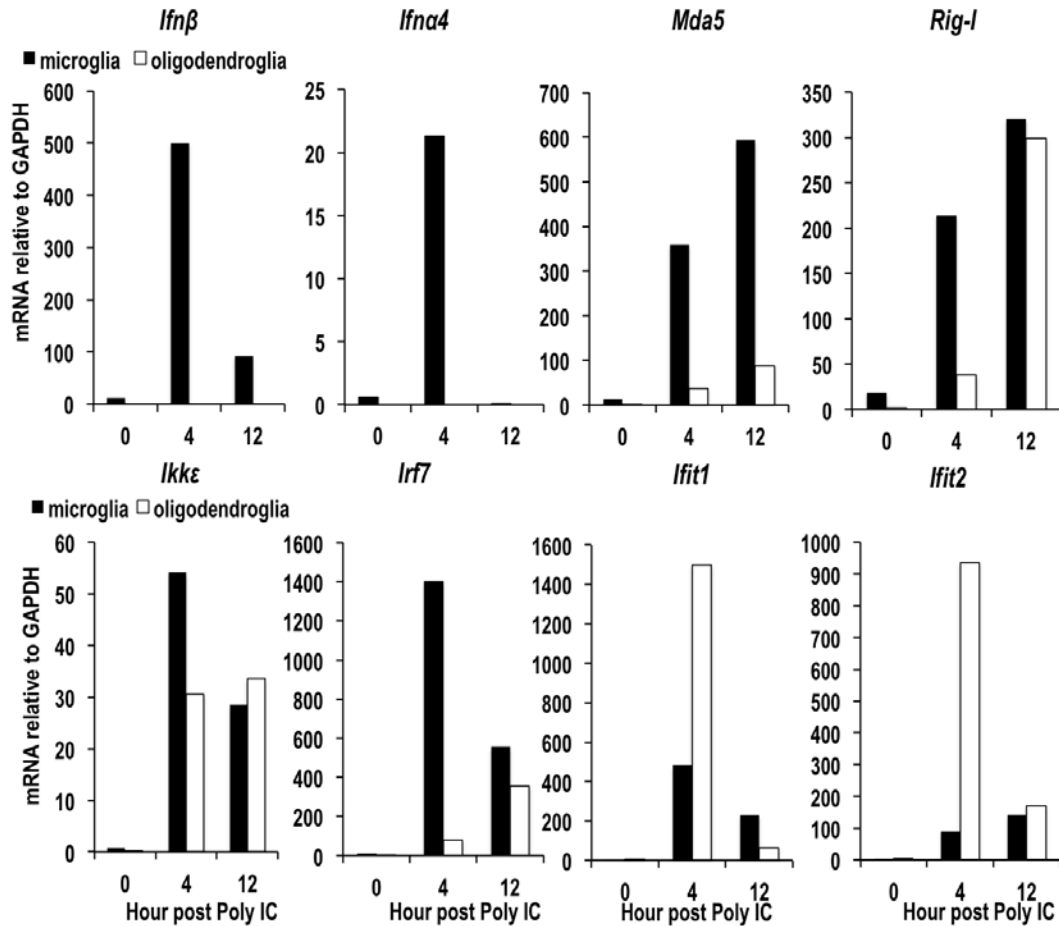


Figure 10. Distinct in vivo responses of oligodendroglia and microglia to poly (I:C). Microglia and oligodendroglia purified from spinal cords at 4 or 12 hours post poly (I:C) injection were analyzed for expression of *Ifnα4*, *Ifnβ*, *Mda5*, *Rig-I*, *Ikkε*, *Irf7*, *Ifit1*, and *Ifit2* transcripts. Data are representative of two independent experiments each with 10 pooled mice per experiment.

2.4 Discussion

PRR initiated innate responses in the CNS are critical for the induction of IFNα/β, as well as proinflammatory cytokines and chemokines. While PRR expression and activation in microglia and astrocytes has been extensively explored *in vitro* (Butchi et al., 2010, Carpentier et al., 2008, Jin et al., 2011, So and Kim, 2009), PRR expression and associated signaling components in glia *in vivo* are poorly defined, especially in oligodendroglia. In this study we compared the capacity of oligodendroglia relative to microglia to mount IFNα/β mediated

innate immune responses. Glial specific responses were monitored within the context of the CNS following intracerebral infection of adult mice with gliatropic JHMV or injection of poly (I:C). Microglia were prominent inducers of *Ifn α / β* mRNA following infection, consistent with IFN α / β induction in primary microglia as well as bone marrow derived macrophages infected with a heterologous MHV (Roth-Cross et al., 2008). However, the inability of oligodendroglia to induce *Ifn α / β* mRNA, despite their high load of viral RNA, contrasted with *in vitro* studies demonstrating MDA5 and RIG-I dependent IFN α / β induction in the infected N20.1 oligodendroglia cell line (Li et al., 2010). This discrepancy likely reflects differences in expression and/or induction of IFN α / β pathway components, rather than distinct viral loads, as even poly (I:C) did not induce *Ifn α / β* in oligodendroglia *in vivo*.

The restricted ability of CoV to induce IFN α / β was recently attributed to the O-methylated cap structure of the viral RNA, making it difficult for the host to distinguish viral from self mRNA (Daffis et al., 2010, Zust et al., 2011). However, in contrast to cultured fibroblasts, bone marrow derived DC, astrocytes and neurons the ability of pDC, macrophages/microglia, and an oligodendroglia cell line to induce IFN α / β via TLR7, MDA5 and MDA5/RIG-I dependent pathways (Cervantes-Barragan et al., 2007, Li et al., 2010, Roth-Cross et al., 2008, Zhou and Perlman, 2007) suggests sufficient PRR activation by viral RNA structures to mediate protective responses in select cell types. Our data indicate that cell type specific basal expression, as well as inducible components in the innate signaling pathway constitute critical signaling thresholds determining IFN α / β induction. In

the adult CNS oligodendroglia differed significantly from microglia in reduced basal transcript levels of viral RNA sensing PRRs and *Ikkε*. However, basal *Irf3* transcripts were only reduced by ~50%, and *Irf7* transcripts were barely detectable in either cell population, consistent with higher basal *Irf3* than *Irf7* levels observed in whole naïve brains (Ousman et al., 2005). Reduced basal PRR levels in oligodendroglia were reminiscent of sparsely expressed PRRs in primary neurons (Carpentier et al., 2008), and supported the superior initiation of *Ifnα/β* responses of microglia. This concept is consistent with the inability of primary cultured neurons and astrocytes to induce IFN α/β expression following MHV infection (Roth-Cross et al., 2008).

Optimal IFN α/β induction requires amplification through IFNAR to elevate PRRs and IRF7 (Honda and Taniguchi, 2006, Honda et al., 2005, Malmgaard et al., 2002). However, in contrast to *Ifnα/β* induction, IFNAR signaling was intact in oligodendroglia. Although IFN α/β protein was below detection in cell free supernatants derived from the JHMV infected CNS by ELISA (data not shown), IFN α/β sufficed to up regulate the ISGs *Mda5*, *Rig-I*, *Stat1*, *Irf7*, *Pkr*, *Ifit2*, and *Adar1* in oligodendroglia. The ability of IFN α/β to induce ISGs was consistent with basal expression of IFNAR chains, as well as basal and inducible levels of *Stat1* and *Irf9* transcripts. Although induction above basal levels was greater in oligodendroglia than microglia for some genes, peak absolute mRNA levels were in general lower compared to those reached in microglia at days 3 and 5 p.i., as exemplified by *Stat1* and *Irf7* mRNA. Furthermore, peak expression for many genes did not correlate with maximal *Ifnα/β* mRNA levels, but rather with peak

IFN γ secretion at day 7 p.i. (Parra et al., 2010, Phares et al., 2011, Puntambekar et al., 2011). Distinct pattern of ISG expression in oligodendroglia compared to microglia may further reside in low *Ikk ϵ* mRNA levels. In addition to mediating PRR signaling, IKK ϵ influences ISG induction through participation in JAK/STAT mediated IFN α/β signaling (Pham and Tenoever, 2010, Tenoever et al., 2007). Although not as severe as the complete abrogation of ISG induction in STAT1^{-/-} mice, IKK ϵ ^{-/-} mice lack induction of ~30% of ISGs, including *Adar1* (Durbin et al., 1996, Tenoever et al., 2007). The biological consequences are demonstrated by impaired clearance of influenza virus infection by IKK ϵ ^{-/-} mice, despite similar expression of IL2, IL6, IL12, IFN γ and RANTES and induction of anti-viral antibody (Tenoever et al., 2007). The paucity of *Ikk ϵ* mRNA and modest, if any, increase of *Irf7* mRNA in oligodendroglia, despite abundant viral and *Mda5* mRNA upregulation, may partially explain the absence of *Iffa*/ β expression and more selective and delayed ISG induction during infection. However, even the strong IFN α/β response elicited in the CNS by poly (I:C) did not overcome the inability of oligodendroglia to induce *Iffa*/ β , despite over 400 fold increases in *Ikk ϵ* and 85-400 fold increases in *Irf7* transcripts relative to those induced by infection. These results suggest additional restrictions intrinsic to oligodendroglia in the initiation of IFN α/β production.

The results thus indicate a reliance of oligodendroglia on external production of IFN α/β to induce an antiviral state. This concept is consistent with data indicating that microglia are a dominant source of IFN α/β within the CNS during JHMV induced encephalomyelitis (Roth-Cross et al., 2008). The biological

relevance of suboptimal IFN α/β responses is clearly evident from differential viral control in both cell types. A direct response to infection by microglia is supported by the correlation between peak viral and *Ifn α/β* mRNA. Furthermore, the early decline in viral RNA, prior to infiltration of T cells, indicates autocrine IFN α/β contributes to the rapid control viral spread in this cell type. By contrast, although oligodendroglia were initially infected to a lesser extent than microglia, viral RNA increased over 2 logs between days 3 and 5 p.i., coincident with the absence of *Ifn α/β* and tentative induction of antiviral ISGs. These data indicate that oligodendroglia thus rely largely on T cell effector function, prominently IFN γ , for viral control (Parra et al., 2010). Oligodendroglia are indeed highly responsive to IFN γ as indicated by upregulation of class I MHC molecules and associated antigen processing components during peak IFN γ , but not IFN α/β induction during JHMV infection (Malone et al., 2008). Moreover, specific blockade of IFN γ receptor signaling on oligodendroglia prolongs JHMV infection in this cell type (Gonzalez et al., 2005, Parra et al., 2010). Whether early events favoring robust infection of oligodendroglia prior to emergence of T cells, contribute to ultimate persistence of JHMV in oligodendroglia, remains to be elucidated.

Overall our results demonstrate a limited role of oligodendroglia as both inducers of, and responders to, IFN α/β compared to microglia. Limited innate antiviral activity may predispose oligodendroglia to be potent responders to IFN γ (Gonzalez et al., 2005, Popko and Baerwald, 1999). While there is no evidence supporting toxicity of IFN α/β (Akwa et al., 1998), more restricted induction of antiviral mediators, especially those also affecting host cell translation, may

circumvent apoptosis and guarantee maintenance of critical myelin housekeeping functions and survival. Our findings also contradict the hypothesis suggesting that virus initiated IFN α/β production by oligodendroglia drives inflammatory responses during viral induced demyelinating disease (Lipton et al., 2007). The low abundance of PRR at basal levels rather provide a mechanism underlying the apparent paucity of oligodendroglia to express cytokines during multiple sclerosis or other CNS inflammatory conditions (Cannella and Raine, 2004, Zeis et al., 2008). Our data thus support the notion that oligodendroglia are defensive players under inflammatory conditions.

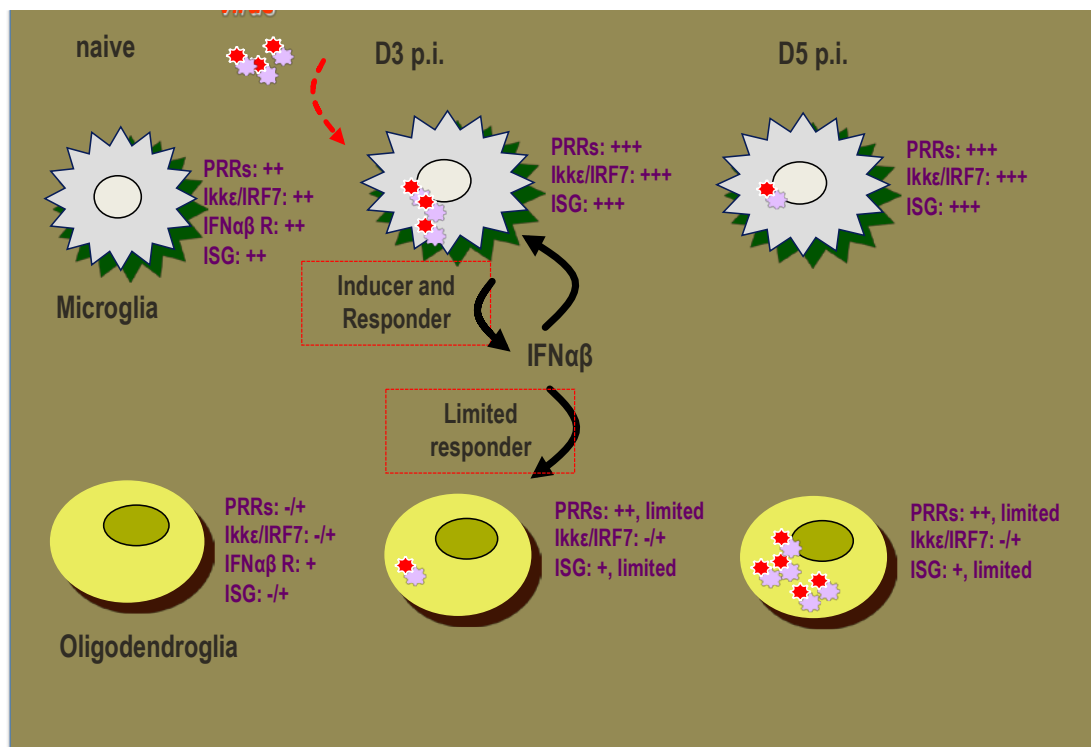


Figure 11. Model for differential innate glia responses to JHMV infection

CHAPTER III

**PKR: UNCONVENTIONAL ROLE OF AN ANTI-VIRAL FACTOR FOLLOWING
CNS INFECTION**

3.1 Abstract

IFN α/β plays an eminent role in restricting viral tropism and limiting dissemination within the CNS following infection with the glia tropic coronavirus JHMV. However, which among the many IFN α/β stimulated innate antiviral factors are protective in the CNS is largely unknown. RNaseL and Protein Kinase RNA dependent (PKR) are the best-characterized innate anti-viral proteins. Although the absence of RNaseL resulted in elevated infection of microglia/macrophages, it was insufficient to alter overall JHMV control or CNS inflammation. Nevertheless, RNaseL deficiency resulted in mortality coincided with accelerated demyelination and axonal degeneration, suggesting RNaseL activation provides protective effects independent of viral control. To identify the role of other innate antiviral pathways in JHMV pathogenesis, we explored a potential contribution of PKR, an inhibitor of host cell translation and modulator of NF κ B mediated gene transcription using PKR deficient mice (PKR $^{-/-}$). Infected

PKR^{-/-} mice exhibited no defect in expression of *Ifnα/β* or induced anti-viral genes *Ifit1* and *Ifit2* suggesting no over deficits in the IFNα/β pathway. Surprisingly, however, PKR deficiency significantly reduced expression of NFκB mediated pro-inflammatory cytokines and chemokines. Viral burden in the CNS was initially increased by ~10-fold in PKR^{-/-} mice relative to wt mice, but histological examination revealed no discernable differences in viral antigen distribution or tropism. Furthermore, virus was subsequently controlled with similar kinetics indicating effective CD8 T cell recruitment and function, although PKR deficiency was associated with more extensive accumulation of infiltrating cells in the perivascular space, Lower *Ii21* and *Ii10* expression further suggested modulation of CD4 T cell activity in the absence of PKR. Lastly, the onset of axonal damage appeared accelerated and demyelination more diffuse in PKR^{-/-} mice. Nevertheless, the overall pathology resembled that of wt rather than RNaseL^{-/-} mice and the absence of PKR did not result in high mortality. A subtle effect of PKR on JHMV pathogenesis was supported by a similar phenotype of mice dually deficient in RNaseL and PKR as in single RNaseL^{-/-} mice. In summary the results suggest that RNaseL and PKR only exert subtle direct antiviral activity during JHMV infection. Moreover, while PKR activation can profoundly influence the cytokine/chemokine milieu without overt consequences on disease, RNaseL activation mediates protective function by mitigating demyelination.

3.2 Introduction

Type-1 IFN signaling initiates transcription of numerous genes resulting in an antiviral state characterized by elevated expression of numerous anti-viral factors (Borden et al., 2007, Trinchieri, 2010). Many of the antiviral molecules directly block viral replication by interfering with translational activity, either by degrading viral and host RNA or directly inhibiting protein synthesis. Nevertheless, effective antiviral functions differ not only between viruses themselves, but also the cell types infected. Moreover, although distinct anti viral factors all minimize viral spread, altered cellular transcriptional and translational profiles can also significantly impact host cell function, for example resulting in apoptosis. The most characterized anti-viral mechanisms are the 2'-5' oligoadenylate synthetase (OAS)/RNaseL and protein kinase double stranded RNA (PKR) pathways (Silverman, 2007b, Silverman, 2007a, Garcia et al., 2007). Both depend on activation of latent enzymes to be functional, which serves to minimize altered cellular functions in non-infected, bystander cells. Cell type dependent antiviral function is illustrated by RNaseL dependent control of West Nile virus (WNV) in MEF, but RNaseL independent IFN β mediated virus clearance in either peripheral or cortical neurons. Furthermore, increased mortality of WNV infected dual RNaseL/PKR^{-/-} mice is attributed to increased peripheral infection, but not enhanced virus dissemination to the CNS (Samuel et al., 2006). Virus dependent protection is highlighted by impaired control of Sindbis virus in the absence of RNaseL and PKR in mouse embryonic fibroblasts (MEF) and bone marrow derived macrophages (Ryman et al., 2002), but IFN β

mediated inhibition of dengue virus is independent of the PKR/RNaseL pathways (Diamond and Harris, 2001). PKR play a crucial role in antiviral defense following vesicular stomatitis virus infection (VSV) *in vitro*. Furthermore, 100% mortality and uncontrolled virus replication was observed in PKR *-/-* mice following intranasal VSV infection (Stojdl et al., 2000).

IFN α/β mediated innate responses are also critical for limiting tropism, controlling virus spread and preventing mortality following infection with the glia tropic, murine coronavirus, JHMV (Ireland et al., 2008). However, the type-1 IFN downstream anti-viral factors mediating protection are largely unknown. RNaseL plays a modest role in reducing infection of macrophage/microglia, but does not alter overall virus clearance in the CNS (Ireland et al., 2009). Surprisingly however, RNaseL mediated protection from accelerated axonal damage, demyelination and death. The pathological differences, independent of viral control, suggested dysregulation of as yet unknown RNaseL functions in the CNS during inflammatory conditions.

Based on uncontrolled JHMV spread in the CNS in absence of IFN α/β signaling, but limited effects of RNaseL, we further explored other antiviral mediators by determining the role of PKR. PKR is an intracellular sensor of stress. Viral dsRNA as well as other ligands such as PKR activating protein (PACT) and polyanionic molecules such as dextran sulfate, chondroitin sulfate, poly (L-glutamine) and heparin can directly activate PKR (Bergeron et al., 2000). In addition to viral RNA, some highly structured cellular RNA molecules, such as Tumor Necrosis factor α (TNF α) and Interferon γ (IFN γ) mRNA also has been

shown to activate PKR (Ben-Asouli et al., 2002, Osman et al., 1999). The ability of PKR to respond to multiple stimuli emphasizes its broader role as a signaling molecule against different types of physiological stress. Activated PKR depicts kinase activity and undergoes autophosphorylation. The main target of phosphorylation by activated PKR is the eukaryotic translation initiation factor, eIF2 α . Phosphorylation of eIF2 α leads to inhibition of translation and induction of apoptosis in host cells, therefore inhibiting viral replication. PKR also induces transcriptional expression of pro-inflammatory genes and IFN α/β by initiating the degradation of I κ B, inducing IRF1 expression and indirectly mediating STAT1 phosphorylation. I κ B degradation leads to activation of downstream transcription factor NF κ B (Kumar et al., 1994, Bonnet et al., 2000). PKR mediated activation of NF κ B is independent of its kinase activity. The N terminus (AA 1-265) of PKR, which includes the dsRNA binding domain (AA 1-181) and third basic domain (AA 181-265) has been shown to activate NF κ B by directly binding and activating the IKK complex (Bonnet et al., 2006). PKR can also associate with TNF receptor associated factor (TRAF) to mediate activation of NF κ B (Gil et al., 2004). Other than inducing pro-inflammatory cytokines, PKR is also demonstrated to be involved in inducing anti-inflammatory cytokine IL10 in monocyte/macrophages in response to polyI:C, LPS and distinct infections such as mycobacterium, and sendai virus (Cheung et al., 2005, Chakrabarti et al., 2008). Several studies also support a link between PKR and cellular immunity. For example, PKR limits HIV replication by reducing surface expression of CD4 T cells *in vitro* in jurkart cells (Nagai et al., 1997). PKR affects ability of CD8 T cells to control replication of

Lymphocytic Choriomeningitis Virus (LCMV) without altering CD8 T cell their effector function (Nakayama et al., 2010). Lastly, impaired proliferation of CD8 T cells in response to mitogen stimulation during systemic lupus erythomatosus (SLE) is associated with increased PKR activation and therefore reduced protein synthesis (Grolleau et al., 2000).

PKR is also implicated to participate in neuro-degenerative processes. Following poliomyelitis infection PKR deficient mice show no difference in virus replication, but were protected from infection mediated extensive spinal cord damage (Scheuner et al., 2003). A separate study links PKR activation as an early biomarker of neuronal cell death in Alzheimer's disease (Peel and Bredesen, 2003). Contribution of PKR in neurotoxicity was attributed to its ability to increase apoptosis by activating fas associated protein with a death domain (FADD) and subsequently activating caspase 3 and 8 in recombinant virus infected cells as well as in A β treated cells and in APP_{SL}PS1 K1 mice (Transgenic mouse to study AD) (Gil and Esteban, 2000, Couturier et al., 2010). In the EAE autoimmune model of multiple sclerosis, PKR is mainly expressed by oligodendroglia, T cells and some macrophages (Chakrabarty et al., 2004). In summary, these findings implicate PKR can control numerous aspects of immunity ranging from direct antiviral activity via translational inhibition, to induction of pro- as well as anti-inflammatory molecules, and modulation of adaptive responses. Moreover, PKR is also demonstrated to contribute in neurotoxicity by inducing apoptotic pathway.

In the absence of PKR we observed higher virus titers early during infection at day 3, 5 and 7 p.i. following JHMV infection. However, virus in PKR^{-/-} mice was subsequently controlled by day 10 p.i., with similar kinetics as in wt mice. This indicated an early antiviral effect of PKR, which was overcome by effective CD8 T cell function. We were therefore surprised that reduced expression of pro-inflammatory cytokines and chemokines such *Il6*, *Ccl5*, and *Cxcl10* had no apparent effect on leukocyte recruitment. Nevertheless, a hallmark of infected PKR^{-/-} mice was accumulation of cells in the perivascular space. Specifically the distribution of CD4 T cells was skewed towards retention in the perivascular space indicating impaired entry into the CNS parenchyma. Moreover, in the absence of PKR, CD4 T cells were impaired in IL10, but not IFN γ production. While these results all indicated substantial immune modulation by PKR, ultimate virus clearance and disease outcome were surprisingly similar to wt mice.

3.3 Results

3.3.1 PKR deficiency does not alter IFN α/β induction, reduces NF κ B mediated gene expression and only affects virus replication modestly in the CNS following JHMV infection

PKR is constitutively expressed at low levels and can signal to activate IFN α/β after binding to dsRNA. Activated PKR can also bind to and degrade the inhibitor of NF κ B (I κ B), resulting in NF κ B activation (Kumar et al., 1994). Once activated NF κ B translocates to the nucleus and regulates expression of pro-inflammatory genes. To initially identify the role of PKR in IFN α/β induction and

NFkB activation in the infected CNS, we determined the expression of IFN α/β and NFkB induced genes using quantitative real time PCR analysis (Figure 12). Induction of *Ifn α 4* and *Ifn β* mRNA peaked in spinal cords at day 5 p.i. in both mice and declined thereafter. Although *Ifn α 4* mRNA levels were similar, *Ifn β* mRNA was reduced at day 5 p.i. in PKR $^{-/-}$ mice. Nevertheless, no differences were observed in expression of the *Ifit1* and *Ifit2* genes, two ISG that are highly sensitive to IFN α/β induction. Both *Ifit1* and *Ifit2* transcripts were highly upregulated by day 5 p.i., remained elevated at day 7 p.i., and declined thereafter (Figure 12A). By contrast, expression of NFkB induced cytokines and chemokines was significantly impaired, albeit not universally (Figure 12B). While the proinflammatory genes *Ccl2*, *Il1 β* , *Il6*, *Tnf α* , *Ccl5* and *Cxcl10* were all upregulated in spinal cords of both groups at day 5 p.i., *Il6*, *Ccl5* and *Cxcl10* were selectively reduced 2-fold in the absence of PKR. *Ccl2* and *Il1 β* mRNA levels both increased to similar relative levels at day 7 p.i., and subsequently declined, demonstrating no overt effect of PKR. *Il6* mRNA remained at 50% the levels of wt mice and declined with similar kinetics at days 7 and 10 p.i. By contrast, *Ccl5* and *Cxcl10* chemokine mRNAs increased by day 7 in wt mice, but remained low throughout days 7 and 10, barely increasing over the day 5 levels in PKR $^{-/-}$ mice. By day 7 p.i. PKR $^{-/-}$ mice also exhibited decreased mRNA levels of *Tnf α* , which was sustained throughout day 10 p.i.

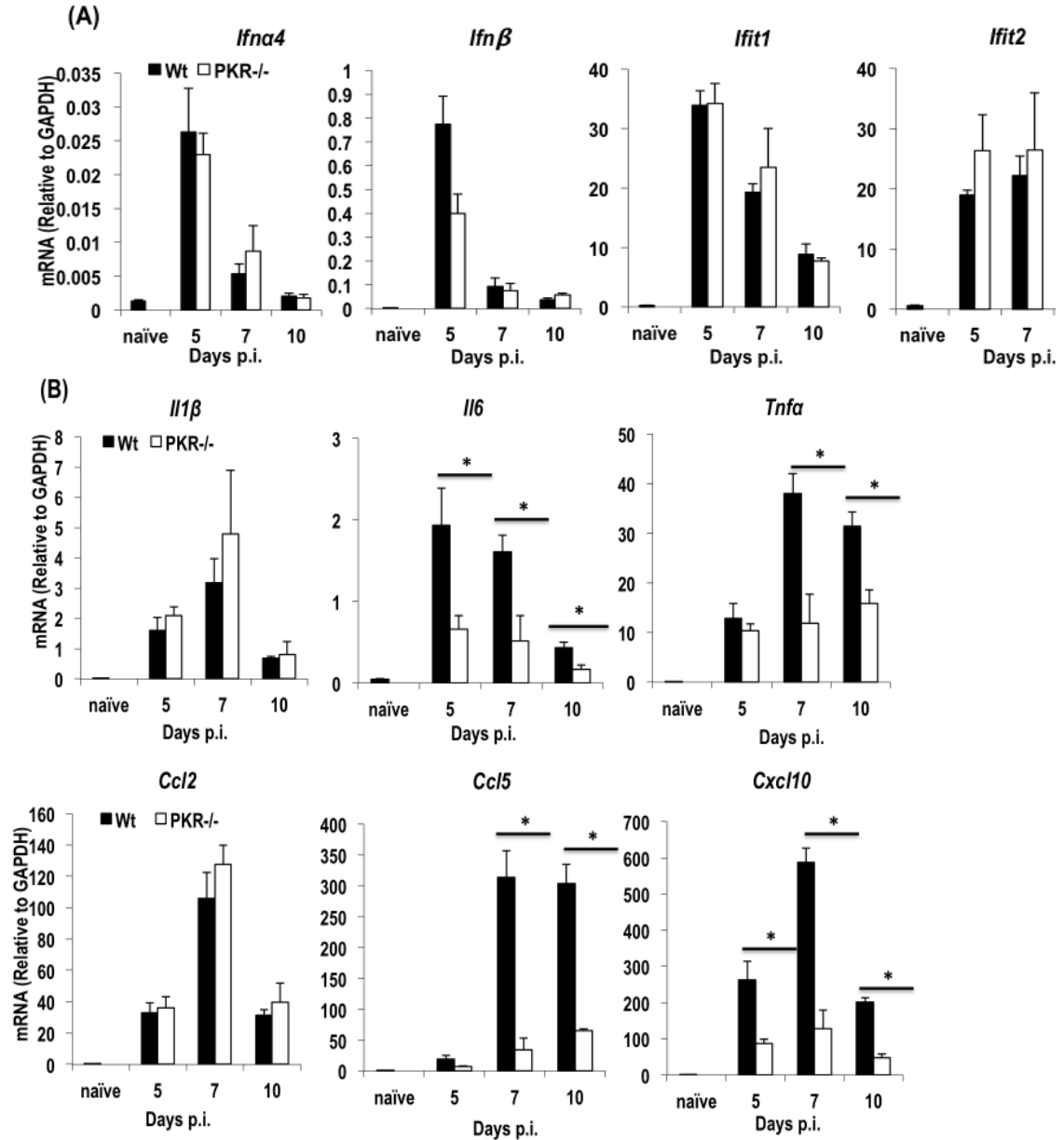


Figure 12. PKR deficiency resulted in reduced expression of NF κ B induced pro-inflammatory genes, but does not alter IFN α/β dependent antiviral genes. Expression of NF κ B and IFN α/β induced genes were determined using Real time PCR analysis. (A) Expression of *Ifna β* and dependent genes *Ifit1* and *Ifit2* from spinal cord of PKR $^{-/-}$ mice and wt mice. (B). Expression of selected NF κ B dependent genes, *Il1 β* , *Il6*, *Tnfa*, *Ccl2*, *Ccl5*, and *Cxcl10* relative to *Gapdh* in spinal cords of PKR $^{-/-}$ and wt mice. Data is represented as average of n = 3 mice/ group/ time-point \pm standard error mean (SEM). * $p \geq .05$.

To determine an affect of PKR on virus replication viral loads in brains and spinal cords were determined by plaque assay and PCR, respectively. Infection is always initiated in the brain and rapidly spreads to spinal cords, where it

preferentially persists. In wt mice, infectious virus peaks at days 3-5 p.i., starts to be controlled at day 7 p.i., and is reduced to undetectable levels by plaque assay by day 14 p.i. We observed ~5-10 fold higher virus titers early during the infection at days 3, 5 and 7 p.i. in PKR^{-/-} mice compared to wt mice; however, at day 10 p.i. virus replication was controlled similarly as wt mice (Figure 13). Analysis of viral RNA in spinal cords revealed no evidence of an early antiviral effect of PKR. Analysis of viral antigen distribution by histology revealed no overt differences in either infected cell numbers or cellular distribution (data not shown). However it is plausible that infectious virus is higher in the absence of PKR if viral mRNA is translated more efficiently. These results indicates that PKR plays a modest antiviral role early during the infection, but virus can be cleared with similar efficiency as in wt mice once CD8 T cells infiltrate to the CNS (days 7-10 p.i.).

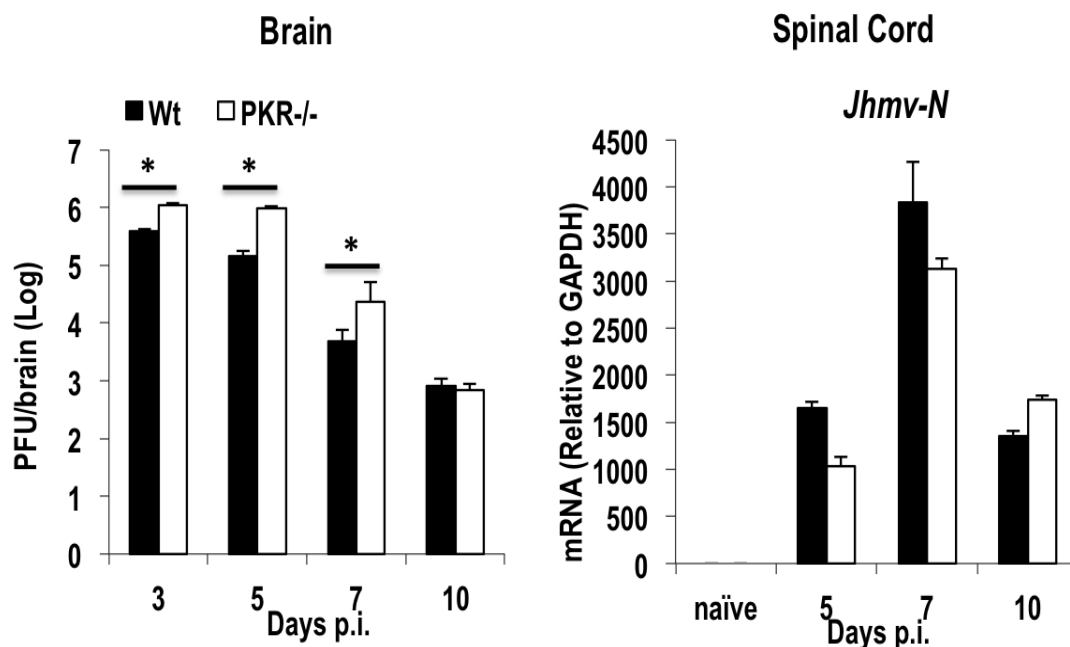


Figure 13. Virus replication in PKR^{-/-} mice is enhanced during early phase of infection but clear with similar kinetics as wt mice. Virus replication in brain was determined by plaque assay on brain supernatants at indicated time-points post infection. Data is re represented as average of n = 3 mice/ group/ time-point ± standard error mean (SEM). (n = 9 mice/group/time-point). Viral RNA was determined in spinal cords relative to *Gapdh*. * p ≥ .05.

3.3.2 Increased CNS T cell infiltration, but accumulation of CD4 T cells in the perivascular space in the absence of PKR

Reduced levels of *Ilf6* and T cell attracting chemokines *Ccl5* and *Cxcl10* suggested alteration in leukocyte infiltration into the CNS, yet efficient virus control contradicted this notion. Therefore, composition of infiltrating cells was determined in CNS of PKR^{-/-} and wt mice using FACS analysis for the cell specific surface markers. We observed no difference in number of overall infiltrates (CD45^{hi} cells) to the CNS in the absence of PKR. Similarly, monocytes infiltrating the CNS, characterized by a CD45^{hi}/F4/80⁺ phenotype, were not statistically different between both mouse groups at any time p.i. consistent with similar monocyte recruiting *Ccl2* expression. CXCL10 and CCL5 expression is reported to attract T cells to the CNS following JHMV infection (Glass et al., 2004, Liu et al., 2001). Therefore alterations in T cell accumulation were determined. Both CD4 and CD8 T cells accumulate in the CNS to maximal levels between 7-10 days following JHMV infection and account for ~ 60% of total CD45^{hi} infiltrates. Compared to wt mice, CD8 T cells were significantly higher at day 7 p.i. and CD4 T cells at both day 7 and 10 p.i. within brain infiltrates in PKR^{-/-} mice (Figure 14).

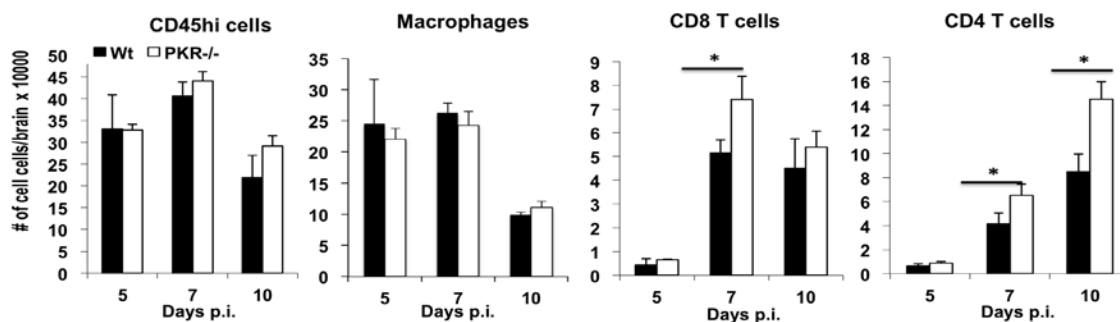


Figure 14. Increased number of infiltrating T cells to the CNS in PKR^{-/-} mice. Number of infiltrating, Total lymphocytes (CD45^{hi}), macrophages (CD45^{hi} F4/80⁺), CD8 T and CD4 T cells derived from the brain of infected wt and PKR^{-/-} mice was determined using flow cytometric analysis. Data is average of three separate experiments \pm standard error mean (SEM). (n = 9 mice/group/time-point). * p \geq .05.

Potential differences in distribution of leukocytes within the CNS in both groups of mice were also analyzed by histochemical analysis of spinal cord sections. Hemotoxylin/eosin staining showed accumulation of infiltrating cells in the perivascular space at day 7 and day 10 p.i. (Figure 15A). To quantify the relative distribution of subtypes of infiltrating lymphocytes, laminin staining was used to visualize the endothelial cells and parenchymal basement membrane to define the outer and inner layers of perivascular space where leukocyte accumulate before trafficking to the parenchyma of the CNS (Savarin et al., 2010). Monocytes have been reported to enhance perivascular accumulation of lymphocytes (Savarin et al., 2010). However, we did not detect any difference in either recruitment of monocyte (Figure 14) or function of monocyte determined by phagocytic ability (data not shown). Furthermore, only a transient increase in CD8 T cell numbers was observed at day 7 p.i. and similar virus control at day 10 p.i. in PKR^{-/-} mice compared to wt (Figure 14) suggested no defect in their functional ability. We specifically focused on CD4 T cells based on their increased numbers at both day 7 and 10 p.i. To distinguish CD4 T cells accumulated in perivascular space compared to total infiltrating CD4 T cells in the spinal cord, sections were stained for laminin and CD4 T cells. In wt mice, CD4 T cells preferentially accumulate in perivascular space at day 7 p.i., accounting to ~50% of total CD4 T cells in the perivascular space, eventually CD4 T cells migrate to the parenchyma at day 10 p.i. as observed only ~20% CD4 T cells retaining in the perivascular space while ~80% localize in parenchyma at this time p.i. (Figure 15B). In the absence of PKR, the frequency

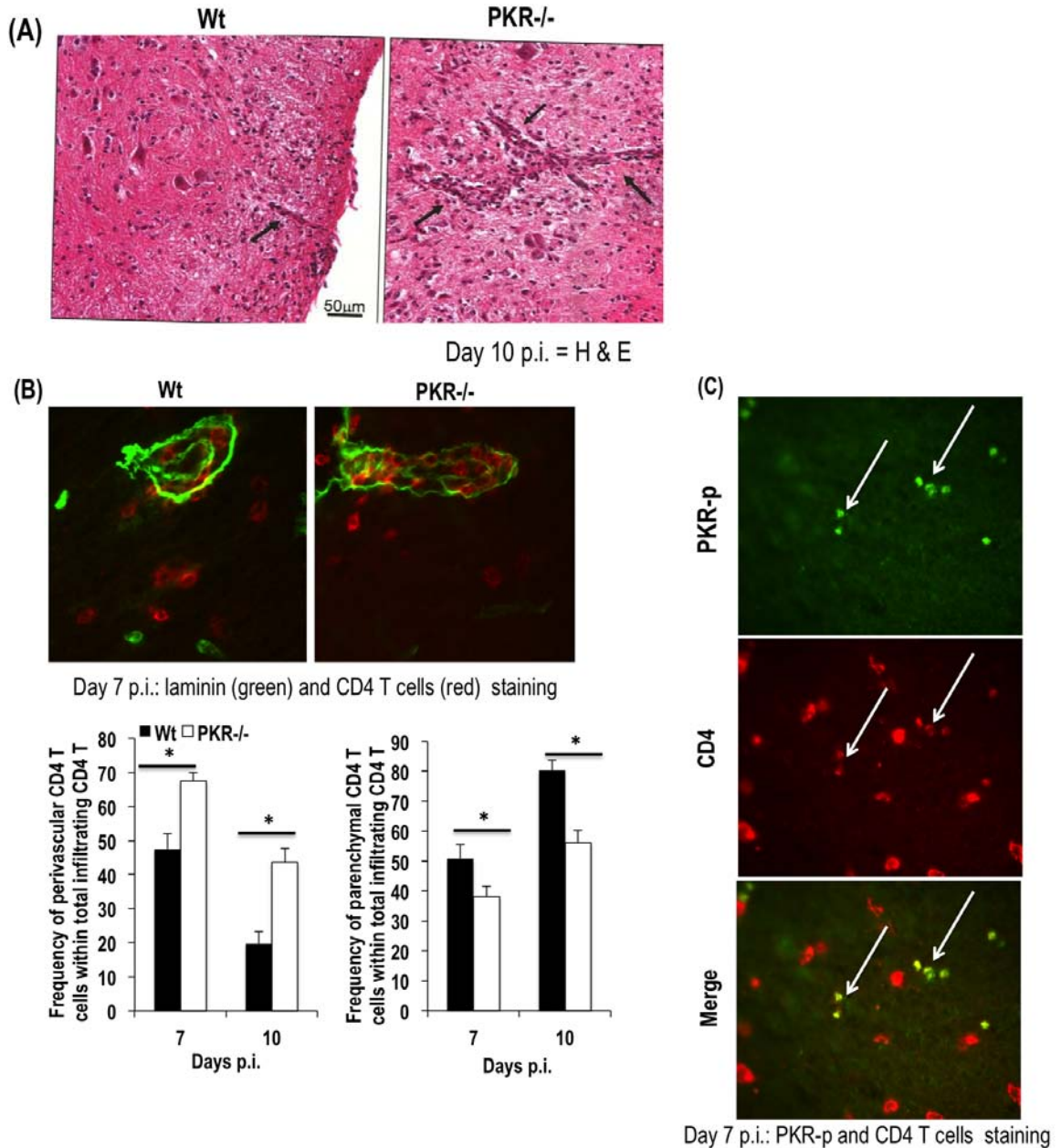


Figure 15. Trafficking of lymphocytes from perivascular space to CNS parenchyma is influenced in PKR-/- mice compared to wt mice. (A) Cross-sections of spinal cords at day 10 p.i. were stained for Hematoxylin and Eosin (H & E). Enhanced perivascular inflammation is consistent with increased T cell accumulation by flow cytometric analysis. Data is representative of three separate experiments. (B) Accumulation of CD4 T cells in the perivascular space was determined using staining spinal cord sections with CD4 and laminin in PKR-/- mice relative to wt mice. Staining of CD and laminin indicates the perivascular accumulation of CD4 T cells. Data is representative of n = 3 mice/ group at day 10 p.i. Quantification of frequency perivascular CD 4 T cells within total infiltrating Cd \$ T cells is presented as graph form. Data is average of total 15 sections between n = 3mice/group/time-point \pm SEM. (C) Expression of activated PKR in infiltrating CD4 T cells to the CNS was determined by double staining spinal cord sections for PKR-p and CD4 in wt mice. Data is repretative of n = 3mice/group at day 7 p.i. * p \geq .05.

of perivascular CD4 T cells was elevated to ~70% at day 7 p.i., which was decreased to ~50% at day 10 p.i. but still remained significantly higher than wt mice. (Figure 15B). Therefore first time we demonstrate that PKR can influence CD4 T cells migration across the glia limitans following JHMV infection. To identify direct role of PKR in regulation of CD4 T cell function, first we analyzed if CD4 T cells express activated PKR (phosphorylated-PKR [PKR-p]) following JHMV infection by utilizing fluorescent microscopy on spinal cord sections. Positive staining for PKR-p in some CD4 positive T cells indicate that not all CD4 T cell can express activate PKR (PKR-p) under viral infection (Figure 15C).

3.3.3 Absence of PKR influences CD4 T cell function

PKR has been implicated in regulating IL10 production in monocyte and CD8 T cell antiviral function (Nakayama et al., 2010, Cheung et al., 2005, Chakrabarti et al., 2008), however its effect on CD4 T cell has not been explored. Co-expression of activated PKR in CD4 T cells, and increased retention of CD4 T cells in perivascular space in absence of PKR would indicate a defect in CD4 T cell function in PKR^{-/-} mice. To investigate the effect of PKR on CD4 T cell activity, expression of cytokines mainly produced by CD4 T cells during JHMV infection was determined using real time PCR analysis. Following JHMV infection, IFN γ is produced by both CD4 as well as CD8 T cells, while IL10 is produced at high level by CD4 T cells and at lower extent by CD8 T cells (Puntambekar et al., 2011) and IL21 is mainly secreted by CD4 T cells (Phares et al., 2011). The absence of PKR did not affect production of IFN γ at either mRNA (Figure 16A) or protein level in the CNS following virus infection. However, *Il10* (~ 6-7 fold) as

well as *Il21* (~ 2 fold) transcripts were reduced at day 7 and 10 p.i. in PKR^{-/-} mice compared to wt mice (Figure 16A).

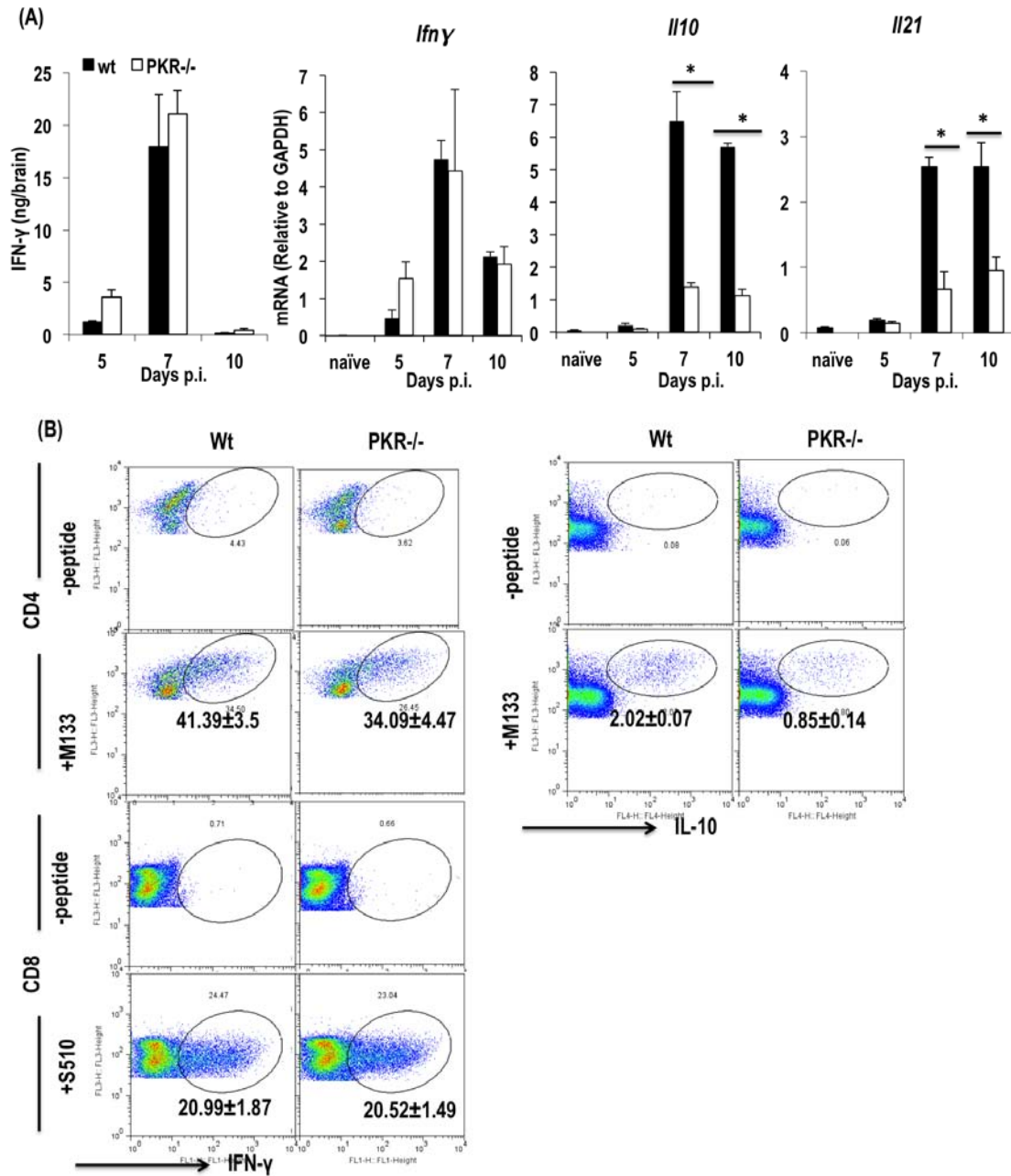


Figure 16. CD4 T cell function is specifically affected in PKR^{-/-} mice relative to wt mice. (A) Effector function of CD4 T cells was assessed by measuring mRNA expression of cytokines mainly produced by CD4 T cells following JHMV infection (high IFN γ , high IL10 and IL21). Data is represented as average of n = 3 mice/group/time-point \pm SEM. (B) Ability of CD8 and CD4 T cells to produce IFN γ and IL10 was determined using intracellular cytokine assay in splenocytes after stimulation with CD⁺ and CD4 specific peptides, S510 and M133, respectively. Frequency of IL10 producing CD4 T cells is presented as representative flow graph and data is also quantified as average of n = 3/group \pm SEM. Reduced effector functions associated primarily with CD4 T cells suggests reduced IL10 may contribute to enhanced pathology. * $p \geq .05$.

Reduced expression of *Il10* and *Il21* in CNS following JHMV infection indicates a defect in CD4 T cell to produce these cytokine in the absence of PKR. To verify a role of PKR in modulating CD4 T cell function, CD4 T cells were activated by peripheral infection and analyzed for cytokine secretion. C57Bl/6 mice were intra peritoneal injected with DM strain of JHMV (plaque variant of JHMV), which produces excellent peripheral response (Stohlman et al., 2008). Splenocytes were isolated 7 days p.i. and stimulated with MHC class II M133 peptide for 5 days to bias composition of spleen cells towards CD4 T cells enriched phenotype. Following restimulation with M133 peptide for 6 hours and then analyzed for IL10 or IFN γ production by intracellular staining. We observed reduced ability of CD4 T cells to secrete IL10 in the absence of PKR, but no defect in their ability to produce IFN γ compared to wt mice (Figure 16B). PKR has been implicated in regulating IL10 expression in monocytes, however first time in this report we demonstrated PKR mediated regulation of IL10 production in CD4 T cells.

3.3.4 PKR deficiency results in more diffuse demyelination, but does not contribute to clinical disease or survival

IL10 deficiency results in exacerbated demyelination following JHMV infection (Trandem et al., 2011). Due to the significant effects of PKR deficiency on IL10 transcription, spinal cords were assessed for myelin loss. Luxol fast blue (LFB) staining on cross sections of spinal cords from infected PKR $^{-/-}$ and wt mice revealed accelerated and more diffuse demyelination in absence of PKR. At day 7 p.i. demyelination was evident by very local vacuolization accompanied by

occasional swollen axons within the lesions in wt mice, but lesions were more pronounced in the absence of PKR, although axonal loss was not yet evident.

Demyelination in both groups was more extensive by day 10 p.i., but more widespread in PKR^{-/-} mice (Figure 17). However, enhanced demyelination did not affect progression or severity of clinical disease or survival rate of PKR^{-/-} compared to wt mice out to 21 days p.i. (Figure 18).

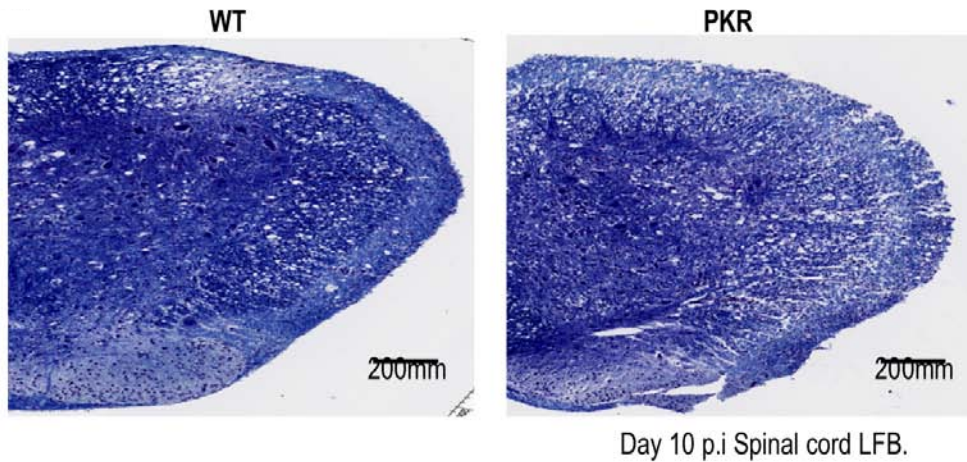


Figure 17. Demyelination but not axonal damage increased in PKR^{-/-} mice. The extent of demyelination was determined by staining cross sections of spinal cord with Luxol fast Blue (LFB) from wt and PKR^{-/-} mice at day 10 p.i. Data is representative of three separate.

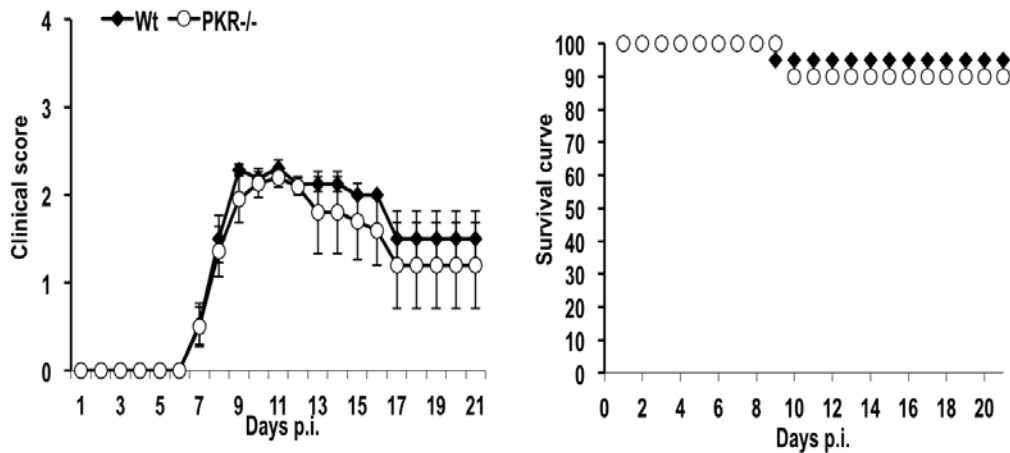


Figure 18. Clinical disease and mortality is not altered in absence of PKR. (Clinical disease and survival rate between wt and PKR^{-/-} mice was determined following intracranial JHMV infection. Data is representative of three separate (n ≥ 15 mice/group/time- point ± SEM).

3.3.5 Dual deficient mice in PKR and RNaseL depicts overall similar phenotype as RNaseL^{-/-} mice

Studies in mice deficient in either RNaseL or PKR indicated modest, but distinct roles in early antiviral function; nevertheless, RNaseL deficiency resulted in mortality, while PKR deficiency did not. To evaluate to what extent reduced elevated viral titers and reduced early proinflammatory responses by PKR deficiency may contribute to pathogenesis in RNaseL^{-/-} mice, mice dually deficient in RNaseL and PKR (DRP^{-/-}) were infected with JHMV. The additional absence of PKR did not influence mortality, severity or progression of clinical disease relative to RNaseL^{-/-} mice (Figure 19A), and ~80% succumbed to infection by day 10-12 p.i. We also observed higher viral burden similar to PKR^{-/-} mice by ~10-fold throughout acute infection, although it declined with kinetics similar to wt and RNaseL^{-/-} mice (Figure 19B). Higher virus titer even at day 10 p.i. in DRP^{-/-} mice (Figure 19B) compared to PKR^{-/-} or wt mice (Figure 13) indicated an additive effect of the absence of both RNaseL and PKR. To assess a defect in T cells potentially contributing to elevated virus titers at day 10 p.i., CNS infiltrating cells were examined for number and composition using flow cytometry. However, no alterations in either total numbers or composition were noted comparing DRP^{-/-} to wt mice (Figure 19C). To confirm a reduction in NFκB dependent pro-inflammatory cytokines/ chemokines (Figure 12B), mRNA expression of pro-inflammatory cytokines *Il6*, *Tnfα* and chemokines *Ccl5* and *Cxcl10* was examined in DRP^{-/-} mice relative to wt mice.

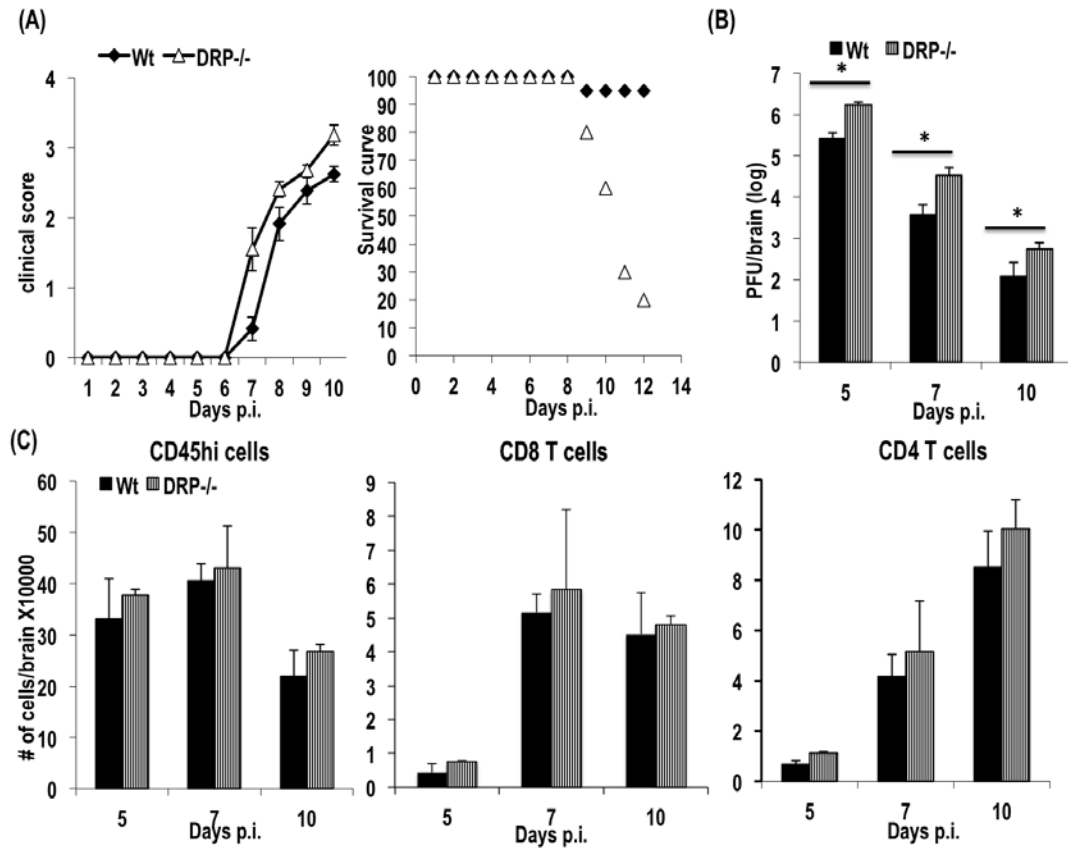


Figure 19. Dually deficient mice in PKR and RNaseL (DRP-/-) demonstrated high virus titers but overall similar phenotype as RNaseL-/- mice. (A) Following intracranial JHMV infection, clinical scores and survival rate were determined between wt and DRP-/- mice. Data is representative of three separate ($n \geq 15$ mice/group/time-point \pm SEM). (B) Virus replication in the CNS of wt and DRP-/- mice following JHMV infection. Data are mean of $n = 9$ mice/group/time-point from three independent experiments \pm SEM. And (C) Flow cytometric analysis of bone marrow derived CD45^{hi} infiltrating lymphocytes within the CNS following JHMV infection. Total number of CD8 and CD4 T cells isolated from the brains of infected mice. Data represents mean from three independent experiments \pm SEM. * $p \geq .05$.

Surprisingly, we did not observe any defect in expression of either cytokines or chemokines in DRP-/- mice compared to wt mice (Figure 20). These results indicate that absence of RNaseL rescued from impaired NF κ B mediated gene expression observed in absence of PKR.

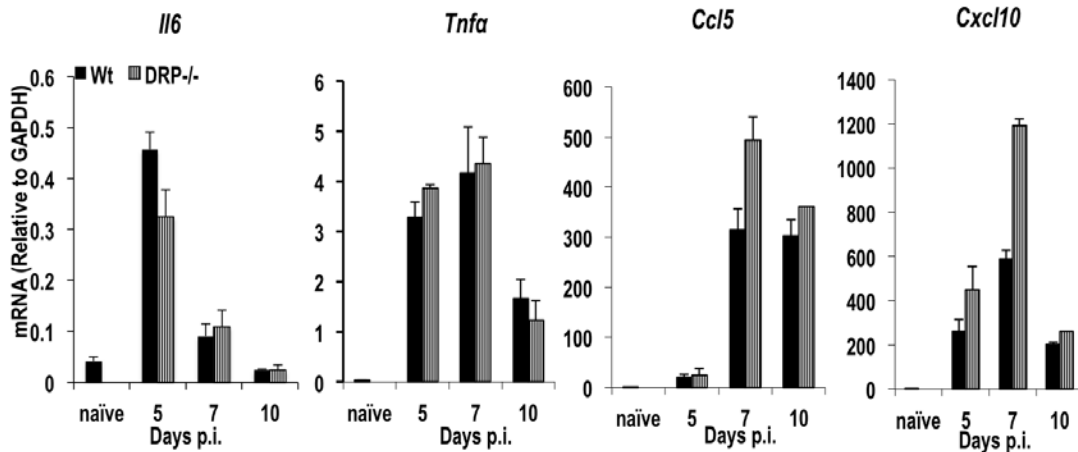


Figure 20. Dual deficiency of PKR and RNaseL reverses PKR mediated reduction in expression of NFκB induced pro-inflammatory genes. Expression of NFκB induced genes *Ii6*, *Tnfa*, *Ccl5*, and *Cxcl10* were determined relative to *Gapdh* in spinal cords of DRP-/- mice relative to wt mice, using real time PCR analysis. Data is represented as average of n = 3 mice/group/time-point ± SEM.

3.4 DISCUSSION

PKR and RNaseL are two well-characterized IFN α/β induced anti-viral molecules. The absence of RNaseL did not affect overall JHMV clearance from the CNS, although virus burden was elevated in CNS derived macrophage/microglia (Ireland et al., 2009). Nevertheless, RNaseL deficiency resulted in high mortality and accelerated demyelination and axonal damage. The limited antiviral effect of RNaseL suggested other anti-viral molecules play a more prominent role in preventing initial viral spread throughout the CNS following JHMV infection. PKR was chosen as a candidate based on its ability to block translation, but also to indirectly inducing IFN α/β production (O'Malley et al., 1986). A recent report further suggested that PKR can affect the ability of CD8 T cells to control virus replication, but without altering effector function in response to LCMV infection (Nakayama et al., 2010). Unlike the LCMV model, the absence of PKR did result in higher virus titers early during JHMV infection, but we could

not detect a cell type specific effect by histology. Furthermore, there were no global defects in expression of IFN α/β or the ISGs, *Ifit1* and *Ifit2*. Similar expansion of virus-specific CD8 T cells and kinetics of viral control also ruled out alterations in the CD8 T cell response.

Reduced expression of cytokine/chemokine such as *Il6*, *Tnf α* , *Ccl5* and *Cxcl10* in the absence of PKR is attributed to defective transcriptional activation of NF κ B mediated pro-inflammatory genes (Brain Williams, 1994, PNAS). All these genes have been reported to play an important role in recruiting and facilitating infiltration of leukocytes through the BBB into the CNS parenchyma. Specifically expression of CXCL10 and CCL5 has been shown to facilitate T cell recruitment, predominantly CD4 T cells to the CNS following JHMV infection (Glass et al., 2004, Liu et al., 2001). It was therefore surprising that the lack of PKR resulted in a transient increase in CNS infiltrating CD8 T cells at day 7 p.i. and significantly higher number of CD4 T cells at day 7 and day 10 p.i. Nevertheless, a large fraction of CD4 T cells accumulated within the perivascular space, suggesting they were inhibited from entering the parenchyma, or were continuously recruited from the periphery. Various studies have indicated the important role of integrins as well as chemokines in migration of lymphocytes across the blood vessels to the perivascular space (Ley et al., 2007). Reduced monocyte infiltration also resulted in increased retention of T cells in the perivascular space following JHMV infection (Savarin et al., 2010). However, we did not observe any deficiency in the monocyte recruiting chemokine *Ccl2*, consistent with similar monocyte infiltration in PKR $^{-/-}$ mice compared to wt mice.

The mechanism underlying enhanced perivascular T cell accumulation may reside in differential positioning of chemokines (McCandless et al., 2006, McCandless et al., 2008, Savarin et al., 2010), or overall reduced proinflammatory cytokine/chemokine expression.

Previous reports have implicated role of PKR in upregulation of the anti-inflammatory cytokine IL10 in a NF κ B, ERK1/2 and JNK1 dependent manner as a response to mycobacterium, bacterial lipopolysaccharide, dsRNA and sendai virus infection (Chakrabarti et al., 2008, Cheung et al., 2005, McCandless et al., 2006, McCandless et al., 2008, Savarin et al., 2010). IL21 has been shown to induce IL10 in a mouse model of autoimmunity of systemic lupus erythematosus (SLE) (Spolski et al., 2009) (Roassne spoliski, 2009, JI). In response to JHMV infection, both IL10 and IL21 are mainly produced by CD4 T cells (Phares et al., 2011, Puntambekar et al., 2011). Here we demonstrated for the first time, that PKR controls the expression of both IL10 and IL21 in CD4 T cells. The inability of CD4 T cells to produce IL10 following *ex vivo* stimulation with peptide (M133) demonstrated that the defect in IL10 was both at the transcriptional and protein level. However, IFN γ production by CD4 T cells was not affected and CD8 T cells were capable of effective viral clearance in PKR^{-/-} mice indicating that PKR specifically affects the ability of CD4 T cells to produce IL21 and IL10.

PKR also exacerbates pathology in various neurological diseases. Strong induction of activated PKR (phosphorylated PKR) in hippocampal neurons has been associated with their loss in pathologies associated with Alzheimer's disease, Huntington disease, and Parkinson's disease (Bando et al., 2005, Peel

and Bredesen, 2003). Similarly, the absence of PKR provides protection from extensive spinal cord damage during poliomyelitis infection (Scheuner et al., 2003). Contrary to these reports, we observed accelerated and more diffuse demyelination in absence of PKR following JHMV CNS infection. The enhanced pathology observed in PKR^{-/-} mice may be attributed to reduced expression of the anti-inflammatory cytokine IL10 (Trandem et al., 2011). IL10 reduces the (Lipton et al., 2007) expression of pro-inflammatory cytokines such as IL6, TNF α and IFN γ expression in the CNS following JHMV infection (Lin et al., 1998). Lastly, although an imbalance between pro- versus anti-inflammatory responses in the CNS has been linked to increased severity of clinical symptoms, progression of clinical disease and mortality was not altered in PKR^{-/-} compared to wt mice. These data supported the notion that IFN γ , which was not altered, drives clinical symptoms following JHMV infection. Moreover, double deficient mice in PKR and RNaseL demonstrated overall similar phenotype as RNaseL^{-/-} mice. This finding would indicate that reduced expression of pro vs anti-inflammatory response observed in PKR^{-/-} mice was mitigated in absence of RNaseL.

In summary, the absence of PKR contributed to increased viral replication, albeit with little consequences on T cell mediated viral control. Surprisingly however, PKR deficiency resulted in significantly reduced expression of both pro- as well as anti-inflammatory responses, without affecting overall pathogenesis. These results are the first to demonstrate numerous effects of PKR at multiple levels in CNS resident cells as well as CD4 T cells. While the role of PKR in

regulating pro- versus anti-inflammatory responses during CNS infection had no overt overall phenotype, its effect in other inflammatory diseases remains to be determined.

CHAPTER IV

IL12, BUT NOT IL23, DEFICIENCY AMELIORATES VIRAL ENCEPHALITIS WITHOUT AFFECTING VIRAL CONTROL¹

Kapil, P., Atkinson, R., Ramakrishna, C., Cua, D.J., Bergmann, C.C. and
Stohlman, S.A.

4.1 Abstract

The relative contribution of IL12 and IL23 to viral pathogenesis has not been extensively studied. IL12p40 mRNA rapidly increases following neurotropic coronavirus infection. Infection of mice defective in both IL12 and IL23 (p40^{-/-}), or IL12 (p35^{-/-}) and IL23 (p19^{-/-}) alone, revealed that the symptoms of coronavirus induced encephalitis are regulated by IL12. IL17 producing cells never exceeded background levels, supporting a redundant role of IL23 in pathogenesis. Viral control, tropism, and demyelination were all similar in p35^{-/-}, p19^{-/-} and wild type (wt) mice. Reduced morbidity in infected IL12 deficient mice was also not associated with altered recruitment or composition of inflammatory cells. However, IFN γ levels and virus specific IFN γ secreting CD4 and CD8 T cells

¹ This work has been published in the form of a research article (Parul Kapil, Roscoe Atkinson, Chadran Ramakrishna, Daniel J. Cua, Cornelia C. Bergmann and Stephen A. Stohlman. 2009 . JVI. 83. 5978-5986).

were all reduced in the CNS of infected p35^{-/-} mice. Transcription of the pro-inflammatory cytokines *Il1β* and *Il6*, but not *Tnf* were initially reduced in infected p35^{-/-} mice, but increased to wild type levels during peak inflammation.

Furthermore, although *Tgfβ* mRNA was not affected, IL10 was increased in the CNS in the absence of IL12. These data suggest that IL12 does not contribute to antiviral function within the CNS, but enhances morbidity associated with viral encephalitis by increasing the ratio of IFN γ to protective IL10.

4.2 Introduction

Resistance to infection, as well as the extent of clinical symptoms, is directly influenced by the pattern and magnitude of cytokine induction. Specifically, interferon gamma (IFN γ) is closely associated with control of many viruses and other intracellular pathogens (Novelli and Casanova, 2004, Scott and Kaufmann, 1991). IFN γ secretion in turn is enhanced by interleukin-12 (IL12), which in concert with the related cytokine IL23, participates in regulating both innate and adaptive immune responses (Hunter, 2005, Langrish et al., 2004, Novelli and Casanova, 2004, Jouanguy et al., 1999, Trinchieri, 2003). IL12 is a heterodimeric cytokine composed of two subunits (IL12p35 and IL12p40) secreted primarily by macrophages and dendritic cells. It is a potent inducer of IFN γ secretion by CD4 T cells, even in the presence of T regulatory cells (King and Segal, 2005). It also increases cytokine secretion as well as cytolytic potential of NK cells and CD8 T cells (Trinchieri, 2003). IL12 is rapidly induced in the periphery and the central nervous system (CNS) following a variety of viral infections (Coutelier et al., 1995, Parra et al., 1997, Trinchieri, 2003, Novelli and

Casanova, 2004); however, its contribution to virus resistance varies depending upon tissue tropism and predominant effector mechanisms employed to control virus replication. For example, IL12 is critical to control murine cytomegalovirus, while it is dispensable for immune responses to lymphocytic choriomeningitis virus; IFN γ is nevertheless required for resistance to both these infections (Orange and Biron, 1996b, Oxenius et al., 1999, Novelli and Casanova, 2004). Although IFN γ is a critical component in the protective host immune response to many viruses, not all viral infections are associated with IL12 mediated enhancement of the IFN γ response (Novelli and Casanova, 2004, Trinchieri, 2003).

IL23 shares both the IL12p40 subunit and the IL12 receptor (IL12R) β 1 subunit with IL12 (Hunter, 2005, Trinchieri, 2003, Langrish et al., 2004) and similar to IL12, IL23 is primarily secreted by macrophages and dendritic cells. The role(s) of IL23 in innate and adaptive immunity have only recently begun to come to light (Hunter, 2005, Langrish et al., 2004). A primary consequence is induction of CD4 T cells secreting IL17, which play a prominent role in neutrophil recruitment to sites of inflammation (Aggarwal et al., 2003, Kolls and Linden, 2004, Langrish et al., 2004, McGeachy and Cua, 2008). Unlike the IL12R, IL23R is not expressed by naïve T cells but is present on memory T cells (McGeachy and Cua, 2008). Differential receptor expression is consistent with IL23 independent induction of IL17 secreting CD4 T cells (Langrish et al., 2004, McGeachy and Cua, 2008); however, it is required for sustained expression of autoimmune T cell effector function associated with autoimmune demyelination of the CNS (Cua et al., 2003, McGeachy and Cua, 2008). During chronic

mycobacterial and HIV infections IL23 functions as a regulator of the protective IFN γ response (Khader et al., 2005, Novelli and Casanova, 2004) but also dampens immune pathology during herpes simplex infection of the eye (Kim et al., 2008). However, IL23 has a limited capacity to influence resistance in the absence of IL12 (Khader et al., 2005, Lieberman et al., 2004).

Infection of the CNS with the neurotropic JHM strain of mouse hepatitis virus (JHMV) induces an acute encephalomyelitis accompanied by myelin loss. Virus replicates in microglia, astrocytes and oligodendroglia, but only rarely in neurons and is controlled by a vigorous inflammatory response localized to the CNS (Bergmann et al., 2006). CD8 T cells exert crucial antiviral functions via perforin and IFN γ mediated mechanisms (Bergmann et al., 2006, Bergmann et al., 2003, Parra et al., 1999); however, recent data indicates that CD4 T cells alone can also mediate virus clearance (Savarin et al., 2008, Stohlman et al., 2008). The critical requirement for IFN γ in combating JHMV infection is demonstrated by prolonged virus replication, and increased clinical disease and mortality in IFN γ deficient mice (Parra et al., 1999). In the absence of IFN γ , virus preferentially resides in oligodendroglia demonstrating a cell specific action of IFN γ within the CNS (Gonzalez et al., 2006). Furthermore, morbidity and mortality are dramatically increased in JHMV infected immunodeficient recipients of CD4 T cells unable to secrete IFN γ (Pewe et al., 2002, Savarin et al., 2008). Although demyelination, a hallmark of JHMV infection, is an immune mediated manifestation of tissue destruction rather than a direct viral cytopathic effect (Bergmann et al., 2006, Matthews et al., 2002), a contribution of IFN γ to myelin

loss is controversial. Similar myelin loss in infected IFN γ ^{-/-} mice compared to controls (Parra et al., 1999), as well as demyelination induced by IFN γ deficient CD4 or gamma delta T cells in the context of immunodeficient hosts implicate an immune component other than IFN γ in contributing to demyelination (Bergmann et al., 2003, Dandekar and Perlman, 2002). By contrast, T cell transferred into infected immunodeficient recipients suggest that IFN γ secretion by CD4 T cells limits demyelination (Pewe et al., 2002), while IFN γ secretion by CD8 T cells contributes to demyelination (Bergmann et al., 2003, Bergmann et al., 2004, Pewe and Perlman, 2002).

IFN γ thus plays a key role in regulating clinical disease, mortality, control of virus replication and myelin loss following JHMV infection of the CNS. To determine the contribution of IL12 to JHMV pathogenesis, as well as a possible indirect contribution of IL23 to myelin loss, antiviral immune responses and tissue damage were examined in infected IL12/IL23 (p40^{-/-}), IL12 (p35^{-/-}), and IL23 (p19^{-/-}) mice. The data demonstrate that IL12 enhances the magnitude of the IFN γ response in the CNS following infection, albeit without affecting viral control. However, decreased clinical disease in IL12 deficient mice indicates that IL12 induced IFN γ and a concomitant reduction in IL10 contributes to the disability associated with JHMV induced encephalomyelitis. By contrast, no differences in demyelination were detected in JHMV infected mice deficient in either IL12 or IL23, suggesting that neither of these cytokines influences virus induced demyelination.

4.3 Results

4.3.1 IL12 enhances JHMV induced encephalitis

Increased transcription of IL12p40 occurs within the CNS rapidly following JHMV infection (Parra et al., 1997) implicating a possible role for IL12 and/or IL23 in the pathogenesis of JHMV encephalitis. Recent data further suggested that IL12p35 mRNA is rapidly induced and that IL23p19 mRNA transcription increases subsequent to virus clearance from the CNS (Held et al., 2008). However, the latter results were not correlated with IL12p40 mRNA expression. As previous reports relied upon semi-quantitative measures of mRNA, we sought to confirm the activation of IL12 and/or IL23 during JHMV infection of the CNS by real time PCR. Expression of p40 mRNA was below detection levels in the CNS of naïve animals, but was rapidly induced following infection (Figure 21), consistent with previous data (Parra et al., 1997). Although p40 mRNA declined rapidly after day 5 post infection (p.i.), it remained above basal levels to day 14 p.i. In contrast to the mRNA encoding the IL12 and IL23 common p40 chain, both the IL12 specific p35 subunit and the IL23 specific p19 subunit were detected at relatively low levels in the CNS of naïve animals (Figure 21). However, expression of both p35 and p19 mRNA remained at or near basal levels following JHMV infection (Figure 21). Despite the inability to detect upregulation of these mRNAs, the increase of IL12/23 p40 mRNA suggested that either IL12 or IL23 may play important roles in the pathogenesis of JHMV.

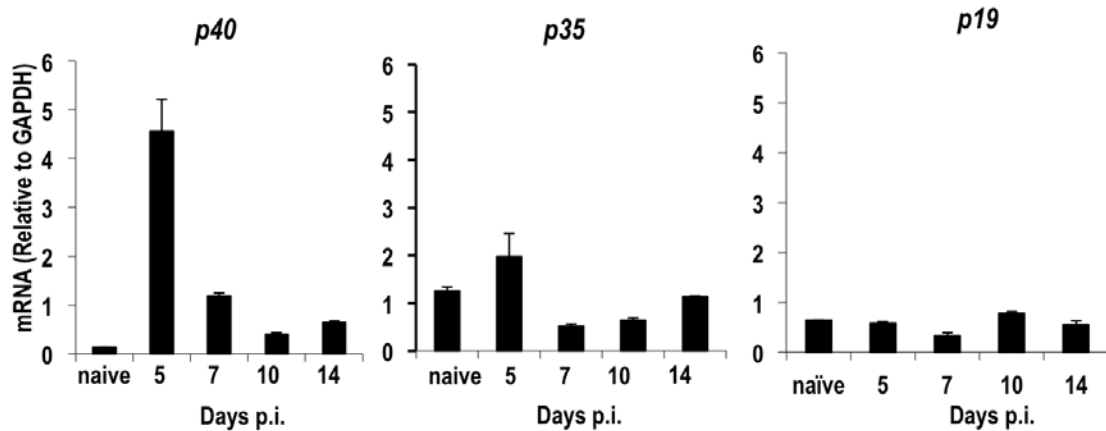


Figure 21. JHMV infection induces IL12p40 expression within the CNS. Expression of IL12p40, IL12p35, and IL23p19 mRNA in the CNSs of JHMV infected mice at various time p.i. The data reflect induction relative to Gapdh, using the following formula: $(2^{[CT(GAPDH) - CT(Target)]}) \times 100$, where C_T is the threshold cycle. The data are the means of three mice per time point \pm the standard error mean (SEM). (Kapil et al., 2009)

The potential role(s) of IL12 and IL23 on JHMV induced encephalomyelitis were thus investigated in IL12/IL-23 deficient ($p40^{-/-}$) mice. Following infection of wt mice clinical symptoms of encephalitis were initially detected at day 7 p.i., progressed to a peak between days 10-12 p.i. and then began to decline (Figure 22). By contrast, initial onset of symptoms was delayed in $p40^{-/-}$ mice (Figure 22). Furthermore, although clinical symptoms in infected $p40^{-/-}$ mice peaked at days 10-12 p.i. similar to wt mice, severity was substantially reduced (Figure 22). To determine a dominant contribution of either IL12 or IL23 to morbidity, progression and severity of clinical disease was examined following infection of mice specifically deficient in either IL12 ($p35^{-/-}$) or IL23 ($p19^{-/-}$). Delayed onset, as well as a significant reduction in peak symptoms, was only observed following infection of IL12 deficient mice (Figure 22). IL23 deficient mice exhibited no difference in onset or maximum clinical symptoms compared to wt mice (Figure 22). Mortality was also similar (~20%) in infected wt and $p19^{-/-}$ mice. By contrast,

mortality in infected p35^{-/-} and p40^{-/-} mice was reduced (~5%) compared to wt mice. These data indicate that IL2, but not IL23, plays a critical role in regulating the morbidity and mortality associated with acute viral encephalitis. Subsequent studies thus focused on analysis of p35^{-/-} mice.

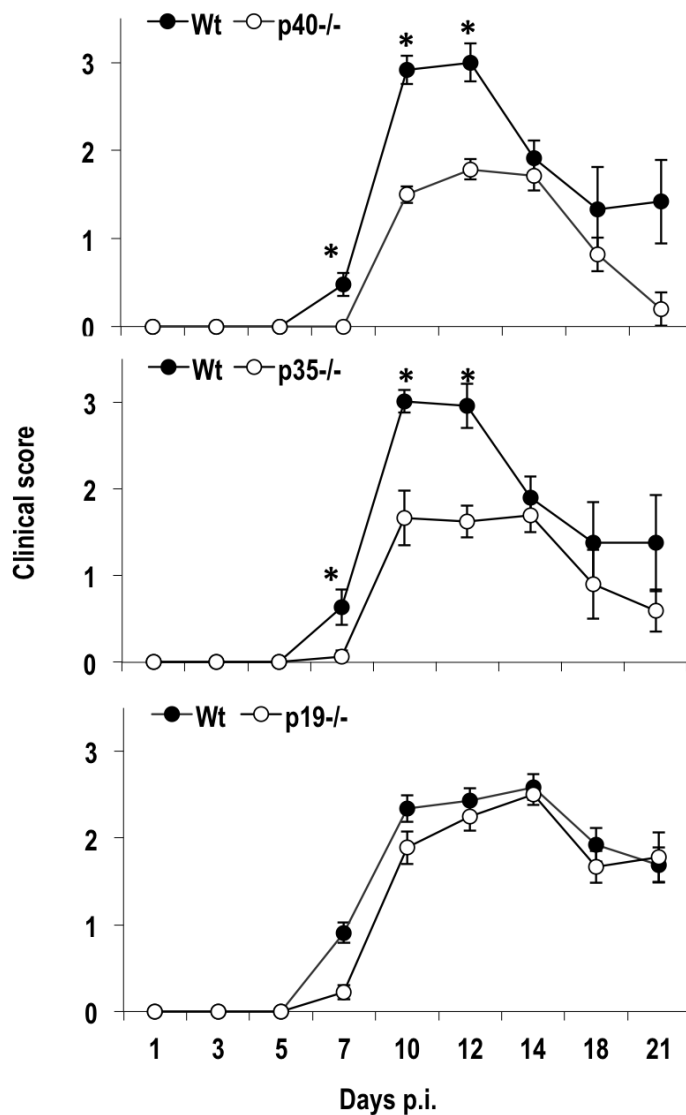


Figure 22. IL12 deficiency decreases the symptoms of virus-induced encephalitis. JHMV infected p40^{-/-}, p35^{-/-}, and p19^{-/-} mice were examined for disease severity at various times p.i. The data are representative of two separate experiments for each strain with n>20 per experiment ± SEM. * p ≤ 0.05 (compared to wt). (Kapil et al., 2009)

Clearance of infectious virus from the CNS of p35^{-/-} and control mice was compared to assess whether reduced morbidity reflected enhanced control of virus replication. Infectious virus peaked in the CNS to similar levels at day 5 p.i. It was subsequently controlled with equal efficiency in both groups and by day 14 p.i. infectious virus was at the limit of detection in both groups of mice (Figure 23). The apparent redundancy of IL12 in clearance of infectious virus is consistent with the absence of altered CNS virus replication in mice treated with anti-IL12 antibody (Held et al., 2008). Similarly, no alteration in virus replication within the CNS was detected in mice treated with anti-IL23 antibody (Held et al., 2008) and no differences were detected in virus replication or clearance comparing JHMV infected p19^{-/-} and wt mice (data not shown). These data indicate that while IL12 plays an important role in the onset and severity of morbidity, it does not influence virus clearance.

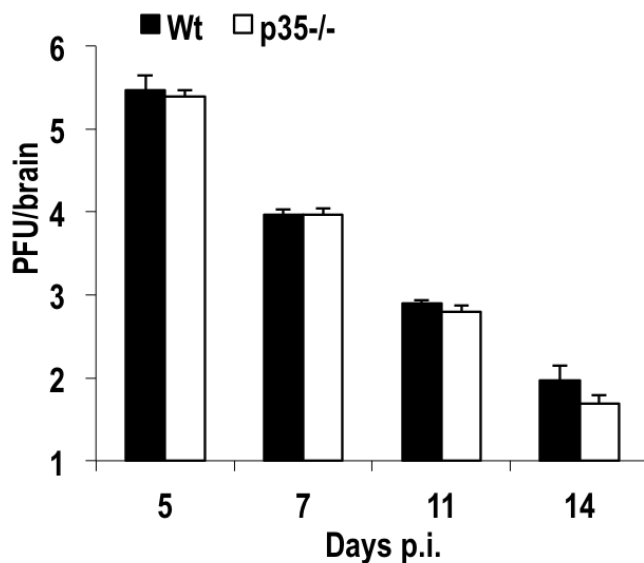


Figure 23. IL12 does not influence control of infectious virus. Virus replication in the CNS of p35^{-/-} and wt mice following JHMV infection. The data are representative of two independent experiments and show the mean of four individual mice per time point \pm SEM. (Kapil et al., 2009)

4.3.2 IL12 does not alter CNS inflammation

Reduced morbidity during acute infection suggested that leukocytes infiltration into the CNS might be altered in the absence of IL12. However, analysis of CD45^{hi} bone marrow derived inflammatory leukocytes showed no difference in overall recruitment into the CNS of JHMV infected p35^{-/-} mice compared to wt mice throughout infection (Figure 24A). Recruitment of inflammatory cells was also similar following infection of p19^{-/-} mice (data not shown). There were also no differences in recruitment of Ly6G⁺ neutrophils or F4/80⁺ monocytes within the CD45^{hi} inflammatory populations at any time point p.i. in either p35^{-/-} or p19^{-/-} mice (data not shown). Lastly, to determine if reduced clinical disease correlated with altered recruitment of T cell subsets, CD8 and CD4 T cells within the infiltrating lymphocyte populations were examined. A slight decrease in total CNS infiltrating CD8 T cells was detected in infected p35^{-/-} relative to wt mice at days 7 and 10 p.i., which only reached statistical significance at day 7 p.i. (Figure 24B). Virus specific tetramer⁺ cells specific for the dominant S510 epitope encoded within the viral spike glycoprotein comprised ~ 40% of CD8 T cells at day 7 and ~60% at day 10 p.i. in both groups (data not shown). Similar recruitment of virus specific CD8 T cells was consistent with the ability of the p35^{-/-} mice to control infectious virus (Figure 23). The absence of IL12 was also associated with a slight decrease in CD4 T cell CNS infiltration throughout infection (Figure 24C), reaching statistical significance at day 10 p.i. In summary, although IL12 did not affect recruitment of innate immune cells, total CD8 and CD4 T cells were reduced at 7 and 10 days p.i., respectively.

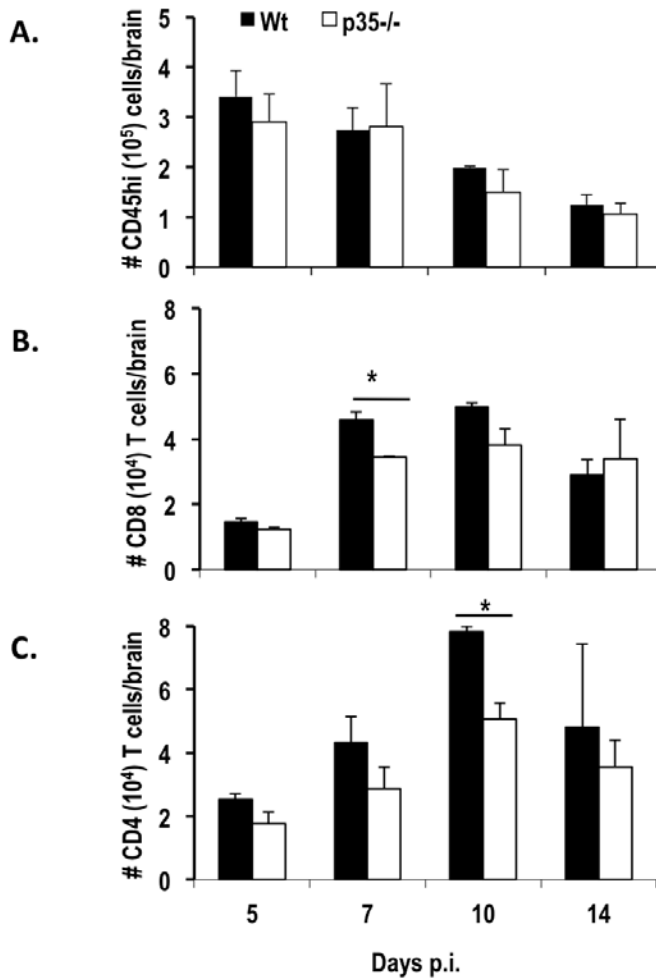


Figure 24. Decreased CD4 T cell recruitment into the CNS of p35^{-/-} mice. (A) Flow Cytometric analysis of bone marrow derived CD45^{hi} infiltrating cells within the CNS following JHMV infection. Total numbers of CD8 T cells (B) and CD4 T cells (C) isolated from the brains of infected mice. The Data represent the mean of three independent experiments \pm SEM. (Kapil et al., 2009).

4.3.3 IFN γ is compromised in the absence of IL12

In addition to its antiviral function (Bergmann et al., 2006, Gonzalez et al., 2006, Parra et al., 1997), IFN γ has been suggested to regulate clinical symptoms during JHMV induced encephalitis (Pewe et al., 2002). IFN γ is primarily secreted by activated T cells during JHMV infection, with no contribution by NK cells (Zuo et al., 2006, Savarin et al., 2008, Bergmann et al., 2006, Gonzalez et al., 2006). Although IL12 is a powerful inducer and enhancer of IFN γ secretion by T cells,

IL12 independent activation of IFN γ producing T cells has been described following a number of viral infections (Novelli and Casanova, 2004, Trinchieri, 2003). Thus, the frequency of CNS derived virus specific T cells producing IFN γ was examined. In the absence of IL12, frequencies of virus specific CD8 and CD4 T cells secreting IFN γ were consistently reduced at day 7 p.i. and. Although slightly variable between independent assays, on average the frequencies of CD4 and CD8 T cells were reduced by 30% - 40% compared to T cells from the CNS of wt mice. Overall, the impact of IL12 deficiency was greater on the CD4 T cell population at day 7 p.i. (Figure 25B). The enhancing affect of IL12 on IFN γ secretion by CD4 T cells becomes especially evident when the data reflect total numbers of virus specific T cells per brain (Figure 25C). At day 10 p.i. the proportion of IFN γ secreting CD8 T cells was comparable in wt and p35^{-/-} mice (~36%); however, the fraction of CD4 T cells secreting IFN γ in the CNS of the p35^{-/-} mice remained at ~60% of wt levels (data not shown). By contrast, no difference in the frequency of IFN γ producing CD4 T cells was detected in CLN (Figure 25D) or spleen (data not shown), excluding a peripheral impairment of T cell activation and expansion. Furthermore, reduced frequencies of virus specific IFN γ producing cells were not attributable to an increase in IL17 secreting cells, as these remained below 0.5% in both the CD4 and CD8 T cell compartments in wt as well as p35^{-/-} mice (data not shown).

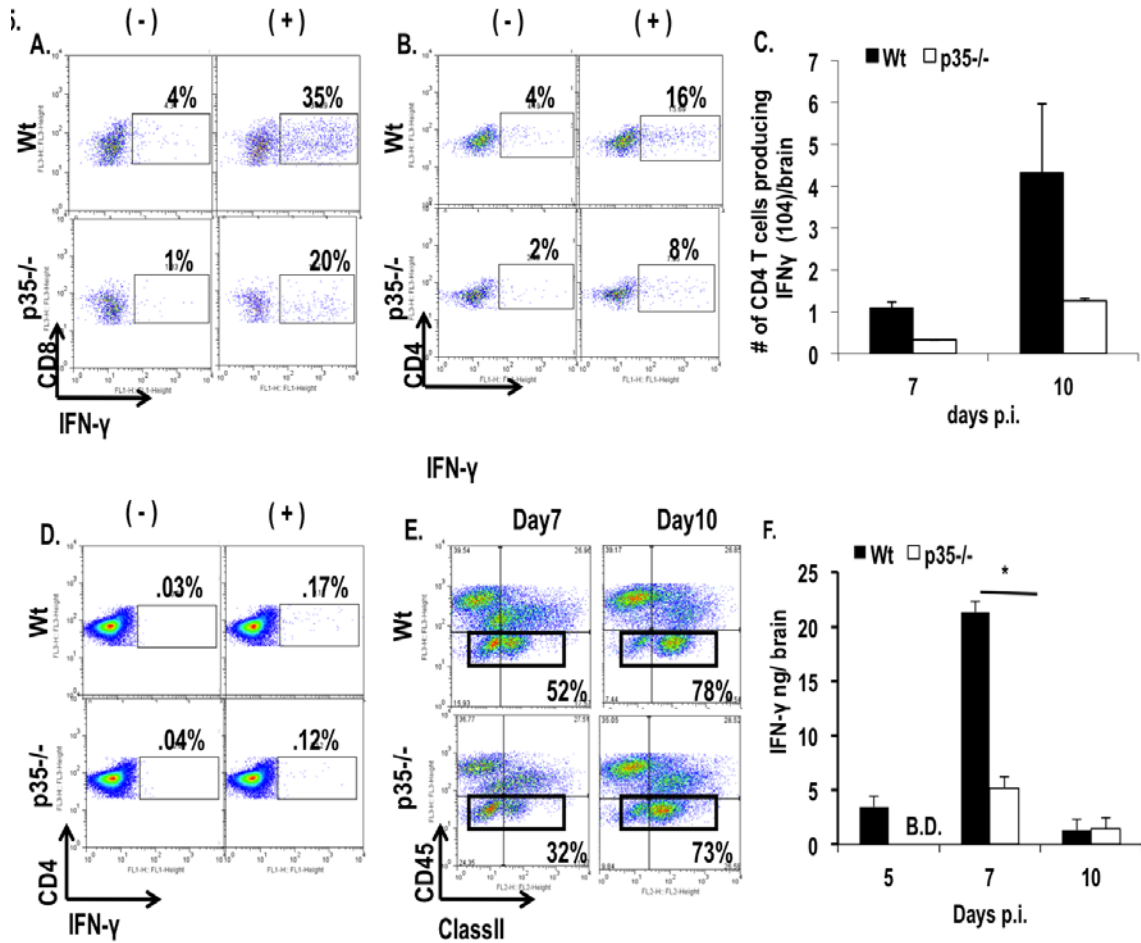


Figure 25. IL12 enhances IFN γ production and Class II expression. Frequencies of CNS derived IFN γ secreting T cells at day 7 p.i. (A) CD8 T cells following stimulation with S510 peptide and (B) CD4 T cells with M133 peptide. Data are representative of two separate experiments analyzing cells combined from n = 4-6 individuals (C) Number of CNS derived CD4 T cells producing IFN γ after ex vivo peptide stimulation in infected wt and p35^{-/-} mice at days 7 and 10 p.i. Data represent the mean of two independent experiments \pm SEM. (D) Frequencies of CLN derived IFN γ secreting CD4 T cells at day 7 p.i. following stimulation in presence or absence of M133 peptide. Data are representative of two separate experiments analyzing cells combined from n = 4-6 individuals (E) IFN γ dependent MHC class II expression on CD45⁺ microglia (boxed cells) at days 7 and 10 p.i. (F) Cell free homogenates of the infected CNS were examined for IFN γ by ELISA. Data show the mean of n = 4 per time point \pm SEM and are representative of two separate experiments. Asterisks indicate statistical significance p \leq 0.05, compared to wt. (Kapil et al., 2009)

During JHMV infection MHC class II expression on microglia correlates with IFN γ levels within the CNS (Bergmann et al., 2003). To determine if the absence of IL12 also compromised IFN γ secretion in the CNS *in vivo*, microglia were examined for upregulation of major histocompatibility complex class II molecules. Microglia from infected p35^{-/-} mice was indeed characterized by an

initial delay in class II expression relative to Wt mice (Figure 25E). However, by day 10 p.i. class II expression on microglia was identical in both groups. IFN γ within the CNS was measured by ELISA to assess to what extent the delay in class II upregulation correlates with IFN γ protein levels. In infected Wt mice, IFN γ was detectable at day 5 p.i., increased significantly by day 7 p.i., and then declined substantially by day 10 p.i. By contrast, in absence of IL12, IFN γ was undetectable at day 5 p.i., and only increased modestly by day 7 p.i. (Figure 25F). IFN γ levels within the CNS were similarly low in both groups by day 10 p.i. (Figure 25F), when infectious virus was already reduced. These data suggest that even under optimal re-stimulation conditions, the capacity of T cells derived from an IL-12 deficient CNS environment to produce IFN γ is reduced (Figure 25C). This deficit was more strongly manifested in vivo, where MHC/antigen density, and thus T cell stimulation, is more limited. Significantly reduced IFN γ levels in the CNS of p35^{-/-} mice correlated with delayed class II expression on microglia and reduced morbidity. Nevertheless, similar and sustained class II expression at day 10 p.i. suggested that the reduced IFN γ in the absence of IL12 were still sufficient to drive optimal class II expression late during infection and sustain viral control.

4.3.4 Viral induced demyelination is IL12 and IL23 independent

IFN γ is critical for the control of JHMV infection in oligodendroglia (Gonzalez et al., 2006, Parra et al., 1999); however, demyelination in the host with an otherwise intact immune system is independent of IFN γ (Gonzalez et al., 2006, Parra et al., 1999). Although demyelination associated with experimental

autoimmune encephalitis is dependent upon IL23 expression (Cua et al., 2003, Langrish et al., 2004, McGeachy and Cua, 2008) the mechanism of myelin loss following JHMV infection is unclear (Matthews et al., 2002). Therefore, potential alterations in inflammation, demyelination and viral tropism in p35^{-/-} and p19^{-/-} mice were compared with Wt mice. Despite the delayed onset of clinical symptoms and reduced severity in p35^{-/-} mice (Figure 22) no difference in inflammation or cells expressing viral antigen were detected compared to wt (Figure 26). Although a slight increase in myelin loss was apparent in infected p35^{-/-} mice (Figure 26) it did not reach statistical significance due to variability between individuals. Similarly, the inability to secrete IL23 did not alter viral induced inflammation or demyelination (Figure 26). These data are consistent with an IFN γ independent mechanism of demyelination (Gonzalez et al., 2006).

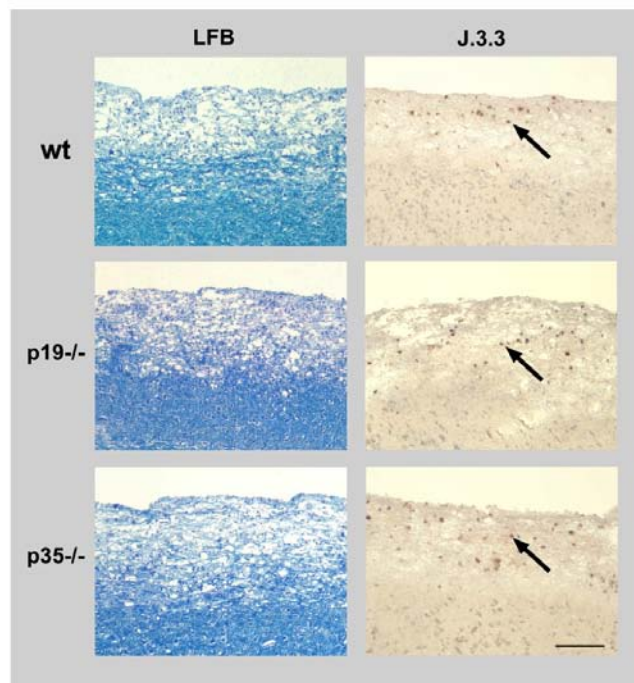


Figure 26. IL12 and IL23 do not influence viral pathogenesis. Longitudinal sections of spinal cords from JHMV infected wt, p35^{-/-} and p19^{-/-} at day 10 p.i. The extent of demyelination as shown by luxol fast blue (LFB). Viral antigen (arrows) detected by immunohistochemical analysis for viral nucleocapsid using mAb J.3.3. Bar = 200 microns. (Kapil et al., 2009)

4.3.5 IL12 regulation of innate cytokine, chemokine and anti-inflammatory cytokines

Ameliorated clinical symptoms in the absence of IL12 suggested three possible mechanisms: 1) diminished activation of pro-inflammatory genes; 2) reduced chemokine expression; or 3) increased activation of anti-inflammatory genes. Expression of genes associated with the acute JHMV response or with induction or severity of clinical disease were compared in $p35^{-/-}$ and wt mice. Based on the crosstalk between IL12 and type I interferons in regulating IFN γ responses (Cousens et al., 1997, Cousens et al., 1999, Orange and Biron, 1996b, Novelli and Casanova, 2004, Trinchieri, 2003), IFN α 4 and IFN β mRNA levels were initially compared. Transcription of both mRNAs in the CNS was reduced by ~40%-50% in the absence of IL12 (data not shown). Nevertheless, the reduction was insufficient to alter infectious virus load or increase the tropism for neurons (Figure 26), previously shown to correlate with the inability to respond to IFN α/β (Ireland et al., 2008). IL12 enhances secretion of IFN γ indirectly via enhanced IL1 β and TNF secretion, thereby initiating production of inducible nitric oxide synthase (iNOS) in addition to other IFN γ inducible genes (Novelli and Casanova, 2004). Decreased IFN γ in the absence of IL12 was indeed reflected in decreased CNS expression of the mRNA encoding *iNos* (data not shown). Furthermore, consistent with their role in regulating clinical symptoms *Il6* and *Il1 β* mRNA were reduced in infected $p35^{-/-}$ mice at day 5 p.i. (Figure 27A). However, no difference in transcription of these genes was detected at day 7 p.i. (Figure 27A), when the $p35^{-/-}$ group exhibited a significant decrease in morbidity (Figure

22). Although expression of *Tnf* mRNA was also slightly reduced in the CNS of infected IL-12^{-/-} mice at day 5p.i., the difference did not reach statistical significance (Figure 27A). These data suggest that the initial decrease in pro-inflammatory cytokines contributes to the delayed onset of clinical symptoms.

Reduced recruitment of T cells into the CNS of infected p35^{-/-} mice suggested a possible defect in chemokine induction following infection in absence of IL12. However, *Cxcl10* mRNA expression was only transiently reduced ~2 fold at day 5p.i. in the absence of IL12. *Cxcl10* mRNA increased to wt levels by day 7 p.i. and no differences were observed in expression of *Cxcl9* or *Ccl5* mRNA (Figure 27B). Although expression levels were equivalent by day 7 p.i., early differences presumably shape the responsiveness to chemokines and cytokines later during infection, thus maintaining overall decreased morbidity.

Based on their association with diminished clinical symptoms of EAE (Prud'homme, 2000), expression of *Tgfβ* and IL10 were examined as down regulatory candidates in JHMV infected p35^{-/-} mice. In contrast to the pro-inflammatory cytokines, no significant alterations in *Tgfβ* mRNA were detected relative to wt controls (Figure 27C). However, IL10 was increased in the CNS of p35^{-/-} mice at days 5, 7 and 10 p.i. (Figure 27D). Decreased morbidity was thus associated with decreased expression of pro-inflammatory cytokines as well as increased expression of the anti-inflammatory cytokine IL10.

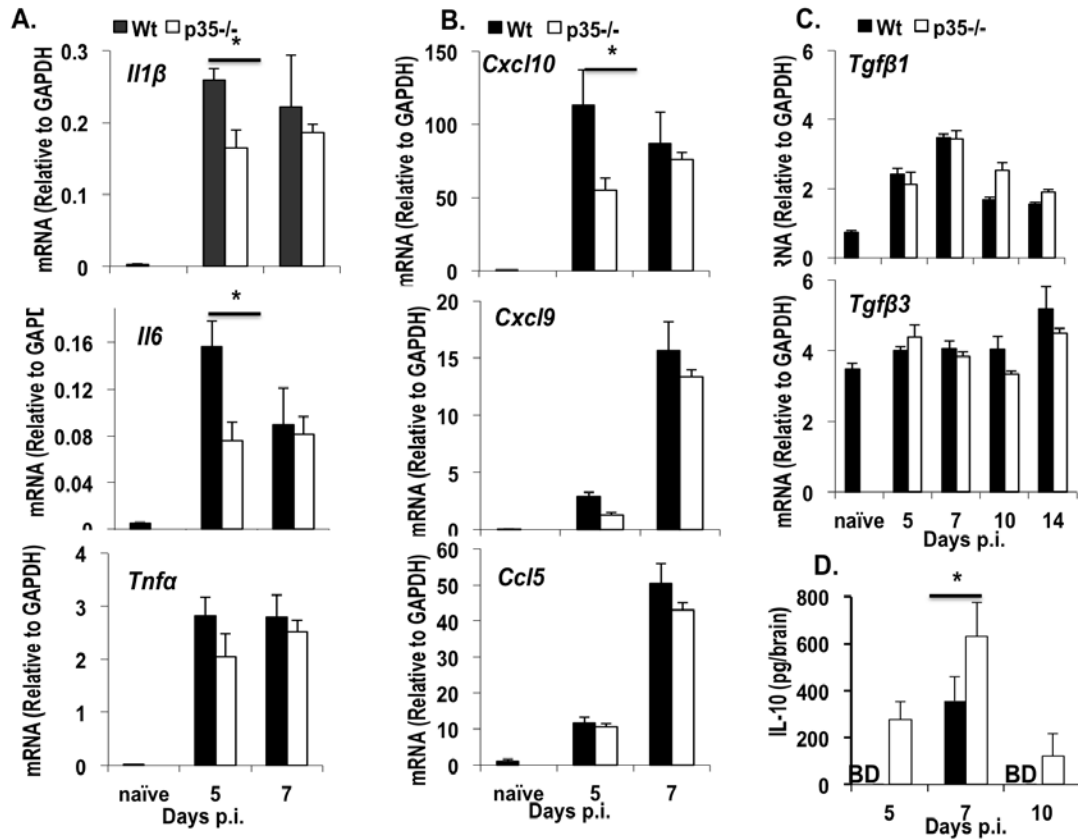


Figure 27. IL12 alters the expression of pro-inflammatory and anti-inflammatory cytokines. Brains from infected wt and p35^{-/-} mice were compared for mRNA expression of pro-inflammatory cytokines (A) *Il1β*, *Il6* and *Tnfα*; chemokines (B) *Cxcl10*, *Cxcl9* and *Ccl5* and the anti-inflammatory cytokines (C) *Tgfb1* and *Tgfb3* by real time PCR. Expression levels were normalized to *Gapdh* using the following formula: $(2^{CT_{(GAPDH)}} - CT_{(Target)}) \times 1000$, where Ct is the threshold cycle. Data represent the mean of three mice per time point \pm SEM. (D) IL10 levels in brains of infected wt and p35^{-/-} mice determined by the ELISA. Data are representative of two experiments (n = 4 per time point) \pm SEM. BD = below detection. Asterisks indicate statistical significance $p \leq 0.05$, compared to wt. (Kapil et al., 2009)

4.4 Discussion

IL12 regulates both innate and adaptive immune responses and plays a major role in controlling bacterial and intracellular protozoa infections predominantly via stimulation of IFN γ (Jouanguy et al., 1999, Langrish et al., 2004, Trinchieri, 2003). Similarly, IL23 contributes to host defense against bacterial infections (Jouanguy et al., 1999, Trinchieri, 2003, Langrish et al., 2004). However, many viral infections resolve without IL12 participation (Trinchieri, 2003) and the contribution(s) of IL23 have not been extensively explored (Held et

al., 2008, Kim et al., 2008, Kohyama et al., 2007, Novelli and Casanova, 2004). Importantly, both cytokines also have the potential to influence the severity of pathological lesions and/or clinical disease (Hunter, 2005, Langrish et al., 2004, Trinchieri, 2003, Novelli and Casanova, 2004). Rapid CNS induction of IL12p40 mRNA in a neurotropic coronavirus induced demyelination model (Parra et al., 1997) thus prompted analysis of the relative contributions of IL12 and IL23 to viral clearance and disease severity. Although quantitative PCR analysis confirmed upregulation of *Il12p40* mRNA (Parra et al., 1997), we were unable to detect statistically significant increases in either *Il12p35* or *Il23p19* mRNA following infection. Discrepancies with the previously reported early *Il12p35* mRNA induction and delayed *Il23p19* mRNA induction following clearance of infectious virus (Held et al., 2008) may reside in distinct viral inoculum doses or our quantitative measurements of PCR replicons. Nevertheless, similar kinetics of virus control in *p35^{-/-}*, and *p40^{-/-}* mice relative to wt mice, are consistent with reports demonstrating no enhancing effects of IL12 on mouse hepatitis virus clearance from the liver and CNS (Held et al., 2008, Schijns et al., 1998). Similarly, infected *p19^{-/-}* mice provided no evidence for IL23 mediated enhancement of host defense (data not shown) consistent with our inability to detect upregulation of p19 transcripts in JHMV infected Wt mice. A transient increase in virus replication observed by treatment with anti-IL23 (Held et al., 2008) could thus not be confirmed in *p19^{-/-}* mice infected with slightly lower virus doses.

A primary role of IL12 is enhancement of cytolytic activity and IFN γ secretion by NK cells as well as T cells (Trinchieri, 2003). Nevertheless, IL12 independent T cell activation and IFN γ secretion has been noted following a number of viral infections including systemic lymphocytic choriomeningitis virus infection (Orange and Biron, 1996a) and Influenza virus infection of the respiratory tract (Monteiro et al., 1998). This may be attributed to type I IFN, which can also promote IFN γ secretion by lymphocytes (Cousens et al., 1999). Type I IFN and IFN γ are both essential to control acute JHMV infection as shown by the inability of either virus induced IFN α/β or IFN γ alone to achieve protection (Ireland et al., 2008, Parra et al., 1999). The absence of an IL12 effect on JHMV clearance from the CNS may thus be attributed to the rapid induction of IFN α (Ireland et al., 2008), which may act as both an inhibitor of IL12 and enhancer of IFN γ production (Cousens et al., 1999). Nevertheless, IFN γ levels were significantly decreased in the CNS of p35^{-/-} mice, suggesting that type I IFN was insufficient to compensate for the absence of IL12 in augmenting IFN γ responses. Indeed, the modest decrease in IFN α/β mRNA levels in p35^{-/-} mice supports a role of IL12 in promoting IFN γ responses locally within the CNS. Impaired NK cell function in this context was ruled out, as NK cells do not contribute to either IFN γ dependent MHC class II expression on microglia or virus control in otherwise immune competent mice (Zuo et al., 2006). Reduced IFN γ correlated with decreased frequencies as well as total numbers of virus specific CD8 and CD4 T cells derived from the CNS of infected p35^{-/-} mice compared to wt mice. However, differences were not observed in frequencies of virus specific IFN- γ producing

CD4 T cells (Figure 25D) or CD8 T cells (Data not shown) in CLN or IFN γ producing CD4 or CD8 T cells in splenocytes (data not shown), consistent with a role of IL12 in directly promoting local T cell mediated IFN γ secretion within the CNS. Although control of JHMV in oligodendrocytes, the predominant cell type infected, is IFN γ dependent (Gonzalez et al., 2006, Parra et al., 1999), no differences in viral tropism, viral antigen distribution or viral clearance were noted comparing p35^{-/-} and wt mice. This suggested that the CD8 T cell response in wt mice, the dominant adaptive effector response controlling viral replication (Bergmann et al., 2006), exceeds the minimum requirement to effectively inhibit viral replication. This is supported by similar results in IL15 and B cell deficient mice, which also show reduced numbers of virus specific CD8 T cells in the CNS following JHMV infection (Ramakrishna et al., 2002, Zuo et al., 2006).

A striking finding was the early effect of IL12 on clinical disease, without alterations in either virus replication or demyelination. A contribution of IL12 to clinical symptoms of viral induced encephalitis, independent of virus load, has not been previously reported to our knowledge and provides a novel insight into viral pathogenesis of the CNS. The absence of a direct influence of IL12 on tissue destruction is consistent with similar findings in infected mice treated with anti-IL12 antibody (Held et al., 2008) and other models of virus induced demyelination. IL12 contributes to limiting Semliki Forest virus infection of neurons, yet has no affect on subsequent demyelination (Keogh et al., 2002). Furthermore IL12 does not influence either the acute phase or demyelination induced by Theiler's murine encephalitis virus (Inoue et al., 1998). The contribution of IFN γ to the

pathogenesis of CNS disease is complex, as it can act as a prominent mediator of pathogenesis during some experimental viral infections, but can also exert anti-inflammatory functions and decrease clinical symptoms (Anghelina et al., 2006, Kim et al., 2008, Savarin et al., 2008), similar to its role in autoimmunity (Kelchtermans et al., 2008). For example, inhibition of IFN γ enhances both morbidity and mortality following Semliki Forest virus, Theilers murine encephalitis virus, and JHMV induced CNS disease (Tomkins et al., 1988, Pullen et al., 1994, Parra et al., 1999).

IFN γ plays a critical role in shaping the inflammatory cells recruited into the CNS (Tran et al., 2000). It is thus difficult to assess how increased virus replication and altered inflammation, e.g. neutrophil accumulation within the CNS, both a result of IFN γ deficiency, contribute to the symptoms of acute encephalitis. This dilemma is evidenced by increased clinical symptoms and mortality of JHMV infected immunodeficient recipients of immune CD4 donor T cells deficient in IFN γ compared to wt CD4 T cells, independent of viral load (Savarin et al., 2008). Both neutrophil and monocyte recruitment in to the CNS, as well as pro-inflammatory cytokine levels were similar in the absence of IL12 at day 7 p.i., correlating reduced clinical disease most prominently with reduced IFN γ levels. The observation that clinical disease is not reduced in infected IL15^{-/-}, despite decreased virus specific CD8 T cells (Zuo et al., 2006), implicates the paucity of total and virus specific CD4 T cells in disease amelioration. Although CD4 T cells may contribute to viral clearance (Stohlman et al., 2008), they are more prominently implicated in the clinical symptoms of encephalitis (Anghelina et al.,

2006). Deletion of the immunodominant CD4 T cell epitope dramatically reduced both clinical symptoms and mortality following a lethal JHMV challenge (Anghelina et al., 2006). Similarly, mutations of the Theiler's murine encephalitis virus immunodominant CD4 T cell epitope ameliorate disease (Palma et al., 2002). Although IL23 dependent IL17 secreting CD4 T cells have recently been implicated in enhancing clinical symptoms during CNS autoimmune disease (Cua et al., 2003, Langrish et al., 2004) the frequencies of IL17 secreting T cells in the JHMV infected CNS remained near background levels in both wt and p35^{-/-} mice. A negligible contribution of IL17 secreting T cells during JHMV pathogenesis is supported by a similar disease course and demyelination in both p19^{-/-} mice and anti-IL23 antibody treated mice (Held et al., 2008) compared to wt mice. In contrast to experimental autoimmune encephalitis (Cua et al., 2003, Langrish et al., 2004), IL23 does not act as either a positive or negative regulator of viral induced CNS inflammation. These data support the notion that the IL12 dependent increase in virus specific IFN γ secreting CD4 T cells contributes to the expression of clinical symptoms. Furthermore, although no evidence for induction of anti-inflammatory TGF β was detected, IL10 was modestly increased in the absence of IL12. JHMV infection of IL10^{-/-} mice resulted in increased encephalitis suggesting that IL12 dependent limitations on IL10 may also contribute to morbidity by increasing CD4 Th1 cell activation.

In summary, the study of JHMV induced encephalitis in IL12 and IL23 deficient mice defined IL12, but not IL23, as a controlling element in the enhanced expression of clinical symptoms during viral encephalitis. Importantly,

the absence of IL12 decreased IFN γ levels within the CNS; however, neither the absence of IL12 or IL23 impeded viral clearance or affected demyelination. These data support the notion that IL12 contributes to morbidity by enhancing IFN γ secreting CD4 T cells and reducing IL10 mediated protection.

CHAPTER V

**KINETIC ANALYSIS OF PRO VERSUS ANTI-INFLAMMATORY GENES
EXPRESSED BY MICROGLIA/MACROPHAGES DURING CORONAVIRUS
MEDIATED CNS INFECTION**

5.1 Abstract

The functional state of tissue macrophage, including CNS resident microglia, can have a significant impact on inflammation and pathogenic outcome in various diseases. Depending on external stimuli macrophages can exist in three major different functional states: the pro-inflammatory (M1) phenotype, anti-inflammatory (M2) phenotype, and deactivated phenotype. Microglia activation and recruitment of monocytes are among the first host responses to JHMV infection of the CNS. In this study we monitored alterations in gene expression by microglia and infiltrated macrophages to assess if these populations are 1) regulated similarly, and 2) acquire an anti inflammatory phenotype as virus is cleared. Initial analysis of $IFN\gamma$, *Il13* and *Il10*, stimuli regulating macrophage differentiation towards a pro vs anti-inflammatory phenotype, respectively, revealed similar upregulation with peak expression of all three cytokines at day 7 post infection (p.i.) in total CNS tissue. RNA analysis of

purified microglia and infiltrating macrophages showed microglia initially expressed the pro-inflammatory *Il12p40*, but subsequently rapidly upregulated anti-inflammatory *Il1ra* and *Ym1/2* (Chitinase like lectins). By contrast, in macrophages expression of *Il1ra* and *Ym1/2* peaked at day 3 (p.i.) and rapidly declined by day 7 p.i. Nevertheless, a strong effect of $IFN\gamma$ was reflected by ~31 fold increase in expression of the M1 associated *iNos* gene in both microglia and macrophages during peak $IFN\gamma$ expression at day 7 p.i. Surprisingly, however, the M2 specific *Arg-1* was also increased by ~72 fold at day 7 p.i. in both cell populations. Furthermore, phagocytic activity was similar in both microglia and macrophages and increased between day 7 and 10 p.i. suggesting increased activation. These results indicate that microglia and infiltrating monocytes exhibit overall similar regulation of pro and anti inflammatory factors at the population level. Moreover, the data suggest that both M1 and M2 populations coexist and are driven by early $IFN\alpha\beta$ as well as T cell mediated $IFN\gamma$ and IL10 production.

5.2 Introduction

Macrophages are innate immune cells that play a crucial role in regulating both innate and adaptive immunity in response to pathogen as well as tissue damage. The functional heterogeneity of macrophages, defined by differential activation states, was recently highlighted for various disease settings (Colton, 2009, Gordon, 2007); an overview of distinct stimuli leading to prominent gene expression characteristics is provided in Table 5.1.

Table 5.1.

Functional Heterogeneity of Macrophages

Activation state	Stimulating agent	General function
Innate activation	LPS, other TLR ligands	Phagocytic activity, Adaptive immunity
Classical activated (M1)	IFN γ , TNF α	Phagocytic activity, Pro-inflammatory cytokine production, Nitric Oxide (NO) production
Alternative activated (M2a; M2)	IL4, IL13	Increased phagocytic activity, Anti-inflammatory cytokine production, Arginase-1 production, tissue repair, reconstruction of extra cellular matrix
Acquired deactivation	TGF β , IL10	Immunosuppression

Macrophages are widely distributed in the body and can be categorized into circulating monocytes and tissue resident macrophages. In the CNS microglia are the resident macrophages, which are originally derived from myeloid progenitors in the yolk sacs (Ginhoux et al., 2010). In the adult CNS,

microglia are on constant surveillance for any perturbation mediated by injury or infection.

As a consequence of CNS injury or infection microglia activation is phenotypically evident by thickening of highly ramified processes. Similar to and in concert with infiltrating macrophages they play an important role in promoting inflammation during microbial infection, but also provide protective roles by limiting ongoing tissue damage and by clearing cellular debris. These dual roles are reflected by the existence of both pro- and anti-inflammatory microglia and macrophages in various CNS inflammatory conditions. Multiple sclerosis (MS) is associated with both intracerebral M1 and M2 cells (Oleszak et al., 1998, Chiang et al., 1996). M2 macrophages were described as foamy cells that can ingest myelin-derived lipids and produce anti-inflammatory cytokines (Boven et al., 2006). The role of pro- and anti-inflammatory microglia and macrophages in MS pathology was further assessed using an experimental demyelinating rodent model termed Experimental Autoimmune Encephalitis (EAE). While, a balance between M1/M2 phenotype of microglia and macrophage resulted in mild EAE, an imbalance towards a prominent M1 phenotype promoted relapsing disease (Mikita et al., 2011). Similarly, perivascular macrophages and microglia exist in a mixed M1/M2 polarized state following HIV infection in the CNS (Benoit et al., 2008). M1 macrophages were relatively short lived, reduced the level of HIV replication but caused neurotoxicity, while an M2 activation state resulted in persistent viral infection but maintained neuronal homeostasis (Cassol et al., 2009). Overall, distinct regulation of microglia relative to infiltrating macrophages,

the co-existence of M1/M2 macrophages and microglia, and the relative contribution in propagating disease or maintaining recovery during CNS infection has not been well studied.

Microglia and macrophage express a wide array of pathogen recognition receptors (PRRs) which can be activated following recognition of pathogen associated molecular patterns (PAMPs), such as DNA and RNA structures (Takeda et al., 2003). Engagement of PRRs leads to induction of $IFN\alpha/\beta$, as well as numerous pro-inflammatory cytokines and chemokines (Takeda and Akira, 2004). $IFN\alpha/\beta$ also induces transcription of the anti-inflammatory factor *Il1ra* in macrophages (Jungo et al., 2001, Sciacca et al., 2000). $IFN\alpha/\beta$ can further polarize macrophages towards an M2 phenotype following infection with *Tropheryma whipplei* (Al Moussawi et al., 2010). These data highlight the plasticity of pro- and anti-inflammatory gene expression by macrophages as a result of numerous autocrine as well as paracrine stimuli. They further suggest the integrative outcome of complex signaling pathways is difficult to predict in vivo, especially in situations where infiltration by T cells provides prominent changes in environmental cues, such as release of $IFN\gamma$ and IL10.

Following intracerebral inoculation, JHMV initially targets ependymal cells and spreads to microglia, astrocytes and oligodendroglia, with oligodendrocytes being the most prominently infected cell type (Ramakrishna et al., 2004); (see Chapter 2). Infection elicits numerous proinflammatory factors resulting in recruitment of leukocytes. Driven by CCL2, monocytes constitute the largest portion of early CNS infiltrating cells (Savarin et al., 2010), and provide further

targets of infection (Ireland et al., 2009). Early infection is characterized mainly by pro-inflammatory cytokines, such as $TNF\alpha$, $IL1\beta$, $IL1\alpha$, $IL6$ and $IL12$ (Bergmann et al., 2006, Parra et al., 1997), with $IFN\gamma$ only prominent as T cells infiltrate the CNS (Parra et al., 1999, Stohlman et al., 1995). Nevertheless, $IL4$, an anti-inflammatory signal, is also induced in response to JHMV infection (Parra et al., 1997). In vitro, infection induces $IL1\beta$ in both primary microglia and macrophage and $IL1\alpha$, $IL6$ and $IL12$ are all induced by microglia (Pearce et al., 1994, Rempel et al., 2004, Rempel et al., 2005, Stohlman et al., 1995). More recent data indicate $IL10$ is prominently produced by T cells (Puntambekar et al., 2011). These findings suggested JHMV infection induces complex cues with the potential to favor both pro- and anti-inflammatory microglia and macrophages.

The studies in this chapter thus set out to address three interrelated questions:

1. Are microglia and macrophage skewed from a prominently proinflammatory to an anti-inflammatory phenotype as virus is controlled or do they reveal a mixed phenotype throughout?
2. Do infiltrating macrophages display overall similar gene expression profiles as microglia over time, indicating exposure to similar environmental cues?
3. How does $IFN\alpha\beta$ influence the microglia/macrophage gene expression with respect to M1/M2 associated genes?

To characterize distinct functional populations, microglia and macrophages were isolated from brains of C57Bl/6 mice at various times post JHMV infection and

mRNA prepared for real time PCR analysis. We detected induction of both pro- and anti-inflammatory factors at the transcript level, suggesting the simultaneous existence of both M1 and M2 phenotypes in both microglia and macrophages. Moreover, the expression profiles were overall similar between resident microglia and the infiltrating macrophages. One exception was high expression of *I11ra* in early infiltrating monocytes, which was IFN α/β signaling dependent. With the exception of early *I11ra*, anti-inflammatory markers already increased between days 5 and 7 p.i., Phagocytic activity of microglia as well macrophages was also increased between days 7 and 10, supporting an increasingly anti-inflammatory phenotype with increased potential to clear dying cells.

5.3 Results

5.3.1 The innate phase of JHMV infection is associated with abundant monocyte recruitment

Many approaches study the activation states of macrophages by *in vitro* stimulation with microbial agonist and cytokines (Murray and Wynn, 2011). However, *in vivo* these cell types are subjected to many different signals dependent on their localization. Resident tissue macrophages exist in an anti-inflammatory state by default to minimize continuous inflammation mediated by homeostatic cell turnover (Murray and Wynn, 2011). Initial warning signals at the site of infection or injury lead to activation of resident macrophages and trigger the recruitment of circulating monocytes. During JHMV infection, CCL2 is the major chemokine recruiting monocytes to the CNS (Savarin et al., 2010). (Figure 28) depicts the kinetics on monocyte recruitment and the relative numbers of

microglia and monocyte derived macrophages in the CNS during the first week of infection. Microglia are characterized as CD45^{lo} F4/80⁺ cells (Figure 28).

Infiltrating macrophages exhibit a CD45^{hi}F4/80⁺ phenotype and comprise ~75% at day 3, and 5 p.i. and ~69% at day 7 p.i. of total infiltrating populations(Figure 28). The frequency of macrophages decline subsequently to ~36% at day 10 p.i. (Figure 28). These data reveals macrophages as a major infiltrating population early following infection, which declines by 2 weeks p.i.

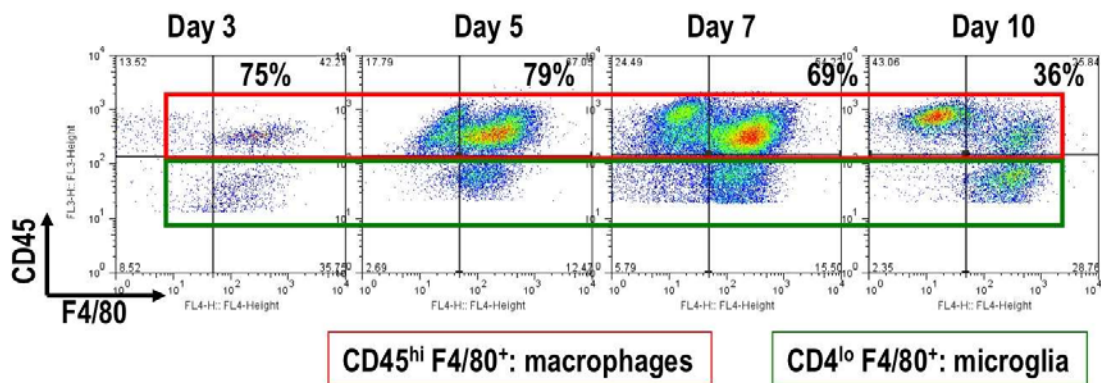


Figure 28. Kinetics of CD45^{hi} F4/80⁺ macrophage, and CD45^{lo} F4/80⁺ microglia in the CNS following JHMV infection. Representative density plots of CNS derived cells stained with CD45 and F4/80 at day 3, 5, 7, and 10 p.i. CNS-infiltrating cells contain a prominent population of CD45^{hi} F4/80⁺ macrophages early during the infection, while microglia are represented as CD45^{lo} F4/80⁺ cells. The data represents three separate experiments at each time point, combining cells from 3-4 mice/time point/experiment.

5.3.2 JHMV replicates in microglia and infiltrating macrophages early during the infection

Following intracerebral infection JHMV spreads to a variety of resident cells. Microglia are one of the initial targets for infection consistent with their expression of the MHV receptor, carcinoembryonic antigen cell adhesion molecule 1 (CECAM-1 or MHVR) (Nakagaki and Taguchi, 2006, Ramakrishna et al., 2004). Similarly a subset of infiltrating macrophages is also infected (Ireland

et al., 2009). As virus replication drives initial PRR dependent innate responses, we compared the relative kinetics of viral replication in microglia and infiltrating macrophages by quantifying the level of viral RNA using primers specific for RNA encoding the nucleocapsid (N) protein, which are found on both genomic and the nested subgenomic RNAs (Baric and Yount, 2000, Schelle et al., 2005).

Microglia and infiltrating macrophages were purified by FACS and RNA viral N RNA expression real time PCR analysis *Gapdh* as a housekeeping gene. Viral RNA expression was maximal at day 3 p.i. and declined by day 5 and 7 p.i. in both microglia and macrophages (Figure 29), indicating innate stimulation decreases coincident with decreasing virus. This is indeed confirmed by kinetics of *Ifn α/β* levels in chapter 2.

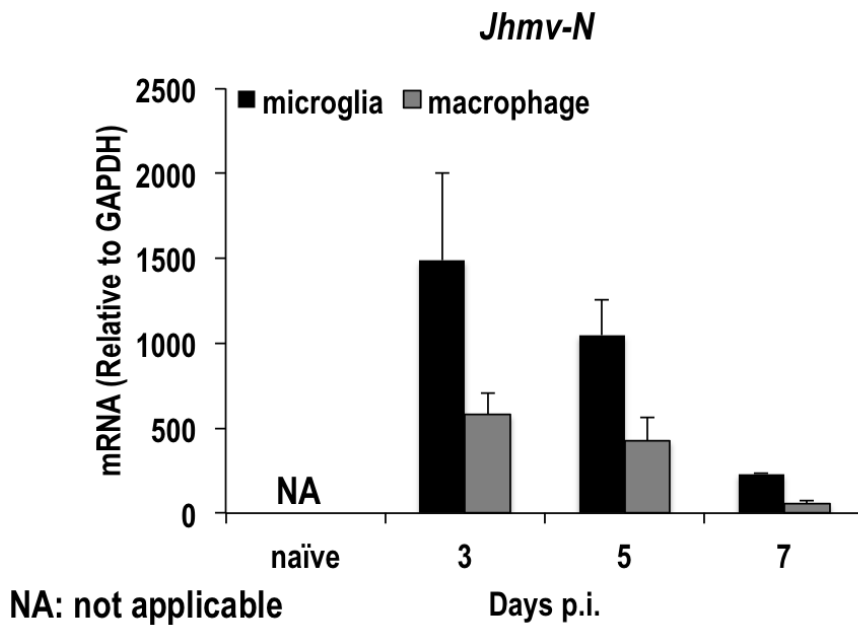


Figure 29. Kinetics of viral RNA in macrophage and microglia. Viral mRNA comprising N-protein encoding sequences was measured in microglia and macrophage populations isolated from brains of JHMV infected C57/Bl6 mice using real time PCR. Numbers depict mRNA levels relative to the house keeping gene GAPDH using the following formula $(2^{[C_T - C_T\{target\}]}) \times 1000$, where C_T is the threshold cycle. The data represent the average values of pooled cells from 5-6 mice of three individual experiments \pm SEM.

5.3.3 Activation of microglia/macrophage following JHMV infection

To further characterize the activation state of microglia and macrophages within the CNS early following JHMV infection, we determined the initial induction of representative pro- and anti-inflammatory factors. The pro-inflammatory cytokine *Il12 p40* was barely detectable in microglia from naïve mice. However, we observed ~200 fold induction in *Il12 p40* as early as day 3 p.i. in microglia which was subsequently downregulated, but still remained ~55 fold and ~5 fold higher at day 5 and 7 p.i. respectively, compared to naïve levels (Figure 30). Similarly, expression of *Il12 p40* peaked at day 3 p.i. in infiltrating macrophages and was subsequently reduced. Overall, *Il12 p40* expression reflected the kinetics and magnitude of virus replication in both populations (Figure 29). These data supported a direct correlation between virus infection and induction of *Il12 p40*.

We also assessed transcription of two genes associated with anti-inflammatory functions. While IL12 promotes IFN γ secretion, the anti-inflammatory factor Ym1/2 has been reported to induce expression of the Th2 cytokines IL13 (yeping cai, 2009, JI). Ym1/2 has been described as secretory protein that shares a close homology with chitinases. (Jin et al., 1998). Ym1 and Ym2 are isomers sharing ~91% similarity and therefore many studies do not differentiate between these isomers and collectively referred as Ym1/2 proteins. In the CNS, Ym1/2 are involved in inducing regeneration of olfactory receptor neurons (Giannetti et al., 2004). A second prominent anti-inflammatory mediator, which counteracts the innate pro-inflammatory cytokines IL1 α and IL1 β , is IL1Ra.

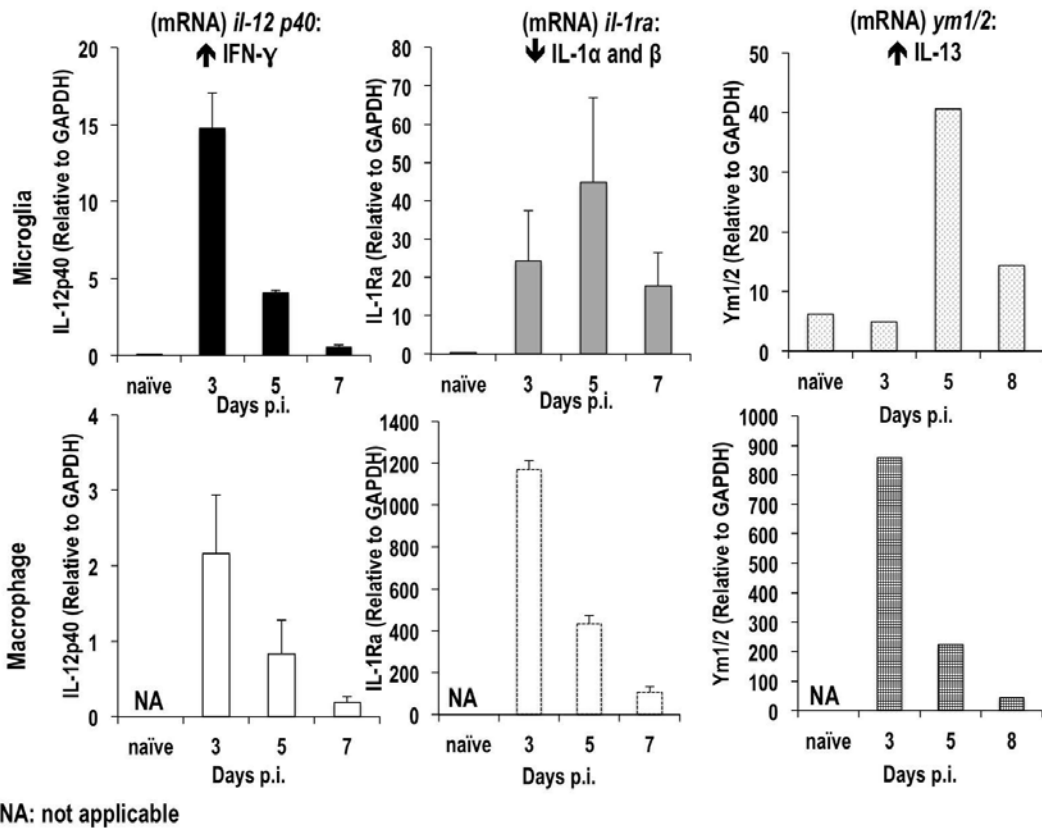


Figure 30. Activation of microglia/macrophages early during JHMV infection. Comparison of transcript levels for the pro-inflammatory cytokine *Il12p40* and anti-inflammatory factors *Il1Ra* and *Ym1/2* in microglia and macrophages isolated from brains of C57BL/6 mice following JHMV infection. Data are all relative to *Gapdh* as described in Fig. 29. Data for *Il12p40* and *Il1Ra* is average of two separate experiments \pm SEM. The data for *Ym1/2* is derived from a single experiment. Data is from pooled cells from 5-6 mice per time-point.

This antagonist competitively binds to IL1 receptor 1 without inducing signal transduction, thereby downregulating IL1 α and β activity (Eisenberg et al., 1990, Seckinger et al., 1987). IL1Ra is also protective during brain injury (Hutchinson et al., 2007). Similar to *Il12 p40*, microglia from naïve mice exhibited very low expression of *Il1ra*, but expression of *Ym1/2* was readily detectable, confirming a prominently anti-inflammatory state prior to infection. However, while *Il-1ra* increased ~74 fold, *Ym1/2* expression stayed at basal level levels in microglia at day 3 p.i. (Figure 30). Expression of *Il1ra* was further induced to ~134 fold at day

5 p.i. and still remained ~52 fold higher over naïve levels at day 7 p.i. (Figure 30). *Ym1/2* was also increased at day 5 p.i., and down-regulated by day 7 p.i., but the maximal increases was only ~6 fold relative to its basal expression (Figure 30). Contrasting delayed induction of anti-inflammatory response genes in microglia, *Il1ra* and *Ym1/2* mRNA levels were overall much higher in infiltrating macrophages at day 3 p.i. Furthermore, although mRNA levels encoding these factors declined progressively in macrophages throughout days 5 and 7, they remained at elevated levels compared to microglia (Figure 30). Overall these data suggest that early infiltrating macrophages contribute substantially to an anti-inflammatory environment.

5.3.4 Expression of cytokines polarizing pro- and anti-inflammatory macrophages in the CNS following JHMV infection

Virus mediated activation of microglia and macrophages lead to induction of various cytokines, which in-turn mediates CNS recruitment of peripherally activated T cells. During intracerebral CNS infections initial activation, differentiation and expansion of T cells takes place in the draining cervical lymph nodes. T cells start accumulating in the CNS as early as day 5 p.i. and increase to maximal numbers between days 7 and 10 (Ireland et al., 2009, Kapil et al., 2009); chapter 4). During this time T cell effector function is further influenced by the CNS environment and responsible for clearance of the vast majority of infectious virus (Bergmann et al., 2003, Bergmann et al., 2004, Gonzalez et al., 2006, Parra et al., 1999, Stohlman et al., 1995). The key antiviral mediator is $IFN\gamma$ (Kapil et al., 2009, Parra et al., 1999), while IL10 production by T cells

dampens T cell pathogenicity (Lin et al., 1998, Trandem et al., 2011). While $\text{IFN}\gamma$ is considered an activating cytokine for macrophages, IL10 mediated signaling to macrophages is associated with deactivation. Expression of these cytokines is thus likely to play a dominant role in influencing macrophage activity. Figure 31 shows the relative levels of $\text{IFN}\gamma$, *Il10* and *Il13*, (a cytokine associated with alternative macrophage activation) in the CNS during JHMV infection. $\text{IFN}\gamma$ protein is detectable in the brain as early as day 5 p.i. peaks at day 7 p.i., and is significantly reduced, yet still detectable by day 10 (Figure 31). Similarly, the deactivation factor *Il10*, predominantly expressed by CD4 T cells (Puntambekar et al., 2011) also peaks at day 7, but stays elevated at day 10 p.i. (Figure 31). Finally, the increase in *Il13* in the brain followed similar kinetics as $\text{IFN}\gamma$ and *Il10*, peaking at day 7 p.i., albeit at considerable lower overall levels. Overall the increases and decreases relative to naïve levels were also less pronounced (Figure 31). The overall expression profiles of $\text{IFN}\gamma$, *Il13* and *Il10* followed similar kinetics as previously described for the anti-inflammatory cytokines *Tgf β* (Kapil et al., 2009) and cytokine *Il4* (Parra et al., 1997). These data clearly demonstrate expression of cytokines known to polarize macrophages into a both pro- and anti-inflammatory phenotypes.

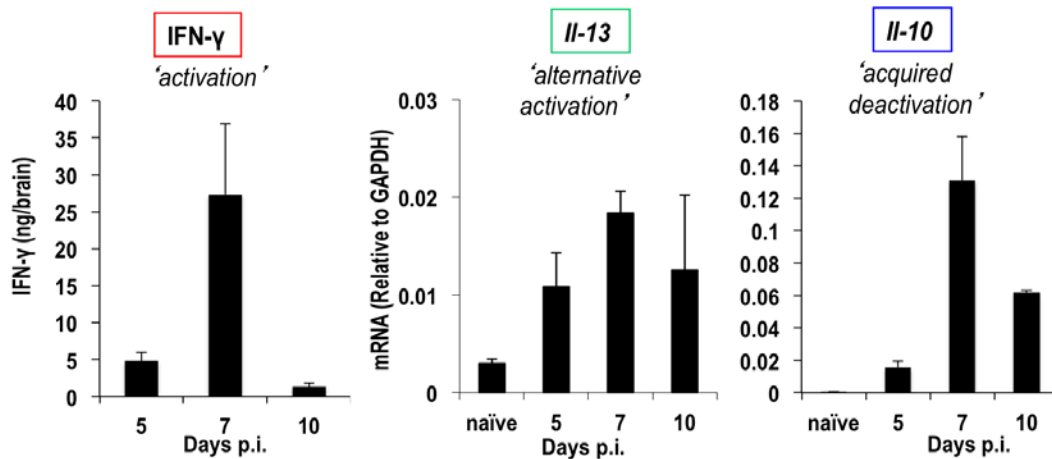


Figure 31. Kinetics of cytokine expression known to polarize distinct microglia/monocyte activation states. Protein levels of the pro-inflammatory cytokine IFN- γ was measured using ELISA and are represented as ng/brain (n=9 mice/time-point). Anti-inflammatory cytokines IL-13 and IL-10 were measured at the transcriptional level using real time PCR (n=6 mice/time-point). Data are represented as relative to GAPDH as depicted in Fig. 29. Values represent the average of three separate experiments \pm SEM.

5.3.5 T cell mediated influence on M1/M2 profiles of microglia and macrophages following JHMV infection

IFN γ induces macrophages to produce iNOS, resulting in a classically activated M1 phenotype (Nathan et al., 1983). iNOS metabolizes amino acids to produce nitric oxide (NO) (Bronte and zenviello, 2005, nat rev immunol). NO provides protection against intracellular pathogens, however, if released in to the extracellular milieu, it can cause damage to the neurons. In contrast, Th2 cytokines, IL4, and IL13 induce production of arginase1 and mediate polarization of macrophage towards an alternatively activated M2 phenotype (Gordon, 2007). Furthermore, overexpression of IL10 in macrophages shown to induce gene expression and activity of arginase1 and reduce production of reactive nitrogen intermediates (Schreiber et al., 2009). Arginase1, expression initiates shift in metabolism of L-arginine from NO production by iNOS towards generation of L-

ornithine, a precursor for polyamines and collagen, which is important for wound healing (Bansal and Ochoa, 2003, Durante et al., 2007). Furthermore, the cytokines IL10 and TGF β induce a deactivated state in macrophages (Mantovani et al., 2004). Based on the presence of both IFN γ and anti-inflammatory cytokines (IL4, *I13*, IL10 and *Tgf β*) in the brain following JHMV infection, we monitored microglia and macrophages for expression of the respective signature M1 /M2 molecules *iNos* and *Arg-1*.

Expression of *iNos* was upregulated ~3 fold at day 5 p.i. and ~31 fold at day 7 p.i. in microglia, compared to naïve levels (Figure 32). Expression of *iNos* was reduced at day 10 p.i. but still remained ~11fold higher than basal level (Figure 32). Expression of *iNos* in infiltrating macrophages follow the similar kinetics as microglia (Figure 32). Increasing *iNos* levels in both microglia and macrophages between days 5 and 7p.i. is consistent with increasing IFN γ mediated signaling. To determine the existence of alternative state macrophages, we monitored expression of arginase1. In microglia expression of *Arg-1* was upregulated ~8 fold at day 5 p.i. and further increased ~70 fold at day 7 p.i. and remained higher at day 10 p.i. relative to basal levels in microglia (Figure 32). Similarly, a major increase in *Arg-1* was apparent in macrophages between days 5 and 7 p.i. (Figure 32). Although, the expression level of *Arg-1* was reduced at day 10 p.i. but still remained elevated compared to day 5 (Figure 32). Overall, these results demonstrate the co-existence of both M1 and M2 specific gene patterns in both microglia and macrophages following JHMV infection. However sustained expression of arginase1 in microglia at day 10 p.i.

indicates a prevalence of anti-inflammatory phenotype in these cells. The data further demonstrate rapid adaptation of macrophages to environmental influences exerted by T cells.

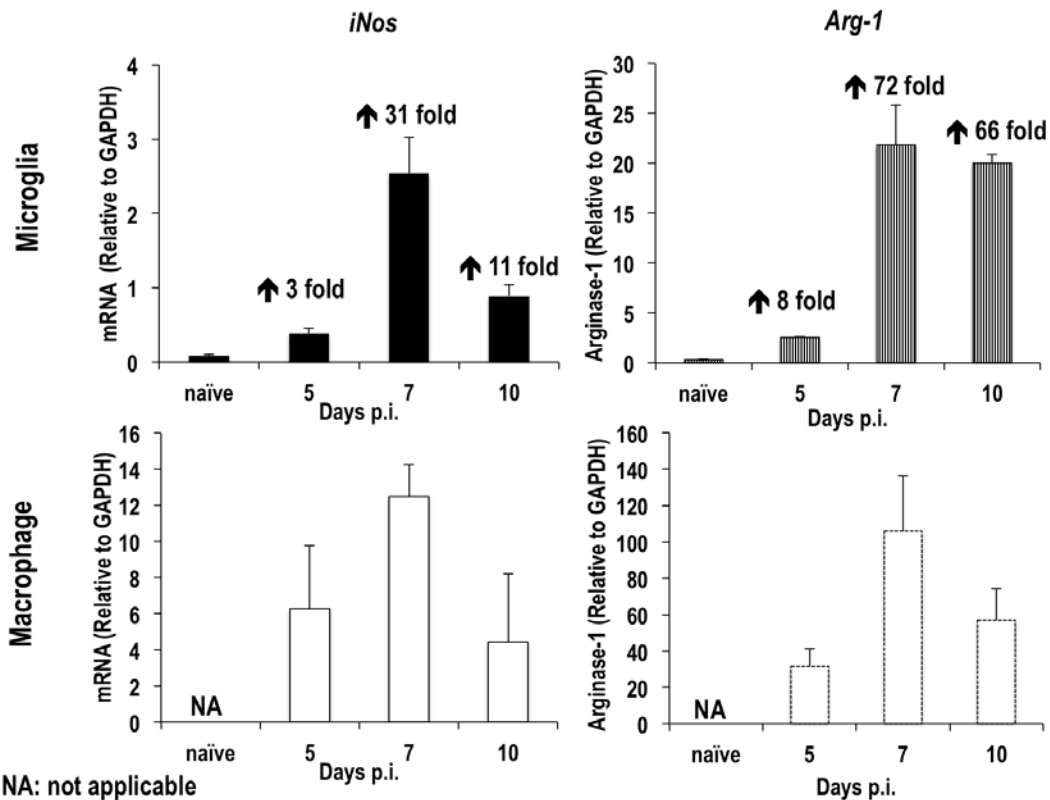


Figure 32. Upregulation of mRNA characteristic of M1/M2. Microglia and macrophages were isolated from infected mice by FACS and RNA analyzed for IFN γ mediated upregulation of *iNos* as a representative M1 specific factors and *Arg1* as a typical M2 specific factor. Expression relative to *Gapdh* was determined by real time PCR. The data represent the average values of pooled cells from 5-6 mice of three individual experiments \pm SEM.

5.3.6 Increasing phagocytic activity of microglia and macrophage following infection

Phagocytosis of myelin debris by activated microglia and macrophages was reported to be an essential response to promote regeneration following MS (Boven et al., 2006). Furthermore, clearance of dead or dying cells by myeloid cells is critical to maintain a healthy microenvironment. To determine the

phagocytic activity of microglia and macrophage following JHMV infection we incubated brain-derived cells with fluorochrome labeled E coli particles (K12 strain) *ex vivo* and monitored the uptake in a phagocytic assay. Both microglia and macrophages showed high phagocytic ability at day 7 p.i. which was further increased at day 10 p.i. (Figure 33). The uptake was ~40% at day 7 and ~80% at day 10 p.i. in both microglia and macrophages (Figure 33). Increased phagocytic activity in microglia and macrophages as T cells accumulate and virus is controlled suggest an overall M2 phenotype. Whether the macrophage populations expressing M1 and M2 associated genes segregate into distinct populations, or represents a mixed phenotype remains to be determined by *in situ* hybridization. Future studies may also utilize bone marrow derived macrophages and primary microglial cultures exposed to external M1 or M2 specific stimuli to further assess gene expression and phagocytic activity *in vitro*.

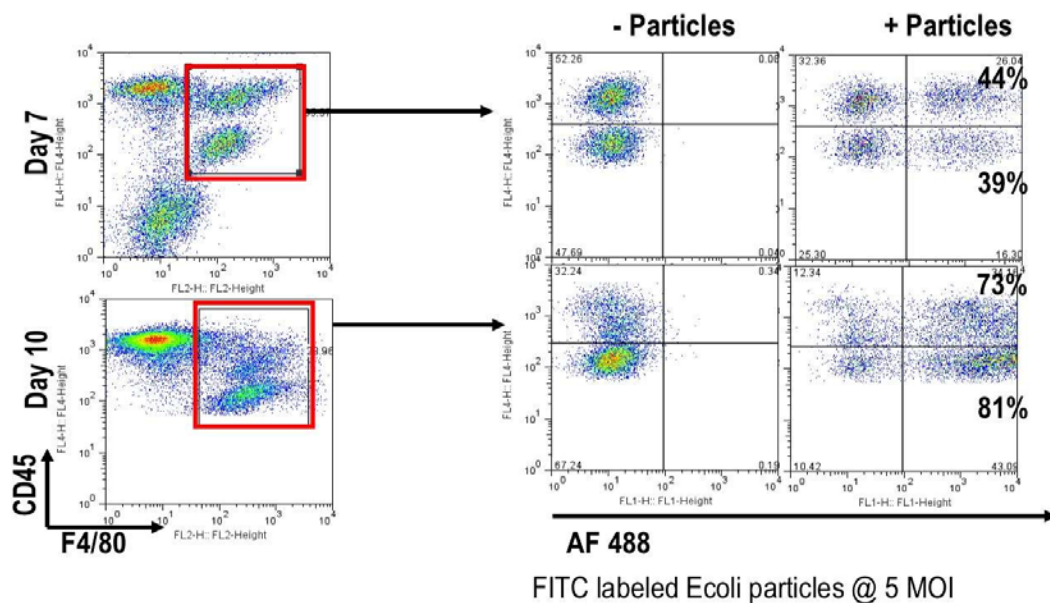


Figure 33. Phagocytic activity of macrophages and microglia is increased as virus is controlled. Phagocytic activity of microglia and macrophages was determined by incubating percol gradient purified brain cells with fluorescein (494/518) labeled E coli particles (E2861) at 5 MOI (5 particles per one cell) at day 7 and day 10 p.i. The data is representative of two separate experiments. Cells were pooled together from 2-3 mice/time-point/experiment.

5.3.7 IFN α/β signaling plays an important role in induction of anti-inflammatory cytokine IL1Ra

IFN α/β induction in microglia initiates induction of various interferon-stimulated genes (ISGs), not only in the same cells, but also in neighboring cells such as oligodendroglia (Chapter 2). These ISGs include pro-inflammatory as well as anti-viral genes. However, IFN α/β also display anti-inflammatory properties as indicated by their ability to induce IL1Ra (Aman et al., 1994, Palmer et al., 2004). The importance of antiviral activity of IFN α/β during JHMV mediated CNS infection was established in mice deficient in IFN receptor chain 1 (IFNAR1 $^{-/-}$). IFNAR mice exhibited uncontrolled virus replication and pro-inflammatory responses and succumbed to infection within 8 days (Ireland et al., 2008). To determine the role of IFN α/β in upregulation of *I1ra*, we initially monitored IFN α/β expression level in microglia and macrophages derived from brain of infected wt mice using real time PCR analysis. The levels of IFN α/β transcripts in microglia and macrophage correlated closely with viral RNA loads in both cell types (Figure 34A). Expression of both *Ifn α* and *Ifn β* transcripts peaked at day 3 p.i. in macrophages and was subsequently reduced at day 5 and 7 p.i. (Figure 34A). In microglia both *Ifn α* and *Ifn β* were upregulated at day 3 p.i.; while *Ifn α* transcripts followed the same trend as in macrophages, expression of *Ifn β* peaked at day 5 p.i. and was reduced at day 7 p.i. (Figure 34A). These data confirmed macrophages and microglia as source of IFN α/β in the CNS (Roth-Cross et al., 2008); Chapter2).

We subsequently isolated mononuclear cells from brains of IFNAR^{-/-} mice and congenic control C57/Bl6 mice at different time post infection following JHMV infection to monitor *I1ra* levels. Induction of *I1ra* was significantly blocked in both microglia and macrophages in absence of IFN α/β signaling (Figure 34B). These results suggested that significantly increased expression of pro-inflammatory molecules in the CNS of JHMV infected IFNAR^{-/-} mice may not only be attributed to uncontrolled viral spread, but also to significantly impaired anti-inflammatory *I1ra* expression.

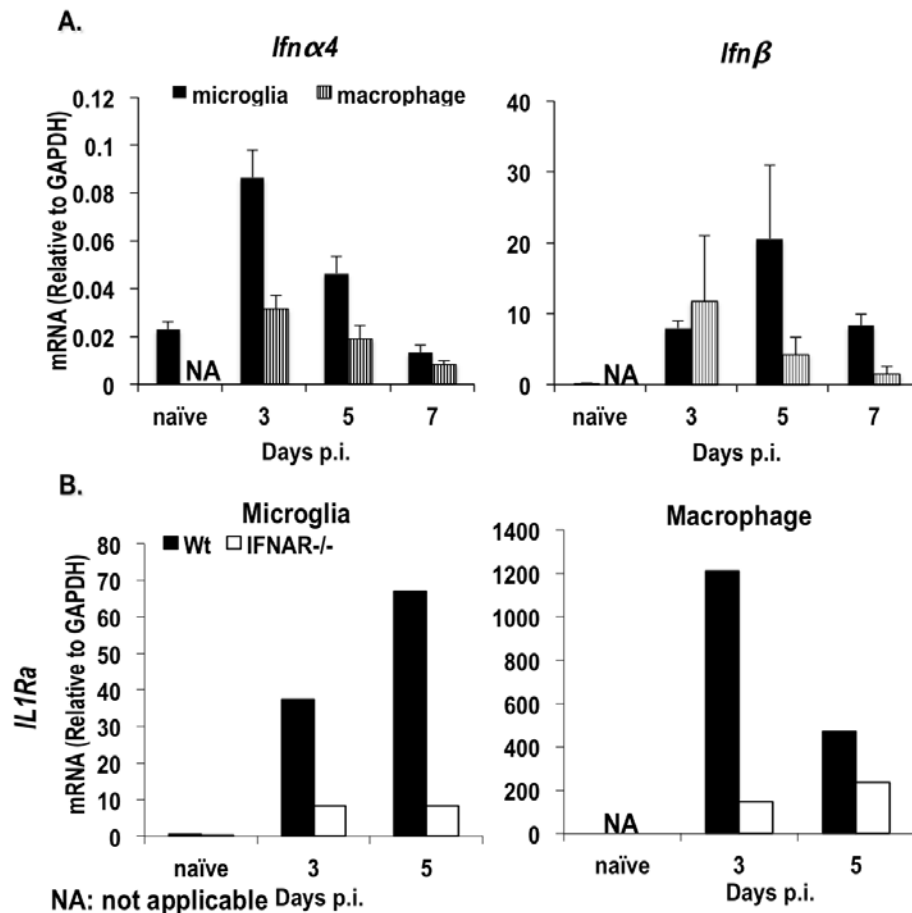


Figure 34. Upregulation of IL1R antagonist mRNA in microglia and macrophage is IFN α/β dependent. (A) *Ifn α* and *Ifn β* transcripts in FACS purified microglia and macrophages were determined using real time PCR. Data represent the average of three separate experiments \pm SEM. (B). *I1ra* transcript levels were determined in both microglia and macrophage isolated by FACS from IFNAR^{-/-} and wt mice following JHMV infection. The data is from a single experiment. All data is presented as relative to *Gapdh*. Cells were pooled together from 5-6 mice/time-point/experiment.

5.4 Discussion

Microglia and macrophages are dynamic cells, which continuously survey their surroundings for pathogenic agents and dangerous signals. In response to extracellular signals they maintain cellular homeostasis by phagocytosis of cellular debris and toxic substances. At the site of infection or injury, activation of microglia and infiltrating macrophages mediates protective effects, but also contributes to tissue damage (Yong and Rivest, 2009). This conflicting behavior can be attributed to the plasticity of these cell types, as both microglia and macrophage can adopt pro- and anti-inflammatory states, thereby exhibiting harmful or protective properties (Mantovani et al., 2004, Michelucci et al., 2009, Mosser, 2003). Polarization of microglia and macrophage towards an M1 phenotype is linked to increased production of pro-inflammatory cytokines and pathophysiology during HIV induced dementia (HAD) and Alzheimer's disease (AD) (Minagar et al., 2002). Treatment with non-steroid anti-inflammatory drugs (NSAIDs) resulted in reduced amyloid plaque burden in mice and reduced risk for AD in humans (Stewart et al., 1997, Szekely et al., 2004, Zandi et al., 2002). Furthermore, M2 macrophages promote virus survival and persistence (Cassol et al., 2009).

During JHMV infection, microglia/macrophages are prominent cell types inducing pro-inflammatory responses, and their uptake of myelin is characteristic of ongoing demyelination during viral persistence. To determine the plasticity of activation states during JHMV mediated CNS infection, microglia and macrophages purified at different times post-infection from infected brains were

characterized for pro- and anti-inflammatory phenotypes. Comparative analysis of transcriptional regulation following CNS infection by JHMV revealed the existence of overlapping pro and anti-inflammatory (M1/M2) polarization in both microglia and macrophages. While an early increase in *Ii12p40* and delayed upregulation of IFN γ stimulated *iNos* readily depicted an M1 phenotype, an early transient increase in *Ym1/2*, followed by delayed upregulation of *Arg-1* characterized an M2 phenotype. A prevalent M2 phenotype coincident with viral control was supported by increased phagocytic potential of both microglia and macrophages between 7 and 10 days p.i. By contrast, transcription of *Ii1ra* was most prominent in infiltrating macrophages during the initial 5 days of infection, suggesting a critical role of early accumulating monocytes in dampening exacerbated pro-inflammatory responses.

The coexistence of M1/M2 or presence of mixed phenotype macrophages is supported by similar observations in distinct model systems. A transcriptome analysis of monocytes during human cytomegalovirus infection reveals an atypical mixed M1/M2 phenotype biased towards an M1 phenotype (Chan et al., 2008). In contrast, patrolling monocytes initially display an M1 phenotype following *Listeria monocytogenes* infection, which subsequently changed to an M2 phenotype during tissue remodeling (Auffray et al., 2007). Furthermore, an imbalance in equilibrium of M1/M2 expression towards M1 phenotype in microglia and macrophage in brain and blood monocytes has been linked to favor relapsing EAE (Mikita et al., 2011). These studies emphasize that distinct functional states of microglia/macrophage play a critical role in final outcome of

disease. An imbalance between various polarization states can result in early termination of protective microbial responses or aggravated progression of autoimmune responses.

IL1Ra is a soluble factor, which competes with IL1 (α and β) for the IL1 receptor (Carter et al., 1990, Seckinger et al., 1987), thus antagonizing IL1 mediated inflammation. IL1 is an innate cytokine, which plays a crucial role in leukocyte extravasation to site of infection or injury (Tamaru et al., 1998). Dysregulation in IL1 is linked with autoimmune and abnormal immune responses (Horai et al., 2000, Nicklin et al., 2000). Exogenous administration of IL1 exacerbates the course of EAE, while administration of IL1Ra suppresses disease (Jacobs et al., 1991, Martin and Near, 1995). IL1Ra production can be induced by various different signals including GMCSF, IL3, IL4 and IFN α/β (Jenkins and Arend, 1993, Sciacca et al., 2000). Both IFN α and IFN β can induce IL1Ra production in different cell types *in vitro*, including monocytes (Jungo et al., 2001, Wan et al., 2008). Importantly, IFN α/β treatment in Hepatitis C viral infection as well as in autoimmune disease such as Rheumatoid Arthritis (RA) induces IL1Ra production in patients (Cotler et al., 2002, Palmer et al., 2004). Consistent with these findings, early expression of *Il1ra* in microglia and macrophages following JHMV infection correlates with peak of induction of *Ifn α/β* in these cell types. Moreover, the significant reduction in *Il1ra* expression in both macrophage and microglia in the absence of IFN α/β signaling (IFNAR $^{-/-}$ mice) supports IFN α/β as critical inducers of IL1Ra in the CNS. Elevated proinflammatory cytokines in the CNS of infected IFNAR mice further support an

anti-inflammatory property of IFN α/β , which may be mediated via IL1Ra following JHMV infection.

In summary, our findings demonstrate the existence of both pro- and anti-inflammatory microglia and macrophages in the CNS following JHMV infection. Moreover, the regulation of characteristic M1 and M2 associated genes in microglia follows similar kinetics as in infiltrating macrophages. While monocyte recruitment is associated with detrimental responses in EAE, their recruitment during JHMV infection does not have adverse consequences (Savarin et al., 2010), perhaps due to their overall more abundant expression of M2 genes. Furthermore, similar disease course when monocyte recruitment is abrogated suggests the function of microglia is sufficient to control inflammation. Finally, IFN α/β is not only crucial in controlling viral dissemination within the CNS (Ireland et al., 2008), but is also required for expression of the anti-inflammatory factor *Il1ra*. Overall, the data indicate a delicate interaction between pro and anti-inflammatory responses in the CNS.

CHAPTER VI

DISCUSSION

In this thesis we have focused on innate responses following gliotropic coronavirus induced encephalomyelitis and how they impact adaptive responses and the pathogenesis. Recognition of viruses by various PRRs provides the first line of defense by activating the transcription factors, NFkB and Interferon Regulatory Factors (IRFs). These early responses limit viral spread by initiating transcription and activation of Interferon (IFN) induced antiviral mediators, such as RNaseL and double stranded RNA-dependent protein kinase (PKR). However they also regulate pro and anti-inflammatory responses, thereby contributing to the tissue damage if not appropriately balanced. There is a growing appreciation of distinct abilities of resident CNS cells to recognize and respond to microorganism, how responses are coordinated following infection *in vivo* is poorly understood.

Studies in mice defective in type1 IFN signaling (IFNAR^{-/-} mice) demonstrated a critical protective role of type1 IFN signaling in preventing virus replication and dissemination following peripheral as well as CNS infection (Cervantes-Barragan et al., 2007, Ireland et al., 2008). Although plasmacytoid

dendritic cells (pDCs) were identified as primary type1 IFN inducers in the periphery, the contribution of CNS resident cells to IFN α/β production *in vivo* was not dissected. Our analysis of the relative contribution of microglia/macrophages and oligodendroglia *in vivo* initiating and propagating IFN α/β responses following coronavirus CNS infection revealed that oligodendroglia are incapable to produce IFN α/β . By contrast, despite being infected at lower levels, microglia initiated IFN α/β expression. Compared to microglia oligodendroglia also mounted a restricted response towards external IFN α/β to induce anti-viral state. Importantly, low basal and delayed inducible levels of mRNA encoding components of the IFN α/β pathway in oligodendroglia was reflected in increasing viral mRNA levels in oligodendroglia at a time when virus was already controlled in microglia. The ineffective innate control in oligodendroglia therefore appears to contribute to preferential virus spread in this cell types prior to accumulation of T cells with anti-viral activity. Nevertheless, although T cells reduce virus load in oligodendroglia, virus still persists preferentially cell in this cell type. Whether a stronger innate response in oligodendroglia could slow virus replication, thereby enhancing the chances of T cells to clear the virus remains to be determined. Oligodendroglia have important function other than myelin formation, including neuronal support by secreting neurotropic factors as well as in neurotransmission. Neurons are cells with little or no regenerative capacity and would be especially vulnerable to inflammation-mediated damage. Therefore, limited and narrowly focused innate responses to infection by oligodendroglia provides a mechanism to avoid attraction of infiltrating cells and to protect their CNS functions.

The role of IFN induced anti-viral genes (is largely unknown in the CNS. We determined role of two well-described IFN induced antiviral genes, RNaseL and Protein Kinase RNA Dependent (PKR) following JHMV infection in the CNS. These latent enzymes are constitutively expressed at lower levels and further upregulated by IFN $\alpha\beta$. When activated by dsRNA these antiviral molecules can directly block viral replication by degrading viral as well as host RNA and by inhibiting protein synthesis. Absence of RNaseL resulted in modest increase in viral burden specifically in macrophage/microglia following JHMV infection in the CNS, without altering overall virus clearance (Ireland et al., 2009). However, unexpectedly RNaseL deficiency resulted in increased axonal damage, demyelination and mortality (Ireland et al., 2009). As RNaseL played a minimum role as an anti-viral factor, we focused on potential role of PKR. PKR activation results in phosphorylation of eIF2 α , an eukaryotic translation initiation factor and Inhibitor of NF κ B (I κ B). Where, Phosphorylation of eIF2 leads to inhibition of translation in the host as well virus, phosphorylation of I κ B leads to activation of potent transcription factor NF- κ B and transcriptional induction of downstream pro- and anti-inflammatory genes. Our studies demonstrated a modest direct antiviral role of PKR, but a strong affect on transcriptional regulation of both and pro-inflammatory genes such as *Il6*, *Tnf α* , *Ccl5*, *Cxcl10*, and anti-inflammatory genes namely *Il10*. Surprisingly, reduced *Il10* mRNA in the CNS, correlated with a direct defect in the ability of CD4 T cells to produce IL10. Furthermore, the absence of PKR resulted in increased accumulation of CD4 T cells in the perivascular space. Diminished *Il10* expression observed in PKR $^{-/-}$ mice was

consistent with enhanced and more diffused demyelination. PKR mediated regulation of IL10 in CD4 T cells suggested a virus independent effect and was consistent with PKR mediated IL10 regulation in macrophages. These results confirmed the notion that antiviral factor also play a significant role in immune regulation and cellular homeostatic functions during CNS inflammation. It may therefore be informative if RNaseL and PKR play a role in non-viral immune mediated demyelinating disease.

During microbial control or injury induced inflammation the host induces countermeasures to limit the tissue damage after virus infection. Macrophage and microglia have been identified to play an ambivalent role in inflammation based on their plasticity to acquire pro to anti-inflammatory phenotype following various CNS infection as well as autoimmune model such as EAE. We therefore explored role of infiltrating macrophage and microglia in regulation of inflammation following JHMV infection. Microglia and infiltrating macrophages exhibited mRNA expression characteristic of pro- as well as anti-inflammatory responses, indicating co-existence of several activation phenotypes. Overall similar expression patterns but different magnitude of gene expression between macrophage and microglia, suggests a cell type specific contribution in regulating pro and anti-inflammatory responses at different stages of infection. Microglia induced IL12p40 expression at ~200 fold as soon as at day 3 p.i. IL12p40 is a common subunit shared by both IL12 and IL23. While IL12 initiates CD4T cells towards IFN γ producing Th1 phenotype; IL23 initiates their activation towards IL17 producing Th17 phenotype. Our results indicate that IL12 but not IL23

deficiency resulted in ameliorated clinical disease without altering virus replication or demyelination. Reduced clinical disease in IL12 deficient mice was attributed to diminished pro-inflammatory response (*Il6*, *Il1β* and $\text{IFN}\gamma$) and increased anti-inflammatory response (IL10). However, reduced level of $\text{IFN}\gamma$ was sufficient to control virus replication in the CNS. These results indicate that balance between pro and anti-inflammatory cytokines dictate a complex interplay between nature of the CNS insult and timing of the cytokine expression during disease.

Therefore, our findings emphasize the importance of cell specific innate immune responses following virus mediated CNS infection using coronavirus model. These studies further underscores the growing understanding of innate immune responses and its collaboration with adaptive immune response to combat acute and persistent infection and their role in successful or pathological outcome in general and in the CNS.

CHAPTER VII

MATERIALS AND METHODS

7.1 Mice

C57BL/6 (H-2D^B) -IL23-deficient (p19^{-/-}) mice were purchased from Schering-Plough, Biopharma (Palo Alto, CA). C57BL/6-IL12- deficient (p35^{-/-}) mice as well as -IL12 and -IL23 (p40^{-/-}) double deficient animals were purchased from Jackson Laboratory (Bar Harbor, ME). Mice expressing green fluorescent protein (GFP) under control of the proteolipid protein (PLP) promoter (PLP-GFP) (Fuss et al., 2000) were backcrossed 6 times with C57BL/6 mice prior to use. Congenic mice were used in subsequent experiments for deficient in type-1 IFN receptor-1 (IFNAR^{-/-}) (Ireland et al., 2008), PKR^{-/-} (Yang et al., 1995) and dual deficient in RNaseL and PKR (DRP^{-/-}) (Zhou et al., 1999). Mice were housed and bred in an accredited animal facility at the Cleveland Clinic, Cleveland, OH in accordance with IACUC guidelines. Age-matched C57BL/6 wild-type mice purchased from the National Cancer Institute (Frederick, MD) were used as controls in all experiments.

7.2 Virus Infection and Clinical Disease

6-7 week old mice were restrained and given an intracerebral injection of 250 plaque forming units (PFU) of the neutralizing monoclonal antibody (mAb) - derived neurotropic John Howard Mueller strain of mouse hepatitis virus (JHMV), variant 2.2v-1, in 30µl of endotoxin free Dulbecco's modified phosphate-buffered saline (PBS). In PKR studies, virus was used at 1000 PFU. Severity of clinical disease was based on post-infection scores graded as 0 = healthy, 1 = ruffled fur and hunch back, 2 = reduced mobility & inability to upright, 3 = paralysis and wasting, and 4 = moribund or dead (Fleming et al., 1986).

7.3 Intracranial Inoculation of Poly (I:C)

TLR3 ligand Poly (I:C) (high molecular weight) was purchased from Invivogen, suspended in endotoxin-free phosphate buffered saline (PBS) to a final concentration of 200 µg/30 µl, aliquoted and stored at -20° C until use. Six week old C57BL/6 mice were injected intracerebrally with 200 µg poly (I:C) in 30 µl sterile PBS, similar to the JHMV infections as described. Brains and spinal cords were removed at 2, 6, 12, and 24, post inoculation, snap frozen in liquid nitrogen, processed and analyzed for mRNA expression.

7.4 Isolation of the Mononuclear Cells and Determination of the Virus Titer

Mononuclear cells were isolated from brain, spleen and cervical lymph nodes (CLN) as previously described (Ireland et al., 2008). Briefly, spleen and CLN tissues were dissociated, washed, and resuspended in RPMI supplemented with 25mM HEPES at 7.2 pH. Additionally, splenocytes were treated with Gey's solution to lyse red blood cells. Brain mononuclear cells were isolated from

individual tissues homogenized in 4 ml of Dulbecco's PBS using chilled Ten-Broeck glass homogenizers (7 ml). Following centrifugation at 400 x g for 7 minutes, clarified supernatants were collected and stored at -80°C. The brain cell pellet was resuspended in a final concentration of 30% Percoll (Pharmacia, Uppsala, Sweden), underlaid with 1 ml of 70% Percoll, and the gradient was centrifuged for 30 min at 800 x g at 4°C. Mononuclear cells were collected from the interface between the 30 and 70% Percoll layers, washed twice with RPMI-HEPES and then viable cells were counted using a hemocytometer-based trypan blue exclusion assay. Virus titer in clarified brain supernatants was determined by plaque assay on a monolayer of DBT cells (a continuous murine astrocytoma cell line), as previously described (Fleming et al., 1986). Briefly, DBT cells were grown in RPMI supplemented with 7% new born calf serum (NBC) and 10% TPB in 20mm petri dish. After 72 hours, confluent monolayer of DBT cells were washed once with RPMI supplemented with TPB and infected with 200µl of brain supernatant, either undiluted or at 10, 100 or 1000 fold dilutions at various time p.i. After 90 minutes incubation, cells were overlaid with 0.6% agarose in RPMI supplemented with 10% TPB. Plaques were counted after 48 hour incubation at 37° C.

7.5 Flow Cytometry

Cells isolated from CNS, Spleen and CLN were incubated with the 10% mouse serum and anti-mouse CD16/32 (clone 2.4G2; BD PharMingen, San Diego, CA) for 15 minutes on ice to block non-specific binding (Kapil et al., 2009). Cells were stained with flurochrome conjugated mAb as described in Table 7.1.

To detect JHMV-specific CD8 T cells, cells were stained with PerCP conjugated anti-CD8 and PE conjugated tetramer H-2D^b-S510. To study the expression of MHC on infiltrating macrophages and on resident brain microglia, cells were stained with the anti- CD45 and F4/80 (Serotec, Raleigh, NJ). CD45^{high} -F4/80 positive cells were distinguished as infiltrating macrophages, while CD45^{low} - F4/80 positive cells were distinguished as microglia.

Table 7.1

Antibodies Utilized in Flow Cytometry

Antibody	Clone	Fluorochrome	vendor
CD4	RM4-5	FITC	BD Pharmingen
CD8	53-6.7	PE	BD Pharmingen
CD45	30-F11	APC, PerCP	BD Pharmingen
MHC Class II	2G9	PE	BD Pharmingen
Ly6G	1A8	FITC	BD Pharmingen
F4/80	C1:A3-1	APC, PE	Serotec
O4	O4	Na*	In house
H-2D ^b -S510 tetramer	-	PE	Beckman-Coulter

7.6 Purification of Cells by Flow Activated Cell Sorting (FACS)

To identify infiltrating macrophages and CNS resident microglia, cells were stained with as described previously in section 6.5 with mAb for the surface receptor for macrophage, microglia and oligodendroglia. Infiltrating macrophages were characterized by their CD45^{hi}/F4/80⁺ phenotype, while CD45^{low}/F4/80⁺ cells

were distinguished as microglia. Mature oligodendroglia, were isolated utilizing transgenic mice (PLP-GFP/B6) that express green fluorescence protein (GFP) under control of an oligodendroglia specific promoter for proteolipid protein, PLP, to (Fuss et al., 2000) in conjunction with CD45 surface staining. Oligodendroglia from IFNAR^{-/-} and Wt control mice were isolated utilizing CD45 and O4 staining. O4 antibody from hybridoma supernatant was obtained from Dr. Stephen Stohlman or Dr. Bruce Trapp's lab. It was titrated for use against cells isolated from PLP-GFP mice and detected with secondary anti-mus IgM (PE). Total protein concentration ranged from 0,1-0.5mg/mL. Staining strategy for specific cell type is described in Table 7.2. Following staining cells were maintained in 1X FACS buffer on ice for sorting. Purified cells were pelleted by centrifugation 400g for 7 minutes at 4⁰ C to remove sheath fluid. Cells were resuspended in trizol and stored at -80⁰ C. Typical yields for 6-7 naïve spinal cords were 40,000-80,000 oligodendroglia and 400,000-600,000 microglia.

Table 7.2

Classification of Cell Types for Identification by Flow

Cell type	Phenotypic classification
Mature oligodendroglia	CD45-ve GFP+ve (using PLP-GFP mice)
Oligodendroglia	CD45-ve O4+ve
Microglia	CD45lo
Macrophage	CD45hi CD11b+ve F4/80+ve

* O4 antibody from hybridoma supernatant was obtained from Dr. Stephen A. Stohlman.

7.7 Correlation between Cell Number and Ct Value

The CNS cell isolation procedure routinely yielded higher numbers of microglia and macrophages compared to oligodendroglia (see section 6.6). To validate that cell numbers were not a factor limiting detection of low abundance mRNA, we evaluated the minimum number of cells needed to achieve reliable PCR products by sorting limiting numbers of brain microglia (CD45^{lo} CD11b⁺) from mice inoculated with the synthetic dsRNA mimic poly (I:C) 4h prior to isolation. Naïve brains were excluded as *Ifn α / β* transcripts were too close to detection thresholds. RNA was isolated from as few as 7500 cells up to 240,000 cells and analyzed for relative expression of *Gapdh*, *Ifn α 4*, and *Ifn β* . *Ifit1* and *Ifit2* transcripts served as representative ISG. Titration curves show that the Ct values for all the genes were in the linear range to *Gapdh* Ct values (Suppl. Figure 3). *Ifn α 4* transcripts that are expressed at low copy number were still in the linear range and reliably detected even below 30,000 cells. In the present study, a minimum of 30,000-40,000 cells obtained from cell preparations of 6-8 mice were thus used for qPCR analysis.

7.8 Ex Vivo Stimulation Of Splenocytes

Spleens were isolated 7 day p.i. from mice injected intraperitoneally with MHV DMN strain at 500 PFU. Splenocytes were isolated as described previously. To bias composition of spleen cells towards CD4 T cells, splenocytes were cultured in RPMI medium 1640 supplemented with 10% FCS, 1% L glutamine, 1% nonessential amino acids, 1% sodium pyruvate, .01% gentamycin and β mercaptoethanol with CD4 specific peptide M133 for 5 days. Stimulated cells

were utilized to determine ability of these cells to produce intercellular cytokines such as IFN γ and IL10.

7.9 Intracellular Detection of Cytokines

Virus-specific production of IFN γ , TNF α and IL17 was evaluated in CNS-, spleen- and CLN-derived CD8 and CD4 T cells. 2×10^6 splenocytes and CLN-derived cells, and 5×10^5 CNS-derived cells were incubated with 3×10^5 EI-4 or CHB3 feeder cells with or without JHMV-specific peptide for the stimulation of CD8 or CD4 T cells. Cells were stimulated either with or without $1 \mu\text{M}$ S510 (CD8-epitope) or $5 \mu\text{M}$ M133 (CD4-epitope) peptide/ml in a total volume of $200 \mu\text{l}$ of RPMI supplemented with 20% fetal calf serum (FCS) for 5 hr at 37°C with $1 \mu\text{l/ml}$ Golgi Stop (BD PharMingen, San Diego, CA). Cytokine production by stimulated cells was detected by intracellular flow cytometry, as previously described (Kapil et al., 2009, Zuo et al., 2006). Briefly, cells were stained for surface expression of CD8, CD4 and CD45, fixed and then permeablized using the Cytotfix/Cytoperm kit (BD PharMingen) according to the manufacturer's protocol. Expression of intracellular cytokine production was detected using FITC conjugated mAb specific for IFN γ , PE conjugated IL17 mAb and APC conjugated IL10 Ab. Cells were analyzed with FACS Calibur flow cytometer (Becton Dickinson, Mountain View, CA) using FlowJo software (TreeStar, Inc., Ashland, OR).

7.10 Phagocytic Assay For Macrophage And Microglia

Escherichia coli (K-12 strain) BioParticles®, Alexa Fluor® 488 (invitrogen) conjugate were used as particle tracers to analyze phagocytosis by infiltrating macrophage and resident microglia cells from CNS of wt mice. Briefly,

mononuclear cells from brain were incubated along with bioparticles. Before using, particles were incubated with opsonizing reagent (invitrogen) in 1xPBS for 1 hour at 37⁰ C and than washed twice with 1XPBS. Cells were incubated with beads for 1 hour at 37⁰ C in 5% CO₂ incubator. Cells were than washed 3X to remove particles from surface and than blocked and stained for CD45 and F4/80 as described previously. To avoid nonspecific signal from beads bound to the surface of microglia/macrophages, cells were quenched with trypan blue for 5 minutes at ice and washed 3X to remove extra dye. Cells were analyzed with FACS Calibur flow cytometer (Becton Dickinson, Mountain View, CA) using FlowJo software (TreeStar, Inc., Ashland, OR).

7.11 ELISA

A sandwich enzyme-linked immunosorbent assay (ELISA)-based system previously described (Kapil et al., 2009) was used to measure concentrations of IFN γ and IL10 protein in brain supernatants. Briefly, ELISA plates were coated with an anti-mouse cytokine capture antibody specific for either IFN γ or IL10 (BD PharMingen, San Diego, CA) at 1 μ g/ml and incubated overnight at 4°C. The plates were washed (0.5% Tween-20 in PBS) and blocked with 10% FCS in PBS for 1 hr at room temperature and washed again. Brain supernatants collected at different time points post-infection were incubated in capture antibody-coated ELISA plates for 2 hr at room temperature. Bound cytokine was detected with a secondary biotinylated detection antibody specific for either IFN γ or IL10 (BD PharMingen) combined with Avidin-Horseradish Peroxidase (Av-HRP) and incubated for 1 hr at room temperature. TMB (BD PharMingen) was used as

colorimetric substrate and the reaction was stopped using sulfuric acid (H₂SO₄). Absorbance levels were measured at 450 nm using a microplate reader (Bio-Rad) and SoftMax Pro software (Molecular Devices, Sunnyvale, CA). Cytokine levels were calculated using a standard curve of known concentrations of commercially available recombinant IFN γ or IL10 protein. Triplicate samples were averaged and standard error was calculated. Data are presented as ng of protein/brain \pm SE.

7.12 Histology and Fluorescent Staining

Spinal cords were fixed in 10% formalin and embedded in paraffin. 10 μ m sections were stained with hematoxylin and eosin or luxol fast blue to evaluate inflammation and myelin loss, respectively. The distribution of viral antigen was determined by immunoperoxidase staining (Vectastain-ABC kit; Vector Laboratory, Burlingame, CA), using the anti-JHMV mAb J.3.3 specific for the carboxyl terminus of the viral nucleocapsid protein as the primary Ab and horse anti-mouse as secondary Ab, and 3, 3'-diaminobenzidine substrate (Vector Laboratory). Sections were scored in a blinded manner for inflammation, demyelination, and viral antigen.

To identify accumulation of CD4 T cells within perivascular space, spinal cord tissues were isolated from perfused wt and PKR^{-/-} mice as described previously (Ireland et al., 2009, Savarin et al., 2010). Tissues were snap frozen in liquid N₂ in OCT and were stored at -80^o C. Spinal cord sections were cut at 12 μ m thickness using microtome and stored at -80^o C. Tissue sections were thawed and fixed with 4% PFA for 20 minutes each at room temperature.

Following permeabilization with 1% tritonX-100 at room temperature, nonspecific antibody binding was blocked using 1% bovine serum albumin and 10% goat serum. For perivascular accumulation of CD4 T cells, spinal cord sections were incubated at 4°C with mouse anti rat CD4 Ab and rabbit anti mouse laminin (Cedarline Laboratories, Ontario, Canada) overnight. Next day, tissue sections were washed and incubated with AF 594 conjugated anti rat and AF488 conjugated anti rabbit (Invitrogen) secondary antibodies at room temperature for 60 minutes. Following wash, sections were mounted with ProLong Gold antifade mounting media containing 4',6-diamidino-2-phenylindole (Invitrogen, Carlsbad, CA). To further determine expression of PKR-p in CD4 T cells, spinal cord sections were incubated at 4°C with mouse anti rat CD4 Ab and rabbit anti mouse PKR-p (Cedarline Laboratories, Ontario, Canada) overnight and processed similarly as described previously.

7.13 Real Time PCR

Tissues were immediately frozen in liquid nitrogen and stored at -80°C. RNA was extracted from CNS tissues dissociated in TRIzol Reagent (Invitrogen, Carlsbad, CA) using sterile Tenbroeck glass homogenizers according to the manufacturer's instructions. Briefly, after chloroform extraction, RNA was precipitated in isopropyl alcohol, washed with 75% ethanol and resuspended in RNase-free water (Gibco, Invitrogen, Grand Island, NY). To remove DNA contamination, RNA was treated with the DNase-treatment Kit (Ambion, Austin, TX), according to the manufacturer's instructions. RNA integrity and concentration were evaluated by electrophoresis on a 1.2% formaldehyde

agarose gel. cDNA was synthesized using 2 ug of total RNA, Moloney Murine Leukemia Virus Reverse Transcriptase (Invitrogen), 10mM dNTP mix, and 20 uM random hexamer primers (Promega). Quantitative real-time PCR was performed for expression levels of cytokines and chemokines, anti-viral genes and anti-inflammatory genes was determined using either SYBR Green chemistry or taqman chemistry (Applied Biosystems, Foster city, CA). List of genes is described in the table form. Expression was compared relative to the endogenous control glyceraldehyde-3-phosphate dehydrogenase (GAPDH) as previously described (Ireland et al., 2008). Reaction conditions for the 7500 Fast Real-Time PCR system (Applied Bio-system) for SYBR green were as follows: 95°C for 10 min and 40 cycles of denaturation at 94°C for 10s, annealing at 60°C for 30s and elongation at 72°C for 30s and for taqman were 95°C for 20 sec as holding temperature and then 40 cycles of denaturation at 95°C for .03s, annealing and extension at 60°C for 30s. All PCR were performed in 10 ul final reaction volumes consisted of specific master mix, 1mM of each primer, and 4 ul cDNA using the ABI 7500 fast PCR machine and 7500 software. Data presented reflect the induction level (n fold) relative to GAPDH, using the following formula,

$$(2^{[CT \{GAPDH\} - CT \{Target\}]}) \times 1000 \text{ where Ct is the threshold cycle.}$$

Table 7.3

List of Primer Sequences/Catalog Number for Genes Utilized in the Study

Gene Name		Primer sequence/ Catalog #
House keeping gene		
1.	Glyceraldehyde 3-phosphate dehydrogenase (<i>Gapdh</i>)	F, 5'-TGCACCACCAACTGCTTAG-3' R, 5'-GGATGCAGGGATGATGTTC-3'
JHMV primers		
1.	Nucleocapsid gene of John Howard Muller strain of coronavirus (<i>JhmvN</i>)	F, 5'-GAGTGCCTATTGCCAATGGAA-3' R, 5'-TTAAAGGAACGTCGGTTGTGTCT-3'
Cytokines		
1.	Interleukin-1 β (<i>Il1β</i>)	Mm01336189_m1
2.	Interleukin-1 receptor antagonist (<i>Il1Ra</i>)	F, 5' AGATAGACATGGTGCCTATTGACCTT-3' R, 5'-CATCTCCAGACTTGGCACAAGA-3'
3.	Interleukin-6 (<i>Il6</i>)	F, 5'-ACACATGTTCTCTGGGAAATCGT-3' R, 5'-AAGTGCATCATCGTTGTTTCATACA-3'
4.	Interleukin-10 (<i>Il10</i>)	F, 5'-TTTGAATTCCCTGGGTGAGAA-3' R, 5'-GCTCCACTGCCTTGCTCTTATT-3'

5.	Interleukin-12p35 (<i>Il12p35</i>)	F, 5'-CACCTTGCCCTCCTAAACC-3' R, 5'-CACCTGGCAGGTCCAGAGA-3'
6.	Interleukin-12p40 (<i>Il12p40</i>)	F, 5'-ACAGCACCAGCTTCTTCATCAG-3' R, 5'-TCTTCAAAGGCTTCATCTGCAA-3'
7.	Interleukin-13 (<i>Il13</i>)	F, 5'-TGACCAACATCTCCAATTGCA-3' R, 5'-TTGTTATAAAGTGGGCTACTTCGATTT-3'
8.	Interleukin-21 (<i>Il21</i>)	F, 5'-GGACAGTATAGACGCTCACGAATG-3' R, 5'-CGTATCGTACTTCTCCACTTGCA-3'
9.	Interleukin-23p19 (<i>Il23p19</i>)	F, 5'-CAGCAGCTCTCTCGGAAT-3' R, 5'-ACAACCATCTTCACACTGGATACG-3'
10.	Interferon- α 4 (<i>Ifnα4</i>)	Mm00833969_s1
11.	Interferon- β (<i>Ifnβ</i>)	Mm00439546_s1
12.	Interferon- γ (<i>Ifnγ</i>)	Mm01168134_m1
13.	Tumor necrosis factor- α (<i>Tnfα</i>)	F, 5'-GCCACCACGCTCTTCTGTCT-3' R, 5'-GGTCTGGGCCATAGAACTGATG-3'
14.	Transforming growth-factor- β 1 (<i>Tgfβ1</i>)	F, 5'-CCCGAAGCGGACTACTATGC-3' R, 5'-CGAATGTCTGACGTATTGAAGAACA-3'
15.	Transforming growth-factor- β 3	F, 5'-CAATTACTGCTCCGCAACCT-3' R, 5'-AGCACCGTGCTATGGGTTGT-3'

	(<i>Tgfβ3</i>)	
Chemo-kines		
1.	Chemokine (C-C motif) ligand 2 (<i>Ccl2</i>)	F, 5'-AGCAGGTGTCCCAAAGAA-3' R, 5'-TATGTCTGGACCCATTCCTT-3'
2.	Chemokine (C-C motif) ligand 5 (<i>Ccl5/Rantes</i>)	F, 5'-GCAAGTGCTCCAATCTTGCA-3' R, 5'-CTTCTCTGGGTTGGCACACA-3'
3.	Chemokine (C-X-C motif) ligand 9 (<i>Cxcl9/Mig</i>)	F, 5'-GACGGTCCGCTGCAACTG-3' R, 5'-GCTTCCCTATGGCCCTCATT-3'
4.	Chemokine (C-X-C motif) ligand 10 (<i>Cxcl10/Ip10</i>)	F, 5'-TGCACGATGCTCCTGCA-3' R, 5'-AGGTCTTTGAGGGATTTGTAGTGG-3'
Cell signaling enzymes		
1.	Nitric oxide synthetase 2 (<i>Nos2</i>)	
2.	Arginase-1 (<i>Arg1</i>)	F, 5' TGGGTGGATGCTCACAGA-3' R, 5'-CAGGTTGCCCATGCAGATT-3'
3.	Chitinase like protein (<i>Ym1/2</i>)	F, 5'-AATATCTGACGGTTCTGAGGAGTAGA G -3' R, 5'-GGCCAACAGAACAGAAGAAAATG-3'
Anti-viral factors		
1.	Protein Kinase RNA dependent (<i>Pkr</i>)	Mm00440966_m1

2.	2'-5'-oligoadenylate synthetase 2 (<i>Oas2</i>)	F, 5'-AAAAATGTCTGCTTCTTGAATTCTGA-3' R, 5'-TGTGCCTTTGGCAGTGGAT-3'
3.	Interferon-induced protein with tetratricopeptide repeats 1 (<i>Ifit1</i>)	Mm00515153_m1
4.	Interferon-induced protein with tetratricopeptide repeats 2 (<i>Ifit2</i>)	Mm00492606_m1
Pathogen Recognition Receptors		
1.	Melanoma differentiation- associated gene-5 (<i>Mda5</i>)	F, 5'-GACACCAGAATTCAAGGGAC-3' R, 5'-GCCACACTTGCAGATAATCTC-3'
2.	Retinoic acid inducible gene I (<i>Rig-I</i>)	F, 5'-GTCAGCACAAACCACAACC-3' R, 5'-GTCTCAACCACTCGAATGTC-3'
3.	Toll like receptor-2 (<i>Tlr2</i>)	Mm00442346_m1

4.	Toll like receptor-3 (<i>Tlr3</i>)	Mm01207404_m1
5.	Toll like receptor-7 (<i>Tlr7</i>)	Mm00446590_m1
Transcription factor		
1.	Interferon regulatory factor-3 (<i>Irf3</i>)	Mm00516779_m1
2.	Interferon regulatory factor-7 (<i>Irf7</i>)	Mm00516788_m1
3.	Signal Transducers and Activators of Transcription (<i>Stat1</i>)	Mm00439531_m1
4.	I-kappa-B kinase epsilon (<i>Ikkε</i>)	Mm00444862_m1

REFERENCES

- Aggarwal, S., Ghilardi, N., Xie, M. H., De Sauvage, F. J. & Gurney, A. L. 2003. 'Interleukin-23 promotes a distinct CD4 T cell activation state characterized by the production of interleukin-17', *Journal of Biological Chemistry*, vol. 278, pp. 1910-4.
- Akwa, Y., Hassett, D. E., Eloranta, M. L., Sandberg, K., Masliah, E., Powell, H., Whitton, J. L., Bloom, F. E. & Campbell, I. L. 1998. 'Transgenic expression of IFN-alpha in the central nervous system of mice protects against lethal neurotropic viral infection but induces inflammation and neurodegeneration', *Journal of Immunology*, vol. 161, pp. 5016-26.
- Al Moussawi, K., Ghigo, E., Kalinke, U., Alexopoulou, L., Mege, J. L. & Desnues, B. 2010. 'Type I interferon induction is detrimental during infection with the Whipple's disease bacterium, *Tropheryma whipplei*', *PLoS Pathogens*, vol. 6, e1000722.
- Alexopoulou, L., Holt, A. C., Medzhitov, R. & Flavell, R. A. 2001. 'Recognition of double-stranded RNA and activation of NF-kappaB by Toll-like receptor 3', *Nature*, vol. 413, pp. 732-8.
- Aman, M. J., Keller, U., Derigs, G., Mohamadzadeh, M., Huber, C. & Peschel, C. 1994. 'Regulation of cytokine expression by interferon-alpha in human bone marrow stromal cells: inhibition of hematopoietic growth factors and induction of interleukin-1 receptor antagonist', *Blood*, vol. 84, pp. 4142-50.

- Anghelina, D., Pewe, L. & Perlman, S. 2006. 'Pathogenic role for virus-specific CD4 T cells in mice with coronavirus-induced acute encephalitis', *American Journal of Pathology*, vol. 169, pp. 209-22.
- Auffray, C., Fogg, D., Garfa, M., Elain, G., Join-Lambert, O., Kayal, S., Sarnacki, S., Cumano, A., Lauvau, G. & Geissmann, F. 2007. 'Monitoring of blood vessels and tissues by a population of monocytes with patrolling behavior', *Science*, vol. 317, pp. 666-70.
- Bando, Y., Onuki, R., Katayama, T., Manabe, T., Kudo, T., Taira, K. & Tohyama, M. 2005. 'Double-strand RNA dependent protein kinase (PKR) is involved in the extrastriatal degeneration in Parkinson's disease and Huntington's disease', *Neurochemistry International*, vol. 46, pp. 11-8.
- Bansal, V. & Ochoa, J. B. 2003. 'Arginine availability, arginase, and the immune response', *Current Opinion in Clinical Nutrition & Metabolic Care*, vol. 6, pp. 223-8.
- Baric, R. S. & Yount, B. 2000. 'Subgenomic negative-strand RNA function during mouse hepatitis virus infection', *Journal of Virology*, vol. 74, pp. 4039-46.
- Barton, G. M. 2008. 'A calculated response: control of inflammation by the innate immune system', *Journal of Clinical Investigation*, vol. 118, pp. 413-20.
- Bass, B. L. 1997. 'RNA editing and hypermutation by adenosine deamination', *Trends in Biochemical Sciences*, vol. 22, pp. 157-62.
- Ben-Asouli, Y., Banai, Y., Pel-Or, Y., Shir, A. & Kaempfer, R. 2002. 'Human interferon-gamma mRNA autoregulates its translation through a

- pseudoknot that activates the interferon-inducible protein kinase PKR', *Cell*, vol. 108, pp. 221-32.
- Benoit, M., Desnues, B. & Mege, J. L. 2008. 'Macrophage polarization in bacterial infections', *Journal of Immunology*, vol. 181, pp. 3733-9.
- Bergeron, J., Benlimame, N., Zeng-Rong, N., Xiao, D., Scrivens, P. J., Koromilas, A. E. & Alaoui-Jamali, M. A. 2000. 'Identification of the interferon-inducible double-stranded RNA-dependent protein kinase as a regulator of cellular response to bulky adducts', *Cancer Research*, vol. 60, pp. 6800-4.
- Bergmann, C., Mcmillan, M. & Stohlman, S. 1993. 'Characterization of the Ld-restricted cytotoxic T-lymphocyte epitope in the mouse hepatitis virus nucleocapsid protein', *Journal of Virology*, vol. 67, pp. 7041-9.
- Bergmann, C. C., Altman, J. D., Hinton, D. & Stohlman, S. A. 1999. 'Inverted immunodominance and impaired cytolytic function of CD8+ T cells during viral persistence in the central nervous system', *Journal of Immunology*, vol. 163, pp. 3379-87.
- Bergmann, C. C., Lane, T. E. & Stohlman, S. A. 2006. 'Coronavirus infection of the central nervous system: host-virus stand-off', *Nature Reviews Microbiology*, vol. 4, pp. 121-32.
- Bergmann, C. C., Parra, B., Hinton, D. R., Chandran, R., Morrison, M. & Stohlman, S. A. 2003. 'Perforin-mediated effector function within the central nervous system requires IFN-gamma-mediated MHC up-regulation', *Journal of Immunology*, vol. 170, pp. 3204-13.

- Bergmann, C. C., Parra, B., Hinton, D. R., Ramakrishna, C., Dowdell, K. C. & Stohlman, S. A. 2004. 'Perforin and gamma interferon-mediated control of coronavirus central nervous system infection by CD8 T cells in the absence of CD4 T cells', *Journal of Virology*, vol. 78, pp. 1739-50.
- Bonavia, A., Arbour, N., Yong, V. W. & Talbot, P. J. 1997. 'Infection of primary cultures of human neural cells by human coronaviruses 229E and OC43', *Journal of Virology*, vol. 71, pp. 800-6.
- Bonnet, M. C., Daurat, C., Ottone, C. & Meurs, E. F. 2006. 'The N-terminus of PKR is responsible for the activation of the NF-kappaB signaling pathway by interacting with the IKK complex', *Cellular Signaling*, vol. 18, pp. 1865-75.
- Bonnet, M. C., Weil, R., Dam, E., Hovanessian, A. G. & Meurs, E. F. 2000. 'PKR stimulates NF-kappaB irrespective of its kinase function by interacting with the IkappaB kinase complex', *Molecular and Cellular Biology*, vol. 20, pp. 4532-42.
- Borden, E. C., Sen, G. C., Uze, G., Silverman, R. H., Ransohoff, R. M., Foster, G. R. & Stark, G. R. 2007. 'Interferons at age 50: past, current and future impact on biomedicine', *Nature Reviews Drug Discovery*, vol. 6, pp. 975-90.
- Boven, L. A., Van Meurs, M., Van Zwam, M., Wierenga-Wolf, A., Hintzen, R. Q., Boot, R. G., Aerts, J. M., Amor, S., Nieuwenhuis, E. E. & Laman, J. D. 2006. 'Myelin-laden macrophages are anti-inflammatory, consistent with foam cells in multiple sclerosis', *Brain*, vol. 129, pp. 517-26.

- Bsibsi, M., Persoon-Deen, C., Verwer, R. W., Meeuwssen, S., Ravid, R. & Van Noort, J. M. 2006. 'Toll-like receptor 3 on adult human astrocytes triggers production of neuroprotective mediators', *Glia*, vol. 53, pp. 688-95.
- Bsibsi, M., Ravid, R., Gveric, D. & Van Noort, J. M. 2002. 'Broad expression of Toll-like receptors in the human central nervous system', *Journal of Neuropathology & Experimental Neurology*, vol. 61, pp. 1013-21.
- Butchi, N. B., Du, M. & Peterson, K. E. 2010. 'Interactions between TLR7 and TLR9 agonists and receptors regulate innate immune responses by astrocytes and microglia', *Glia*, vol. 58, pp. 650-64.
- Cannella, B. & Raine, C. S. 2004. 'Multiple sclerosis: cytokine receptors on oligodendrocytes predict innate regulation', *Annals of Neurology*, vol. 55, pp. 46-57.
- Carpentier, P. A., Begolka, W. S., Olson, J. K., Elhofy, A., Karpus, W. J. & Miller, S. D. 2005. 'Differential activation of astrocytes by innate and adaptive immune stimuli', *Glia*, vol. 49, pp. 360-74.
- Carpentier, P. A., Duncan, D. S. & Miller, S. D. 2008. 'Glial toll-like receptor signaling in central nervous system infection and autoimmunity', *Brain, Behavior, and Immunity*, vol. 22, pp. 140-7.
- Carter, D. B., Deibel, M. R., Jr., Dunn, C. J., Tomich, C. S., Laborde, A. L., Slightom, J. L., Berger, A. E., Bienkowski, M. J., Sun, F. F., & Mcewan, R. N. 1990. 'Purification, cloning, expression and biological characterization of an interleukin-1 receptor antagonist protein', *Nature*, vol. 344, pp. 633-8.

- Carty, M. & Bowie, A. G. 2011. 'Evaluating the role of Toll-like receptors in diseases of the central nervous system', *Biochemical Pharmacology*, vol. 81, pp. 825-37.
- Cassol, E., Cassetta, L., Rizzi, C., Alfano, M. & Poli, G. 2009. 'M1 and M2a polarization of human monocyte-derived macrophages inhibits HIV-1 replication by distinct mechanisms', *Journal of Immunology*, vol. 182, pp. 6237-46.
- Castro, R. F. & Perlman, S. 1996. 'Differential antigen recognition by T cells from the spleen and central nervous system of coronavirus-infected mice', *Virology*, vol. 222, pp. 247-51.
- Cervantes-Barragan, L., Züst, R., Weber, F., Spiegel, M., Lang, K. S., Akira, S., Thiel, V. & Ludewig, B. 2007. 'Control of coronavirus infection through plasmacytoid dendritic-cell-derived type I interferon', *Blood*, vol. 109, pp. 1131-7.
- Chakrabarti, A., Sadler, A. J., Kar, N., Young, H. A., Silverman, R. H. & Williams, B. R. 2008. 'Protein kinase R-dependent regulation of interleukin-10 in response to double-stranded RNA', *Journal of Biological Chemistry*, vol. 283, pp. 25132-9.
- Chakrabarty, A., Danley, M. M. & Levine, S. M. 2004. 'Immunohistochemical localization of phosphorylated protein kinase R and phosphorylated eukaryotic initiation factor-2 alpha in the central nervous system of SJL mice with experimental allergic encephalomyelitis', *Journal of Neuroscience Research*, vol. 76, pp. 822-33.

- Chan, G., Bivins-Smith, E. R., Smith, M. S., Smith, P. M. & Yurochko, A. D. 2008. 'Transcriptome analysis reveals human cytomegalovirus reprograms monocyte differentiation toward an M1 macrophage', *Journal of Immunology*, vol. 181, pp. 698-711.
- Cheung, B. K., Lee, D. C., Li, J. C., Lau, Y. L. & Lau, A. S. 2005. 'A role for double-stranded RNA-activated protein kinase PKR in Mycobacterium-induced cytokine expression', *Journal of Immunology*, vol. 175, pp. 7218-25.
- Chiang, C. S., Powell, H. C., Gold, L. H., Samimi, A. & Campbell, I. L. 1996. 'Macrophage/microglial-mediated primary demyelination and motor disease induced by the central nervous system production of interleukin-3 in transgenic mice', *Journal of Clinical Investigation*, vol. 97, pp. 1512-24.
- Colonna, M. 2007. 'TLR pathways and IFN-regulatory factors: to each its own'. *European Journal of Immunology*, vol. 37, pp. 306-9.
- Colton, C. A. 2009. 'Heterogeneity of microglial activation in the innate immune response in the brain', *Journal of NeuroImmune Pharmacology*, vol. 4, pp. 399-418.
- Conrady, C. D., Drevets, D. A. & Carr, D. J. 2010. 'Herpes simplex type I (HSV-1) infection of the nervous system: is an immune response a good thing?' *Journal of NeuroImmune Pharmacology*, vol. 220, pp. 1-9.
- Cotler, S. J., Craft, T., Ferris, M., Morrissey, M., Mccone, J., Reddy, K. R., Conrad, A., Jensen, D. M., Albrecht, J. & Taylor, M. W. 2002. 'Induction of IL-1Ra

- in resistant and responsive hepatitis C patients following treatment with IFN-con1', *Journal of Interferon & Cytokine Research*, vol. 22, pp. 549-54.
- Cousens, L. P., Orange, J. S., Su, H. C. & Biron, C. A. 1997. 'Interferon-alpha/beta inhibition of interleukin 12 and interferon-gamma production in vitro and endogenously during viral infection', *Proceedings of the National Academy of Sciences of the United States of America*, vol. 94, pp. 634-9.
- Cousens, L. P., Peterson, R., Hsu, S., Dorner, A., Altman, J. D., Ahmed, R. & Biron, C. A. 1999. 'Two roads diverged: interferon alpha/beta- and interleukin 12-mediated pathways in promoting T cell interferon gamma responses during viral infection', *Journal of Experimental Medicine*, vol. 189, pp. 1315-28.
- Coutelier, J. P., Van Broeck, J. & Wolf, S. F. 1995. 'Interleukin-12 gene expression after viral infection in the mouse', *Journal of Virology*, vol. 69, pp. 1955-8.
- Couturier, J., Morel, M., Pontcharraud, R., Gontier, V., Fauconneau, B., Paccalin, M. & Page, G. 2010. 'Interaction of double-stranded RNA-dependent protein kinase (PKR) with the death receptor signaling pathway in amyloid beta (A β)-treated cells and in APPSLPS1 knock-in mice', *Journal of Biological Chemistry*, vol. 285, pp. 1272-82.
- Cua, D. J., Sherlock, J., Chen, Y., Murphy, C. A., Joyce, B., Seymour, B., Lucian, L., To, W., Kwan, S., Churakova, T., Zurawski, S., Wiekowski, M., Lira, S. A., Gorman, D., Kastelein, R. A. & Sedgwick, J. D. 2003. 'Interleukin-23

rather than interleukin-12 is the critical cytokine for autoimmune inflammation of the brain', *Nature*, vol. 421, pp. 744-8.

Daffis, S., Szretter, K. J., Schriewer, J., Li, J., Youn, S., Errett, J., Lin, T. Y., Schneller, S., Zust, R., Dong, H., Thiel, V., Sen, G. C., Fensterl, V., Klimstra, W. B., Pierson, T. C., Buller, R. M., Gale, M., Jr., Shi, P. Y. & Diamond, M. S. 2010. '2'-O methylation of the viral mRNA cap evades host restriction by IFIT family members', *Nature*, vol. 468, pp. 452-6.

Dakhama, A., Lee, Y. M., Ohnishi, H., Jing, X., Balhorn, A., Takeda, K. & Gelfand, E. W. 2009. 'Virus-specific IgE enhances airway responsiveness on reinfection with respiratory syncytial virus in newborn mice', *Journal of Allergy and Clinical Immunology*, vol. 123, pp. 138-145.

Dandekar, A. A. & Perlman, S. 2002. 'Virus-induced demyelination in nude mice is mediated by gamma delta T cells', *American Journal of Pathology*, vol. 161, pp. 1255-63.

Delhaye, S., Paul, S., Blakqori, G., Minet, M., Weber, F., Staeheli, P. & Michiels, T. 2006. 'Neurons produce type I interferon during viral encephalitis', *Proceedings of the National Academy of Sciences of the United States of America*, vol. 103, pp. 7835-40.

Diamond, M. S. & Harris, E. 2001. 'Interferon inhibits dengue virus infection by preventing translation of viral RNA through a PKR-independent mechanism', *Virology*, vol. 289, pp. 297-311.

Domanski, P., Witte, M., Kellum, M., Rubinstein, M., Hackett, R., Pitha, P. & Colamonici, O. R. 1995. 'Cloning and expression of a long form of the beta

- subunit of the interferon alpha beta receptor that is required for signaling', *Journal of Biological Chemistry*, vol. 270, pp. 21606-11.
- Dong, Y. & Benveniste, E. N. 2001. 'Immune function of astrocytes', *Glia*, vol. 36, pp. 180-90.
- Durante, W., Johnson, F. K. & Johnson, R. A. 2007. 'Arginase: a critical regulator of nitric oxide synthesis and vascular function', *Clinical and Experimental Pharmacology and Physiology*, vol. 34, pp. 906-11.
- Durbin, J. E., Hackenmiller, R., Simon, M. C. & Levy, D. E. 1996. 'Targeted disruption of the mouse Stat1 gene results in compromised innate immunity to viral disease', *Cell*, vol. 84, pp. 443-50.
- Eisenberg, S. P., Evans, R. J., Arend, W. P., Verderber, E., Brewer, M. T., Hannum, C. H. & Thompson, R. C. 1990. 'Primary structure and functional expression from complementary DNA of a human interleukin-1 receptor antagonist', *Nature*, vol. 343, pp. 341-6.
- Engelhardt, B. & Ransohoff, R. M. 2005. 'The ins and outs of T-lymphocyte trafficking to the CNS: anatomical sites and molecular mechanisms', *Trends in Immunology*, vol. 26, pp. 485-95.
- Fleming, J. O., Trousdale, M. D., El-Zaatari, F. A., Stohlman, S. A. & Weiner, L. P. 1986. 'Pathogenicity of antigenic variants of murine coronavirus JHM selected with monoclonal antibodies', *Journal of Virology*, vol. 58, pp. 869-75.
- Fleming, J. O., Wang, F. I., Trousdale, M. D., Hinton, D. R. & Stohlman, S. A. 1993. 'Interaction of immune and central nervous systems: contribution of

- anti-viral Thy-1+ cells to demyelination induced by coronavirus JHM', *Regional Immunology*, vol. 5, pp. 37-43.
- Fuss, B., Mallon, B., Phan, T., Ohlemeyer, C., Kirchhoff, F., Nishiyama, A. & Macklin, W. B. 2000. 'Purification and analysis of in vivo-differentiated oligodendrocytes expressing the green fluorescent protein', *Developmental Biology*, vol. 218, pp. 259-74.
- Galea, I., Bechmann, I. & Perry, V. H. 2007. 'What is immune privilege (not)?' *Trends in Immunology*, vol. 28, pp. 12-8.
- Garcia, M. A., Meurs, E. F. & Esteban, M. 2007. 'The dsRNA protein kinase PKR: virus and cell control', *Biochimie*, vol. 89, pp. 799-811.
- Giannetti, N., Moyse, E., Ducray, A., Bondier, J. R., Jourdan, F., Propper, A. & Kastner, A. 2004. 'Accumulation of Ym1/2 protein in the mouse olfactory epithelium during regeneration and aging', *Neuroscience*, vol. 123, pp. 907-17.
- Gil, J. & Esteban, M. 2000. 'The interferon-induced protein kinase (PKR), triggers apoptosis through FADD-mediated activation of caspase 8 in a manner independent of Fas and TNF-alpha receptors', *Oncogene*, vol. 19, pp. 3665-74.
- Gil, J., Garcia, M. A., Gomez-Puertas, P., Guerra, S., Rullas, J., Nakano, H., Alcami, J. & Esteban, M. 2004. 'TRAF family proteins link PKR with NF-kappa B activation', *Molecular and Cellular Biology*, vol. 24, pp. 4502-12.
- Ginhoux, F., Greter, M., Leboeuf, M., Nandi, S., See, P., Gokhan, S., Mehler, M. F., Conway, S. J., Ng, L. G., Stanley, E. R., Samokhvalov, I. M. & Merad,

- M. 2010. 'Fate mapping analysis reveals that adult microglia derive from primitive macrophages', *Science*, vol. 330, pp. 841-5.
- Glass, W. G., Hickey, M. J., Hardison, J. L., Liu, M. T., Manning, J. E. & Lane, T. E. 2004. 'Antibody targeting of the CC chemokine ligand 5 results in diminished leukocyte infiltration into the central nervous system and reduced neurologic disease in a viral model of multiple sclerosis', *Journal of Immunology*, vol. 172, pp. 4018-25.
- Gonzalez, J. M., Bergmann, C. C., Fuss, B., Hinton, D. R., Kangas, C., Macklin, W. B. & Stohlman, S. A. 2005. 'Expression of a dominant negative IFN-gammareceptor on mouse oligodendrocytes', *Glia*, vol. 51, pp. 22-34.
- Gonzalez, J. M., Bergmann, C. C., Ramakrishna, C., Hinton, D. R., Atkinson, R., Hoskin, J., Macklin, W. B. & Stohlman, S. A. 2006. 'Inhibition of interferon-gamma signaling in oligodendroglia delays coronavirus clearance without altering demyelination', *American Journal of Pathology*, vol. 168, pp. 796-804.
- Gordon, S. 2007. 'Macrophage heterogeneity and tissue lipids', *Journal of Clinical Investigation*, vol. 117, pp. 89-93.
- Griffin, D. E. 2003. 'Immune responses to RNA-virus infections of the CNS', *Nature Reviews Immunology*, vol. 3, pp. 493-502.
- Grolleau, A., Kaplan, M. J., Hanash, S. M., Beretta, L. & Richardson, B. 2000. 'Impaired translational response and increased protein kinase PKR expression in T cells from lupus patients', *Journal of Clinical Investigation*, vol. 106, pp.1561-8.

- Hanisch, U. K. 2002. 'Microglia as a source and target of cytokines', *Glia*, vol. 40, pp. 140-55.
- Hanke, M. L. & Kielian, T. 2011. 'Toll-like receptors in health and disease in the brain: mechanisms and therapeutic potential', *Clinical Science (London)*, vol. 121, pp. 367-87.
- Held, K. S., Glass, W. G., Orlovsky, Y. I., Shamberger, K. A., Petley, T. D., Branigan, P. J., Carton, J. M., Beck, H. S., Cunningham, M. R., Benson, J. M. & Lane, T. E. 2008. 'Generation of a protective T-cell response following coronavirus infection of the central nervous system is not dependent on IL-12/23 signaling', *Viral Immunology*, vol. 21, pp. 173-88.
- Hoek, R. M., Ruuls, S. R., Murphy, C. A., Wright, G. J., Goddard, R., Zurawski, S. M., Blom, B., Homola, M. E., Streit, W. J., Brown, M. H., Barclay, A. N. & Sedgwick, J. D. 2000. 'Down-regulation of the macrophage lineage through interaction with OX2 (CD200)', *Science*, vol. 290, pp. 1768-71.
- Honda, K. & Taniguchi, T. 2006. 'IRFs: master regulators of signalling by Toll-like receptors and cytosolic pattern-recognition receptors', *Nature Reviews Immunology*, vol. 6, pp. 644-58.
- Honda, K., Yanai, H., Negishi, H., Asagiri, M., Sato, M., Mizutani, T., Shimada, N., Ohba, Y., Takaoka, A., Yoshida, N. & Taniguchi, T. 2005. 'IRF-7 is the master regulator of type-I interferon-dependent immune responses', *Nature*, vol. 434, pp. 772-7.
- Horai, R., Saijo, S., Tanioka, H., Nakae, S., Sudo, K., Okahara, A., Ikuse, T., Asano, M. & Iwakura, Y. 2000. 'Development of chronic inflammatory

arthropathy resembling rheumatoid arthritis in interleukin 1 receptor antagonist-deficient mice', *Journal of Experimental Medicine*, vol. 191, pp. 313-20.

Hosking, M. P., Liu, L., Ransohoff, R. M. & Lane, T. E. 2009. 'A protective role for ELR+ chemokines during acute viral encephalomyelitis', *PLoS Pathogens*, vol. 5, pp. e1000648.

Houtman, J. J. & Fleming, J. O. 1996. 'Dissociation of demyelination and viral clearance in congenitally immunodeficient mice infected with murine coronavirus JHM', *Journal For Neurovirology*, vol. 2, pp. 101-10.

Hunter, C. A. 2005. 'New IL-12-family members: IL-23 and IL-27, cytokines with divergent functions', *Nature Reviews Immunology*, vol. 5, pp. 521-31.

Hutchinson, P. J., O'connell, M. T., Rothwell, N. J., Hopkins, S. J., Nortje, J., Carpenter, K. L., Timofeev, I., Al-Rawi, P. G., Menon, D. K. & Pickard, J. D. 2007. 'Inflammation in human brain injury: intracerebral concentrations of IL-1alpha, IL-1beta, and their endogenous inhibitor IL-1ra', *Journal of Neurotrauma*, vol. 24, pp. 1545-57.

Inoue, A., Koh, C. S., Yamazaki, M., Yahikozawa, H., Ichikawa, M., Yagita, H. & Kim, B. S. 1998. 'Suppressive effect on Theiler's murine encephalomyelitis virus-induced demyelinating disease by the administration of anti-IL-12 antibody', *Journal of Immunology*, vol. 161, pp. 5586-93.

Ireland, D. D., Stohlman, S. A., Hinton, D. R., Atkinson, R. & Bergmann, C. C. 2008. 'Type I interferons are essential in controlling neurotropic

- coronavirus infection irrespective of functional CD8 T cells', *Journal of Virology*, vol. 82, pp. 300-10.
- Ireland, D. D., Stohlman, S. A., Hinton, D. R., Kapil, P., Silverman, R. H., Atkinson, R. A. & Bergmann, C. C. 2009. 'RNase L mediated protection from virus induced demyelination', *PLoS Pathogens*, vol. 5, pp. e1000602.
- Jacobs, C. A., Baker, P. E., Roux, E. R., Picha, K. S., Toivola, B., Waugh, S. & Kennedy, M. K. 1991. 'Experimental autoimmune encephalomyelitis is exacerbated by IL-1 alpha and suppressed by soluble IL-1 receptor', *Journal of Immunology*, vol. 146, pp. 2983-9.
- Jenkins, J. K. & Arend, W. P. 1993. 'Interleukin 1 receptor antagonist production in human monocytes is induced by IL-1 alpha, IL-3, IL-4 and GM-CSF', *Cytokine*, vol. 5, pp. 407-15.
- Jin, H. M., Copeland, N. G., Gilbert, D. J., Jenkins, N. A., Kirkpatrick, R. B. & Rosenberg, M. 1998. 'Genetic characterization of the murine Ym1 gene and identification of a cluster of highly homologous genes', *Genomics*, vol. 54, pp. 316-22.
- Jin, Y. H., Kim, S. J., So, E. Y., Meng, L., Colonna, M. & Kim, B. S. 2011. 'Melanoma differentiation-associated gene 5 is critical for protection against Theiler's virus-induced demyelinating disease', *Journal of Virology*.
- Johnson, M. D., Gold, L. I. & Moses, H. L. 1992. 'Evidence for transforming growth factor-beta expression in human leptomeningeal cells and transforming growth factor-beta-like activity in human cerebrospinal fluid', *Laboratory Investigation*, vol. 67, pp. 360-8.

- Jouanguy, E., Doffinger, R., Dupuis, S., Pallier, A., Altare, F. & Casanova, J. L. 1999. 'IL-12 and IFN-gamma in host defense against mycobacteria and salmonella in mice and men', *Current Opinion in Immunology*, vol. 11, pp. 346-51.
- Jungo, F., Dayer, J. M., Modoux, C., Hyka, N. & Burger, D. 2001. 'IFN-beta inhibits the ability of T lymphocytes to induce TNF-alpha and IL-1beta production in monocytes upon direct cell-cell contact', *Cytokine*, vol. 14, pp. 272-82.
- Kapil, P., Atkinson, R., Ramakrishna, C., Cua, D. J., Bergmann, C. C. & Stohlman, S. A. 2009. 'Interleukin-12 (IL-12), but not IL-23, deficiency ameliorates viral encephalitis without affecting viral control', *Journal of Virology*, vol. 83, pp. 5978-86.
- Kato, H., Takeuchi, O., Sato, S., Yoneyama, M., Yamamoto, M., Matsui, K., Uematsu, S., Jung, A., Kawai, T., Ishii, K. J., Yamaguchi, O., Otsu, K., Tsujimura, T., Koh, C. S., Reis E Sousa, C., Matsuura, Y., Fujita, T. & Akira, S. 2006. 'Differential roles of MDA5 and RIG-I helicases in the recognition of RNA viruses', *Nature*, vol. 441, pp. 101-5.
- Kawai, T. & Akira, S. 2007. 'Antiviral signaling through pattern recognition receptors', *Journal of Biochemistry*, vol. 141, pp. 137-45.
- Kawai, T. & Akira, S. 2009. 'The roles of TLRs, RLRs and NLRs in pathogen recognition', *International Immunology*, vol. 21, pp. 317-37.
- Kelchtermans, H., Billiau, A. & Matthys, P. 2008. 'How interferon-gamma keeps autoimmune diseases in check', *Trends in Immunology*, vol. 29, pp.479-86.

- Keogh, B., Atkins, G. J., Mills, K. H. & Sheahan, B. J. 2002. 'Avirulent Semliki Forest virus replication and pathology in the central nervous system is enhanced in IL-12-defective and reduced in IL-4-defective mice: a role for Th1 cells in the protective immunity', *Journal of NeuroImmune Pharmacology*, vol. 125, pp. 15-22.
- Khader, S. A., Pearl, J. E., Sakamoto, K., Gilmartin, L., Bell, G. K., Jelley-Gibbs, D. M., Ghilardi, N., Desauvage, F. & Cooper, A. M. 2005. 'IL-23 compensates for the absence of IL-12p70 and is essential for the IL-17 response during tuberculosis but is dispensable for protection and antigen-specific IFN-gamma responses if IL-12p70 is available', *Journal of Immunology*, vol. 175, pp. 788-95.
- Kim, B., Sarangi, P. P., Azkur, A. K., Kaistha, S. D. & Rouse, B. T. 2008. 'Enhanced viral immunoinflammatory lesions in mice lacking IL-23 responses', *Microbes and Infection*, vol. 10, pp. 302-12.
- King, I. L. & Segal, B. M. 2005. 'Cutting edge: IL-12 induces CD4+CD25- T cell activation in the presence of T regulatory cells', *Journal of Immunology*, vol. 175, pp. 641-5.
- Kohyama, S., Ohno, S., Isoda, A., Moriya, O., Belladonna, M. L., Hayashi, H., Iwakura, Y., Yoshimoto, T., Akatsuka, T. & Matsui, M. 2007. 'IL-23 enhances host defense against vaccinia virus infection via a mechanism partly involving IL-17', *Journal of Immunology*, vol. 179, pp. 3917-25.
- Kolls, J. K. & Linden, A. 2004. 'Interleukin-17 family members and inflammation', *Immunity*, vol. 21, pp. 467-76.

- Kumar, A., Haque, J., Lacoste, J., Hiscott, J. & Williams, B. R. 1994. 'Double-stranded RNA-dependent protein kinase activates transcription factor NF-kappa B by phosphorylating I kappa B', *Proceedings of the National Academy of Sciences of the United States of America*, vol. 91, pp.6288-92.
- Langrish, C. L., Mckenzie, B. S., Wilson, N. J., De Waal Malefyt, R., Kastelein, R. A. & Cua, D. J. 2004. 'IL-12 and IL-23: master regulators of innate and adaptive immunity', *Immunological Review*, vol. 202, pp. 96-105.
- Levy, D. E. & Garcia-Sastre, A. 2001. 'The virus battles: IFN induction of the antiviral state and mechanisms of viral evasion', *Cytokine & Growth Factor Reviews*, vol. 12, pp. 143-56.
- Ley, K., Laudanna, C., Cybulsky, M. I. & Nourshargh, S. 2007. 'Getting to the site of inflammation: the leukocyte adhesion cascade updated', *Nature Reviews Immunology*, vol. 7, pp. 678-89.
- Li, J., Liu, Y. & Zhang, X. 2010. 'Murine coronavirus induces type I interferon in oligodendrocytes through recognition by RIG-I and MDA5', *Journal of Virology*, vol. 84, pp. 6472-82.
- Lieberman, L. A., Cardillo, F., Owyang, A. M., Rennick, D. M., Cua, D. J., Kastelein, R. A. & Hunter, C. A. 2004. 'IL-23 provides a limited mechanism of resistance to acute toxoplasmosis in the absence of IL-12', *Journal of Immunology*, vol. 173, pp. 1887-93.
- Lin, M. T., Hinton, D. R., Marten, N. W., Bergmann, C. C. & Stohlman, S. A. 1999. 'Antibody prevents virus reactivation within the central nervous system', *Journal of Immunology*, vol. 162, pp. 7358-68.

- Lin, M. T., Hinton, D. R., Parra, B., Stohlman, S. A. & Van Der Veen, R. C. 1998. 'The role of IL-10 in mouse hepatitis virus-induced demyelinating encephalomyelitis', *Virology*, vol. 245, pp. 270-80.
- Lipton, H. L., Liang, Z., Hertzler, S. & Son, K. N. 2007. 'A specific viral cause of multiple sclerosis: one virus, one disease', *Annals of Neurology*, vol. 61, pp. 514-23.
- Liu, M. T., Keirstead, H. S. & Lane, T. E. 2001. 'Neutralization of the chemokine CXCL10 reduces inflammatory cell invasion and demyelination and improves neurological function in a viral model of multiple sclerosis', *Journal of Immunology*, vol. 167, pp. 4091-7.
- Malmgaard, L., Salazar-Mather, T. P., Lewis, C. A. & Biron, C. A. 2002. 'Promotion of alpha/beta interferon induction during in vivo viral infection through alpha/beta interferon receptor/STAT1 system-dependent and -independent pathways', *Journal of Virology*, vol. 76, pp. 4520-5.
- Malone, K. E., Stohlman, S. A., Ramakrishna, C., Macklin, W. & Bergmann, C. C. 2008. 'Induction of class I antigen processing components in oligodendroglia and microglia during viral encephalomyelitis', *Glia*, vol. 56, pp. 426-35.
- Mantovani, A., Sica, A., Sozzani, S., Allavena, P., Vecchi, A. & Locati, M. 2004. 'The chemokine system in diverse forms of macrophage activation and polarization', *Trends in Immunology*, vol. 25, pp. 677-86.

- Martin, D. & Near, S. L. 1995. 'Protective effect of the interleukin-1 receptor antagonist (IL-1ra) on experimental allergic encephalomyelitis in rats', *Journal of NeuroImmune Pharmacology*, vol. 61, pp. 241-5.
- Masters, P. S. 2006. 'The molecular biology of coronaviruses'. *Advances in Virus Research*, vol. 66, pp. 193-292.
- Matthews, A. E., Weiss, S. R. & Paterson, Y. 2002. 'Murine hepatitis virus--a model for virus-induced CNS demyelination', *Journal For Neurovirology*, 8, 76-85.
- Mccandless, E. E., Wang, Q., Woerner, B. M., Harper, J. M. & Klein, R. S. 2006. 'CXCL12 limits inflammation by localizing mononuclear infiltrates to the perivascular space during experimental autoimmune encephalomyelitis', *Journal of Immunology*, vol. 177, pp. 8053-64.
- Mccandless, E. E., Zhang, B., Diamond, M. S. & Klein, R. S. 2008. 'CXCR4 antagonism increases T cell trafficking in the central nervous system and improves survival from West Nile virus encephalitis', *Proceedings of the National Academy of Sciences of the United States of America*, vol. 105, pp. 11270-5.
- Mcgavern, D. B. & Kang, S. S. 2011. 'Illuminating viral infections in the nervous system', *Nature Reviews Immunology*, vol. 11, pp. 318-29.
- Mcgeachy, M. J. & Cua, D. J. 2008. 'Th17 cell differentiation: the long and winding road', *Immunity*, vol. 28, pp. 445-53.
- Mckimmie, C. S., Johnson, N., Fooks, A. R. & Fazakerley, J. K. 2005. 'Viruses selectively upregulate Toll-like receptors in the central nervous system',

Biochemical and Biophysical Research Communications, vol. 336, pp. 925-33.

Michelucci, A., Heurtaux, T., Grandbarbe, L., Morga, E. & Heuschling, P. 2009.

'Characterization of the microglial phenotype under specific pro-inflammatory and anti-inflammatory conditions: Effects of oligomeric and fibrillar amyloid-beta', *Journal of NeuroImmune Pharmacology*, vol. 210, pp. 3-12.

Mikita, J., Dubourdieu-Cassagno, N., Deloire, M. S., Vekris, A., Biran, M., Raffard,

G., Brochet, B., Canron, M. H., Franconi, J. M., Boiziau, C. & Petry, K. G.

2011. 'Altered M1/M2 activation patterns of monocytes in severe relapsing experimental rat model of multiple sclerosis. Amelioration of clinical status by M2 activated monocyte administration', *Multiple Sclerosis Journal*, vol. 17, pp. 2-15.

Minagar, A., Shapshak, P., Fujimura, R., Ownby, R., Heyes, M. & Eisdorfer, C.

2002. 'The role of macrophage/microglia and astrocytes in the pathogenesis of three neurologic disorders: HIV-associated dementia, Alzheimer disease, and multiple sclerosis', *Journal of the Neurological Sciences*, vol. 202, pp. 13-23.

Minagawa, H., Sakai, Y., Li, Y., Ishibashi, T., Inomata, H. & Mori, R. 1997.

'Suppression of infectious virus spread and corneal opacification by the combined use of recombinant interferon beta and interleukin-10 following corneal infection with herpes simplex virus-1 in mice', *Antiviral Research*, vol. 36, pp. 99-105.

- Mogensen, T. H. 2009. 'Pathogen recognition and inflammatory signaling in innate immune defenses', *Clinical Microbiology Reviews*, vol. 22, pp. 240-73.
- Monteiro, J. M., Harvey, C. & Trinchieri, G. 1998. 'Role of interleukin-12 in primary influenza virus infection', *Journal of Virology*, vol. 72, pp. 4825-31.
- Mosser, D. M. 2003. 'The many faces of macrophage activation', *Journal of Leukocyte Biology*, vol. 73, pp. 209-12.
- Mosser, D. M. & Zhang, X. 2008. 'Interleukin-10: new perspectives on an old cytokine', *Immunological Review*, vol. 226, pp. 205-18.
- Murray, P. J. & Wynn, T. A. 2011. 'Protective and pathogenic functions of macrophage subsets', *Nature Reviews Immunology*, vol. 11, pp. 723-37.
- Nagai, K., Wong, A. H., Li, S., Tam, W. N., Cuddihy, A. R., Sonenberg, N., Mathews, M. B., Hiscott, J., Wainberg, M. A. & Koromilas, A. E. 1997. 'Induction of CD4 expression and human immunodeficiency virus type 1 replication by mutants of the interferon-inducible protein kinase PKR', *Journal of Virology*, vol. 71, pp. 1718-25.
- Nakagaki, K. & Taguchi, F. 2006. 'Receptor-independent spread of a neurotropic murine coronavirus MHV-JHMV in mixed neural culture', *Advances in Experimental Medicine and Biology*, vol. 581, pp. 327-30.
- Nakayama, Y., Plisch, E. H., Sullivan, J., Thomas, C., Czuprynski, C. J., Williams, B. R. & Suresh, M. 2010. 'Role of PKR and Type I IFNs in viral control during primary and secondary infection', *PLoS Pathogens*, vol. 6, pp. e1000966.

- Nathan, C. F., Murray, H. W., Wiebe, M. E. & Rubin, B. Y. 1983. 'Identification of interferon-gamma as the lymphokine that activates human macrophage oxidative metabolism and antimicrobial activity', *Journal of Experimental Medicine*, vol. 158, pp. 670-89.
- Neumann, H., Misgeld, T., Matsumuro, K. & Wekerle, H. 1998. 'Neurotrophins inhibit major histocompatibility class II inducibility of microglia: involvement of the p75 neurotrophin receptor', *Proceedings of the National Academy of Sciences of the United States of America*, vol. 95, pp. 5779-84.
- Nicklin, M. J., Hughes, D. E., Barton, J. L., Ure, J. M. & Duff, G. W. 2000. 'Arterial inflammation in mice lacking the interleukin 1 receptor antagonist gene', *Journal of Experimental Medicine*, vol. 191, pp. 303-12.
- Novelli, F. & Casanova, J. L. 2004. 'The role of IL-12, IL-23 and IFN-gamma in immunity to viruses', *Cytokine & Growth Factor Reviews*, vol. 15, pp. 367-77.
- O'malley, R. P., Mariano, T. M., Siekierka, J. & Mathews, M. B. 1986. 'A mechanism for the control of protein synthesis by adenovirus VA RNAI', *Cell*, vol. 44, pp. 391-400.
- Okun, E., Griffioen, K. J., Lathia, J. D., Tang, S. C., Mattson, M. P. & Arumugam, T. V. 2009. 'Toll-like receptors in neurodegeneration', *Brain Research Reviews*, vol. 59, pp. 278-92.
- Oleszak, E. L., Zaczynska, E., Bhattacharjee, M., Butunoi, C., Legido, A. & Katsetos, C. D. 1998. 'Inducible nitric oxide synthase and nitrotyrosine are found in monocytes/macrophages and/or astrocytes in acute, but not in

- chronic, multiple sclerosis', *Clinical and Diagnostic Laboratory Immunology*, vol. 5, pp. 438-45.
- Olson, J. K., Girvin, A. M. & Miller, S. D. 2001. 'Direct activation of innate and antigen-presenting functions of microglia following infection with Theiler's virus', *Journal of Virology*, vol. 75, pp. 9780-9.
- Olson, J. K. & Miller, S. D. 2004. 'Microglia initiate central nervous system innate and adaptive immune responses through multiple TLRs', *Journal of Immunology*, vol. 173, pp. 3916-24.
- Olson, J. K. & Miller, S. D. 2009. 'The innate immune response affects the development of the autoimmune response in Theiler's virus-induced demyelinating disease', *Journal of Immunology*, vol. 182, pp. 5712-22.
- Orange, J. S. & Biron, C. A. 1996a. 'An absolute and restricted requirement for IL-12 in natural killer cell IFN-gamma production and antiviral defense. Studies of natural killer and T cell responses in contrasting viral infections', *Journal of Immunology*, vol. 156, pp. 1138-42.
- Orange, J. S. & Biron, C. A. 1996b. 'Characterization of early IL-12, IFN- α , and TNF effects on antiviral state and NK cell responses during murine cytomegalovirus infection', *Journal of Immunology*, vol. 156, pp. 4746-56.
- Osman, F., Jarrous, N., Ben-Asouli, Y. & Kaempfer, R. 1999. 'A cis-acting element in the 3'-untranslated region of human TNF- α mRNA renders splicing dependent on the activation of protein kinase PKR', *Genes & Development*, vol. 13, pp. 3280-93.

- Ousman, S. S., Wang, J. & Campbell, I. L. 2005. 'Differential regulation of interferon regulatory factor (IRF)-7 and IRF-9 gene expression in the central nervous system during viral infection', *Journal of Virology*, vol. 79, pp. 7514-27.
- Oxenius, A., Karrer, U., Zinkernagel, R. M. & Hengartner, H. 1999. 'IL-12 is not required for induction of type 1 cytokine responses in viral infections', *Journal of Immunology*, vol. 162, pp. 965-73.
- Palma, J. P., Yauch, R. L., Kang, H. K., Lee, H. G. & Kim, B. S. 2002. 'Preferential induction of IL-10 in APC correlates with a switch from Th1 to Th2 response following infection with a low pathogenic variant of Theiler's virus', *Journal of Immunology*, vol. 168, pp. 4221-30.
- Palmer, G., Mezin, F., Juge-Aubry, C. E., Plater-Zyberk, C., Gabay, C. & Guerne, P. A. 2004. 'Interferon beta stimulates interleukin 1 receptor antagonist production in human articular chondrocytes and synovial fibroblasts', *Annals of the Rheumatic Diseases*, vol. 63, pp. 43-9.
- Parra, B., Hinton, D. R., Lin, M. T., Cua, D. J. & Stohlman, S. A. 1997. 'Kinetics of cytokine mRNA expression in the central nervous system following lethal and nonlethal coronavirus-induced acute encephalomyelitis', *Virology*, vol. 233, pp. 260-70.
- Parra, B., Hinton, D. R., Marten, N. W., Bergmann, C. C., Lin, M. T., Yang, C. S. & Stohlman, S. A. 1999. 'IFN-gamma is required for viral clearance from central nervous system oligodendroglia', *Journal of Immunology*, vol. 162, pp. 1641-7.

- Parra, G. I., Bergmann, C. C., Phares, T. W., Hinton, D. R., Atkinson, R. & Stohlman, S. A. 2010. 'Gamma interferon signaling in oligodendrocytes is critical for protection from neurotropic coronavirus infection', *Journal of Virology*, vol. 84, pp. 3111-5.
- Paul, S., Ricour, C., Sommereyns, C., Sorgeloos, F. & Michiels, T. 2007. 'Type I interferon response in the central nervous system', *Biochimie*, vol. 89, pp. 770-8.
- Pearce, B. D., Hobbs, M. V., Mcgraw, T. S. & Buchmeier, M. J. 1994. 'Cytokine induction during T-cell-mediated clearance of mouse hepatitis virus from neurons in vivo', *Journal of Virology*, vol. 68, pp. 5483-95.
- Peel, A. L. & Bredesen, D. E. 2003. 'Activation of the cell stress kinase PKR in Alzheimer's disease and human amyloid precursor protein transgenic mice', *Neurobiology of Disease*, vol. 14, pp. 52-62.
- Pewe, L., Haring, J. & Perlman, S. 2002. 'CD4 T-cell-mediated demyelination is increased in the absence of gamma interferon in mice infected with mouse hepatitis virus', *Journal of Virology*, vol. 76, pp. 7329-33.
- Pewe, L. & Perlman, S. 2002. 'Cutting edge: CD8 T cell-mediated demyelination is IFN-gamma dependent in mice infected with a neurotropic coronavirus', *Journal of Immunology*, vol. 168, pp. 1547-51.
- Pham, A. M. & Tenoever, B. R. 2010. 'The IKK Kinases: Operators of Antiviral Signaling', *Viruses*, vol. 2, pp. 55-72.

- Phares, T. W., Marques, C. P., Stohlman, S. A., Hinton, D. R. & Bergmann, C. C. 2011. 'Factors supporting intrathecal humoral responses following viral encephalomyelitis', *Journal of Virology*, vol. 85, pp. 2589-98.
- Piccinini, A. M. & Midwood, K. S. 2010. 'DAMPening inflammation by modulating TLR signalling', *Mediators of Inflammation*.
- Popko, B. & Baerwald, K. D. 1999. 'Oligodendroglial response to the immune cytokine interferon gamma', *Neurochemical Research*, vol. 24, pp. 331-8.
- Prud'homme, G. J. 2000. 'Gene therapy of autoimmune diseases with vectors encoding regulatory cytokines or inflammatory cytokine inhibitors', *Journal of Gene Medicine*, vol. 2, pp. 222-32.
- Pullen, L. C., Miller, S. D., Dal Canto, M. C., Van Der Meide, P. H. & Kim, B. S. 1994. 'Alteration in the level of interferon-gamma results in acceleration of Theiler's virus-induced demyelinating disease', *Journal of NeuroImmune Pharmacology*, vol. 55, pp. 143-52.
- Puntambekar, S. S., Bergmann, C. C., Savarin, C., Karp, C. L., Phares, T. W., Parra, G. I., Hinton, D. R. & Stohlman, S. A. 2011. 'Shifting hierarchies of interleukin-10-producing T cell populations in the central nervous system during acute and persistent viral encephalomyelitis', *Journal of Virology*, vol. 85, pp. 6702-13.
- Ramakrishna, C., Bergmann, C. C., Holmes, K. V. & Stohlman, S. A. 2004. 'Expression of the mouse hepatitis virus receptor by central nervous system microglia', *Journal of Virology*, vol. 78, pp. 7828-32.

- Ramakrishna, C., Stohlman, S. A., Atkinson, R. D., Shlomchik, M. J. & Bergmann, C. C. 2002. 'Mechanisms of central nervous system viral persistence: the critical role of antibody and B cells', *Journal of Immunology*, vol. 168, pp. 1204-11.
- Rempel, J. D., Murray, S. J., Meisner, J. & Buchmeier, M. J. 2004. 'Differential regulation of innate and adaptive immune responses in viral encephalitis', *Virology*, vol. 318, pp. 381-92.
- Rempel, J. D., Quina, L. A., Blakely-Gonzales, P. K., Buchmeier, M. J. & Gruol, D. L. 2005. 'Viral induction of central nervous system innate immune responses', *Journal of Virology*, vol. 79, pp. 4369-81.
- Rose, K. M. & Weiss, S. R. 2009. 'Murine coronavirus cell type dependent interaction with the type I Interferon response', *Viruses*, vol. 1, pp. 689-712.
- Roth-Cross, J. K., Bender, S. J. & Weiss, S. R. 2008. 'Murine coronavirus mouse hepatitis virus is recognized by MDA5 and induces type I interferon in brain macrophages/microglia', *Journal of Virology*, vol. 82, pp. 9829-38.
- Ryman, K. D., White, L. J., Johnston, R. E. & Klimstra, W. B. 2002. 'Effects of PKR/RNase L-dependent and alternative antiviral pathways on alphavirus replication and pathogenesis', *Viral Immunology*, vol. 15, pp. 53-76.
- Samuel, C. E. 2001. 'Antiviral actions of interferons', *Clinical Microbiology Reviews*, vol. 14, pp. 778-809.
- Samuel, M. A., Whitby, K., Keller, B. C., Marri, A., Barchet, W., Williams, B. R., Silverman, R. H., Gale, M., Jr. & Diamond, M. S. 2006. 'PKR and RNase L contribute to protection against lethal West Nile Virus infection by

- controlling early viral spread in the periphery and replication in neurons', *Journal of Virology*, vol. 80, pp. 7009-19.
- Savarin, C., Bergmann, C. C., Hinton, D. R., Ransohoff, R. M. & Stohlman, S. A. 2008. 'Memory CD4+ T-Cell-Mediated Protection from Lethal Coronavirus Encephalomyelitis', *Journal of Virology*, vol. 82, pp. 12432-40.
- Savarin, C., Stohlman, S. A., Atkinson, R., Ransohoff, R. M. & Bergmann, C. C. 2010. 'Monocytes regulate T cell migration through the glia limitans during acute viral encephalitis', *Journal of Virology*, vol. 84, pp. 4878-88.
- Schelle, B., Karl, N., Ludewig, B., Siddell, S. G. & Thiel, V. 2005. 'Selective replication of coronavirus genomes that express nucleocapsid protein', *Journal of Virology*, vol. 79, pp. 6620-30.
- Scheuner, D., Gromeier, M., Davies, M. V., Dorner, A. J., Song, B., Patel, R. V., Wimmer, E. J., Mclendon, R. E. & Kaufman, R. J. 2003. 'The double-stranded RNA-activated protein kinase mediates viral-induced encephalitis', *Virology*, vol. 317, pp. 263-74.
- Schijns, V. E., Haagmans, B. L., Wierda, C. M., Kruithof, B., Heijnen, I. A., Alber, G. & Horzinek, M. C. 1998. 'Mice lacking IL-12 develop polarized Th1 cells during viral infection', *Journal of Immunology*, vol. 160, pp. 3958-64.
- Schijns, V. E., Wierda, C. M., Van Hoeij, M. & Horzinek, M. C. 1996. 'Exacerbated viral hepatitis in IFN-gamma receptor-deficient mice is not suppressed by IL-12', *Journal of Immunology*, vol. 157, pp. 815-21.
- Schreiber, T., Ehlers, S., Heitmann, L., Rausch, A., Mages, J., Murray, P. J., Lang, R. & Holscher, C. 2009. 'Autocrine IL-10 induces hallmarks of

- alternative activation in macrophages and suppresses antituberculosis effector mechanisms without compromising T cell immunity', *Journal of Immunology*, vol. 183, pp. 1301-12.
- Sciacca, F. L., Canal, N. & Grimaldi, L. M. 2000. 'Induction of IL-1 receptor antagonist by interferon beta: implication for the treatment of multiple sclerosis', *Journal For Neurovirology*, vol. 6 Suppl. 2, pp. S33-7.
- Scott, P. & Kaufmann, S. H. 1991. 'The role of T-cell subsets and cytokines in the regulation of infection', *Immunology Today*, vol. 12, pp. 346-8.
- Seckinger, P., Lowenthal, J. W., Williamson, K., Dayer, J. M. & Macdonald, H. R. 1987. 'A urine inhibitor of interleukin 1 activity that blocks ligand binding', *Journal of Immunology*, vol. 139, pp. 1546-9.
- Sen, G. C. 2001. 'Viruses and interferons', *Annual Review of Microbiology*, vol. 55, pp. 255-81.
- Serafini, B., Columba-Cabezas, S., Di Rosa, F. & Aloisi, F. 2000. 'Intracerebral recruitment and maturation of dendritic cells in the onset and progression of experimental autoimmune encephalomyelitis', *American Journal of Pathology*, vol. 157, pp. 1991-2002.
- Sharma, A. & Maheshwari, R. K. 2009. 'Oligonucleotide array analysis of Toll-like receptors and associated signalling genes in Venezuelan equine encephalitis virus-infected mouse brain', *Journal of General Virology*, vol. 90, pp. 1836-47.
- Shrestha, B., Gottlieb, D. & Diamond, M. S. 2003. 'Infection and injury of neurons by West Nile encephalitis virus', *Journal of Virology*, vol. 77, pp. 13203-13.

- Silverman, R. H. 2007a. 'A scientific journey through the 2-5A/RNase L system', *Cytokine & Growth Factor Reviews*, vol. 18, pp. 381-8.
- Silverman, R. H. 2007b. 'Viral encounters with 2',5'-oligoadenylate synthetase and RNase L during the interferon Antiviral Research response', *Journal of Virology*, vol. 81, pp. 12720-9.
- Skinner, M. A. & Siddell, S. G. 1983. 'Coronavirus JHM: nucleotide sequence of the mRNA that encodes nucleocapsid protein', *Nucleic Acids Research*, vol. 11, pp. 5045-54.
- So, E. Y. & Kim, B. S. 2009. 'Theiler's virus infection induces TLR3-dependent upregulation of TLR2 critical for proinflammatory cytokine production', *Glia*, vol. 57, pp. 1216-26.
- Spolski, R., Kim, H. P., Zhu, W., Levy, D. E. & Leonard, W. J. 2009. 'IL-21 mediates suppressive effects via its induction of IL-10', *Journal of Immunology*, vol. 182, pp. 2859-67.
- Stetson, D. B. & Medzhitov, R. 2006. 'Type I interferons in host defense', *Immunity*, vol. 25, pp. 373-81.
- Stewart, M. J., Smoak, K., Blum, M. A. & Sherry, B. 2005. 'Basal and reovirus-induced beta interferon (IFN-beta) and IFN-beta-stimulated gene expression are cell type specific in the cardiac protective response', *Journal of Virology*, vol. 79, pp. 2979-87.
- Stewart, W. F., Kawas, C., Corrada, M. & Metter, E. J. 1997. 'Risk of Alzheimer's disease and duration of NSAID use', *Neurology*, vol. 48, pp. 626-32.

- Stohlman, S. A., Bergmann, C. C., Van Der Veen, R. C. & Hinton, D. R. 1995. 'Mouse hepatitis virus-specific cytotoxic T lymphocytes protect from lethal infection without eliminating virus from the central nervous system', *Journal of Virology*, vol. 69, pp. 684-94.
- Stohlman, S. A., Hinton, D. R., Parra, B., Atkinson, R. & Bergmann, C. C. 2008. 'CD4 T cells contribute to virus control and pathology following central nervous system infection with neurotropic mouse hepatitis virus', *Journal of Virology*, vol. 82, pp. 2130-9.
- Stojdl, D. F., Abraham, N., Knowles, S., Marius, R., Brasey, A., Lichty, B. D., Brown, E. G., Sonenberg, N. & Bell, J. C. 2000. 'The murine double-stranded RNA-dependent protein kinase PKR is required for resistance to vesicular stomatitis virus', *Journal of Virology*, vol. 74, pp. 9580-5.
- Suh, H. S., Brosnan, C. F. & Lee, S. C. 2009. 'Toll-like receptors in CNS viral infections', *Current Topics in Microbiology and Immunology*, vol. 336, pp. 63-81.
- Szekely, C. A., Thorne, J. E., Zandi, P. P., Ek, M., Messias, E., Breitner, J. C. & Goodman, S. N. 2004. 'Nonsteroidal anti-inflammatory drugs for the prevention of Alzheimer's disease: a systematic review', *Neuroepidemiology*, vol. 23, pp. 159-69.
- Takeda, K. & Akira, S. 2004. 'TLR signaling pathways', *Seminars in Immunology*, vol. 16, pp. 3-9.
- Takeda, K., Kaisho, T. & Akira, S. 2003. 'Toll-like receptors', *Annual Review of Immunology*, vol. 21, pp. 335-76.

- Tamaru, M., Tomura, K., Sakamoto, S., Tezuka, K., Tamatani, T. & Narumi, S. 1998. 'Interleukin-1beta induces tissue- and cell type-specific expression of adhesion molecules in vivo', *Arteriosclerosis, Thrombosis, and Vascular Biology*, vol. 18, pp. 1292-303.
- Tenoever, B. R., Ng, S. L., Chua, M. A., Mcwhirter, S. M., Garcia-Sastre, A. & Maniatis, T. 2007. 'Multiple functions of the IKK-related kinase IKKepsilon in interferon-mediated antiviral immunity', *Science*, vol. 315, pp. 1274-8.
- Tomkins, P. T., Ward, G. A. & Morris, A. G. 1988. 'Role of interferon-gamma in T-cell responses to Semliki Forest virus-infected murine brain cells', *Immunology*, vol. 63, pp. 355-62.
- Tran, E. H., Prince, E. N. & Owens, T. 2000. 'IFN-gamma shapes immune invasion of the central nervous system via regulation of chemokines', *Journal of Immunology*, vol. 164, pp. 2759-68.
- Trandem, K., Jin, Q., Weiss, K. A., James, B. R., Zhao, J. & Perlman, S. 2011. 'Virally expressed interleukin-10 ameliorates acute encephalomyelitis and chronic demyelination in coronavirus-infected mice', *Journal of Virology*, vol. 85, pp. 6822-31.
- Trinchieri, G. 2003. 'Interleukin-12 and the regulation of innate resistance and adaptive immunity', *Nature Reviews Immunology*, vol. 3, pp. 133-46.
- Trinchieri, G. 2010. 'Type I interferon: friend or foe?' *Journal of Experimental Medicine*, vol. 207, pp. 2053-63.

- Van Noort, J. M. & Bsibsi, M. 2009. 'Toll-like receptors in the CNS: implications for neurodegeneration and repair', *Progress in Brain Research*, vol. 175, pp. 139-48.
- Vilcek, J. 2006. 'Fifty years of interferon research: aiming at a moving target', *Immunity*, vol. 25, pp. 343-8.
- Wan, L., Lin, C. W., Lin, Y. J., Sheu, J. J., Chen, B. H., Liao, C. C., Tsai, Y., Lin, W. Y., Lai, C. H. & Tsai, F. J. 2008. 'Type I IFN induced IL1-Ra expression in hepatocytes is mediated by activating STAT6 through the formation of STAT2: STAT6 heterodimer', *Journal of Cellular and Molecular Medicine*, vol. 12, pp. 876-88.
- Wang, F. I., Stohlman, S. A. & Fleming, J. O. 1990. 'Demyelination induced by murine hepatitis virus JHM strain (MHV-4) is immunologically mediated', *Journal of NeuroImmune Pharmacology*, vol. 30, pp. 31-41.
- Weiner, L. P. 1973. 'Pathogenesis of demyelination induced by a mouse hepatitis', *Archives of Neurology*, vol. 28, pp. 298-303.
- Xu, J., Zhong, S., Liu, J., Li, L., Li, Y., Wu, X., Li, Z., Deng, P., Zhang, J., Zhong, N., Ding, Y. & Jiang, Y. 2005. 'Detection of severe acute respiratory syndrome coronavirus in the brain: potential role of the chemokine mig in pathogenesis', *Clinical Infectious Diseases*, vol. 41, pp. 1089-96.
- Yang, Y. L., Reis, L. F., Pavlovic, J., Aguzzi, A., Schafer, R., Kumar, A., Williams, B. R., Aguet, M. & Weissmann, C. 1995. 'Deficient signaling in mice devoid of double-stranded RNA-dependent protein kinase', *EMBO Journal*, vol. 14, pp. 6095-106.

- Yeh, E. A., Collins, A., Cohen, M. E., Duffner, P. K. & Faden, H. 2004. 'Detection of coronavirus in the central nervous system of a child with acute disseminated encephalomyelitis', *Pediatrics*, vol. 113, pp. e73-6.
- Yong, V. W. & Rivest, S. 2009. 'Taking advantage of the systemic immune system to cure brain diseases', *Neuron*, vol. 64, pp. 55-60.
- Zandi, P. P., Anthony, J. C., Hayden, K. M., Mehta, K., Mayer, L. & Breitner, J. C. 2002. 'Reduced incidence of AD with NSAID but not H2 receptor antagonists: the Cache County Study', *Neurology*, vol. 59, pp. 880-6.
- Zeis, T., Graumann, U., Reynolds, R. & Schaeren-Wiemers, N. 2008. 'Normal-appearing white matter in multiple sclerosis is in a subtle balance between inflammation and neuroprotection', *Brain*, vol. 131, pp. 288-303.
- Zhou, A., Paranjape, J. M., Der, S. D., Williams, B. R. & Silverman, R. H. 1999. 'Interferon action in triply deficient mice reveals the existence of alternative antiviral pathways', *Virology*, vol. 258, pp. 435-40.
- Zhou, H. & Perlman, S. 2007. 'Mouse hepatitis virus does not induce Beta interferon synthesis and does not inhibit its induction by double-stranded RNA', *Journal of Virology*, vol. 81, pp. 568-74.
- Zuo, J., Stohlman, S. A., Hoskin, J. B., Hinton, D. R., Atkinson, R. & Bergmann, C. C. 2006. 'Mouse hepatitis virus pathogenesis in the central nervous system is independent of IL-15 and natural killer cells', *Virology*, vol. 350, pp. 206-15.
- Zust, R., Cervantes-Barragan, L., Habjan, M., Maier, R., Neuman, B. W., Ziebuhr, J., Szretter, K. J., Baker, S. C., Barchet, W., Diamond, M. S., Siddell, S. G.,

Ludewig, B. & Thiel, V. 2011. 'Ribose 2'-O-methylation provides a molecular signature for the distinction of self and non-self mRNA dependent on the RNA sensor Mda5', *Nature Immunology*, vol. 12, pp. 137-43.

APPENDICES

APPENDIX A
LIST OF ABBREVIATIONS

wt:	Wild-type
IL:	Interleukin
IL1Ra:	Interleukin receptor antagonist
IFN:	Interferon
Ko:	Knock-out
IP:	Intra peritoneal
IC:	Intracerebral
p.i.:	Post-infection
NFkB:	Nuclear factor kappa beta
JHMV:	John Howard Muller strain of coronavirus
PKR:	Protein Kinase RNA dependent
OAS-2:	2'5' Oligoadenylate synthetase
STAT:	Signal transducer and activator of transcription
IFIT:	Interferon-induced protein with tetratricopeptide repeats
SC:	Spinal cord
CD:	Cluster of differentiation
mAb:	Monoclonal Antibody
MHC:	Major Histocompatibility Complex
TNF:	Tumor necrosis factor
PRR:	Pathogen recognition receptor
PAMP:	Pathogen associated molecular pattern

MDA-5:	Melanoma Differentiation-Associated Gene 5
RIG-I:	Retinoic acid inducible gene-I
TLR:	Toll like receptor
IRF:	Interferon regulatory factor
ISG:	Interferon stimulated genes
CoV:	Coronavirus
HIV:	Human immunodeficiency virus
WNV:	West Nile virus
LCMV:	Lymphocytic choriomeningitis Virus
HCMV:	Human cytomegalovirus
HSV:	Herpes simplex virus
JCV:	John Cunningham virus
EAE:	Experimental autoimmune encephalitis
MS:	Multiple sclerosis
Poly I:C:	Polyinosinic-polycytidylic acid